FEDERAL UNIVERSITY OF ITJAUBA

POST GRADUATION PROGRAM OF MECHANICAL ENGINEERING - DOCTORATE

IEM – INSTITUTE OF MECHANICAL ENGINEERING

THIAGO LUIZ LARA OLIVEIRA

ANALYSIS OF MILLING IN COMPOSITE MATERIAL BY NON-DESTRUCTIVE METHODS

Itajubá – Minas Gerais - Brazil

August/2021

UNIVERSIDADE FEDERAL DE ITAJUBÁ

PROGRAMA DE PÓS-GRADUAÇÃO EM ENGENHARIA MECÂNICA - DOUTORADO

IEM – INSTITUTO DE ENGENHARIA MECÂNICA

THIAGO LUIZ LARA OLIVEIRA

ANÁLISE DO FRESAMENTO DE MATERIAIS COMPOSITOS POR MÉTODOS NÃO DESTRUTIVOS

Itajubá – Minas Gerais - Brasil

Agosto/2021

UNIVERSITÉ FEDERALÉ D'ITAJUBÁ

ÉCOLE DOCTORALE D'INGENERIE MECÁNIQUE

IEM – INSTITUT DE INGENERIE MÉCANIQUE

THIAGO LUIZ LARA OLIVEIRA

ANALYSE DU FRAISAGE DES MATÉRIAUX COMPOSITES PAR MÉTHODES NON DESTRUCTIVES

Itajubá – Minas Gerais - Brésil

Août/2021

UNIVERSIDADE FEDERAL DE ITAJUBÁ

POST GRADUATION PROGRAM OF MECHANICAL ENGINEERING - DOCTORATE

Thiago LUIZ LARA OLIVEIRA

ANALYSIS OF MILLING IN COMPOSITE MATERIAL BY NON-DESTRUCTIVE METHODS

Doctoral thesis submitted to the Post Graduation Program of Mechanical Engineering as part of the requirements for obtaining the title of Doctor of Science in Mechanical Engineering.

Concentration Area: Process, Materials and Project.

Advisor: PhD. Prof. Antonio Carlos Ancelotti Jr.

Co-advisor: PhD. Prof. Sebastião Simões Da Cunha Jr.

Co-advisor Abroad: PhD. Prof. Redouane Zitoune

Itajubá – MG – Brazil

August/2021

Acknowledgments

This project would not have been possible without the support of many people, specially my tutors, friends and family. My supervisor Doctor Antonio Carlos Ancelotti Junior, I am glad for the opportunity to work with him, for his guidance, teaching and friendship for this years. I would like to thanks Doctor Redouane Zitoune for my enlightening year at ICA, in which I was able to grow as a person and as a professional. Doctor Sebastião Simões da Cunha Junior, for his constant aid during my work development.

Thanks to Universidade Federal de Itajubá, with all the support from the personal that I have received and the many opportunities to grow professionally, as well as Institut Clement Ader that provided me an outstanding research experience. To all UNIFEI and ICA professors, for the teaching and incentive. My PhD colleagues, Daniel, Lorena, Diego, Olivia, Alan, Fernanda, Tamara, Thiago, Vinícius, Lorraine, Akshay, Nguyen and Xavier for all aid that you guys gave me, the lessons and the specially the friendship.

Thank you my parents, for the love, support and patience, especially for understanding my usual absence and respect of my life choice to go further in this career. My parents who were always a sample of courage and dedication to work. Thank you my family for supporting me in the hard and in the good times. Thank you my friend Marlon Mendes Oliveira, especially for your friendship.

Thanks to all my friends, brothers and sisters of friendship, which have been part of my personal and professional life, and that will remain present on my life. Thanks to all people that have been passing in my life, you all were once part of my life, somehow will always be, we shared experiences together, learned together and I am glad to have met and have been with you all.

"Those who don't take control of their own lives become mere spectators of their own existence."

Author

“Courage is the first of human qualities because it is the quality which guarantees the others.”

Aristotle

“Yea, something invulnerable, unburiable is with me, something that would rend rocks asunder: it is called my will. Silently doth it proceed, and unchanged throughout the years.” – “Yea, thou art still for me the demolisher of all graves: Hail to thee, my will! And only where there are graves are there resurrections.”

Friedrich Nietzsche

ABSTRACT

In aerospace industry, composite materials offer several advantages, such as high weight-to-strength ratio and corrosion resistance. Aerospace materials are costly and have high safety standards, frequently using non-destructive testing in order to evaluate the material without incurring in further damage. Acoustic emission is a non-destructive testing method, which allows the signal processing to evaluate material performance during mechanical tests for determining material defects, for example. This study focused in the machining process of composite plates, in terms of surface finishing evaluation with comprehension of process phenomenology using non-destructive testing. Manufacturing processes are complex, especially the machining of composite materials, due to their specific properties and characteristics. The detection and prediction of surface finishing and occurrence of defects during manufacturing using non-destructive techniques is industrially useful, in terms of increasing automated manufacturing systems to increase productivity and quality control. The aim of this study is to show the possibility of online monitoring of the cutting process and to understand mechanism behind variables of control, with comparisons of different milling parameters and focusing in their impacts in acoustic emission signals, infrared thermography and surface finishing. The results indicates the relationship between cutting process and acoustic emission signals, with a key differentiation of other studies because it shows the not only the capability of detecting anomalies during cutting process and to predict surface quality by acoustic emission signal analysis, but also that is possible to develop new methods of monitoring in real time machined surface of composite parts quality using acoustic emission signals.

Keywords: AE signals; CFRP; milling; smart machining; NDT.

RESUMO

Na indústria aeroespacial, polímeros reforçados com fibra de carbono oferecem diversas vantagens, como uma melhor relação entre resistência por peso ou mesmo resistência a corrosão. A análise de sinais obtidos pela emissão acústica tem sido bem sucedida para avaliar ensaios mecânicos e também para determinar defeitos no material. Esse trabalho é focado no processo de usinagem por fresamento de materiais compósitos de resina epóxi e fibra de carbono, em termos de avaliação da qualidade superficial e com compreensão da fenomenologia do processo por ensaios não destrutivos, principalmente emissão acústica e análise de temperatura por infravermelho. Durante o processo de usinagem, o monitoramento do processo com vistas à detecção e predição da qualidade superficial e ocorrência de defeitos é industrialmente útil, podendo aumentar a automatização dos sistema de fabricação, incrementar a produtividade e prover maior controle de qualidade. O objetivo deste estudo foi de mostrar que é possível implementar um sistema de monitoramento em tempo real do processo de corte, com o entendimento dos mecanismos e variáveis de influência. As comparações dos diferentes parâmetros empregados durante o fresamento e seus efeitos nos sinais obtidos pela técnica de emissão acústica e variações de temperatura, permitiram relacionar esses métodos com a qualidade superficial. Os resultados indicam que os ensaios não destrutivos podem servir de indicativo para o estado de qualidade superficial das placas de fibra de carbono-epóxi, também são sensíveis às alterações dos parâmetros de usinagem. Além disso, a análise por emissão acústica obteve melhor desempenho do que a análise por termografia infravermelho no monitoramento do fresamento desses materiais.

Palavras-Chave: Emissão acústica; materiais compósitos; fresamento; END.

RÉSUMÉ

Dans l'industrie aérospatiale, les plaques composites renforcées de fibres longues offrent de nombreux avantages. Les matériaux aérospatiaux ont un coût élevé et ont un niveau de sécurité élevé, de sorte que les structures doivent être évaluées sans endommager le matériau. L'émission acoustique est une méthode de CND, qui permet au traitement du signal d'évaluer les performances du matériau. Des études récentes ont analysé l'EA lors de l'usinage, afin de surveiller les outils d'usinage ou qualité d'usinage des matériaux métalliques. Cette étude s'est concentrée sur le processus d'usinage des structures composites en carbone/époxy, en envisageant l'évaluation de la qualité de la surface avec compréhension de la phénoménologie des processus à l'aide d'analyses de CND axées sur les caractéristiques des signaux d d'émission acoustique et de la température d'usinage. L'usinage des matériaux composites est un procédé complexe, en raison de leurs propriétés et caractéristiques spécifiques. La prédiction de l'état de surface après usinage et/ou de détection des imperfections durant la phase de fabrication sont nécessaires sur le plan industriel, pour augmenter la productivité et améliorer le contrôle qualité. L'objectif de cette étude est de montrer la possibilité d'un suivi en ligne du processus de fraisage et de comprendre le mécanisme derrière les variables de contrôle, comparaison des paramètres de fraisage et en se concentrant sur leurs impacts dans les signaux EA et de l'état de surface. Les résultats indiquent la relation entre le processus de coupe et les signaux EA, avec la capacité de détecter les anomalies pendant le processus de coupe et de prédire l'état de surface par analyse des signaux EA, montrant qu'il est possible de développer de nouvelles méthodes de surveillance en temps réel de l'état de surface usinée à l'aide d'émission acoustique.

Mots clés : signaux AE ; CFRP ; fraisage ; usinage intelligent ; CND.

List of Figures

List of Tables

Table of Contents

1. Introduction

Composite materials are often related to aeronautic, naval and automotive industries, where the increasing potential of having their mechanical properties improved for a wide range of different applications allows them to replace conventional materials. Nowadays fibre reinforced polymers are the main aircraft components and often them are reinforced with glass or carbon fibres (1,2,3).The machining of composite materials is a complex secondary manufacturing process, with a complex mechanism that impacts on material quality and machining tools life span (4). Compared to metal process of cutting, machining of composite materials cause rapid tool wear and often significant damage to machined surfaces.

Regarding the interaction between machined surface and cutting tool, machining parameters and material characteristics influence the phenomenology of damage in composite materials during manufacturing (5). Composite materials have a heterogeneous and anisotropic structure, these characteristics make machining parameters, tool wear and material damages in machining a complex field of study (6). Cutting fluids, for example, are often necessary and used in metal machining processes. However, for composite materials the use of cutting fluids showed diverse results, depending on cutting fluid components (7). Machinability of composite materials is related to material characteristics, for example, fibres have high hardness, are abrasive and brittle. Thus, despite material damage caused by machining, a hazard dust is produced during the process and may affect human healthy (8).

As the manufacturing process by itself can produce damage in composite materials, several techniques have been employed for monitoring the fabrication stages, such as cutting forces, mechanical vibration and acoustic emission. The cutting forces evaluation is influenced by machining parameters and workpiece, it is perhaps the most common parameter for monitoring

machining process and is related to tool wear, surface finishing and chip formation (9,10,11,12,13).

Machining processes have a variety of principles for the phenomenon of cutting. Fewer processes are used in machining of composite materials, namely: drilling, turning, grinding, milling and trimming. Thus, drilling operations are focused in making cylindrical holes, grinding of composite materials aims to improve surface finishing, while turning is meant to be used for cylindrical components in order to achieve dimensional tolerances or split parts. Milling and trimming operations in composite materials frequently uses the same mechanism of cutting, with trimming operations aiming contour shape or divide the material in several parts and the milling term being often associated to machining of complex shapes within material area (14).

There are several studies about machining parameters influences on the cutting of carbon fibre reinforced polymer (CFRP) plates, concerning mainly material damage in terms of surface integrity and mechanical properties were widely described. Surface integrity comprises surface properties and characteristics, such as, topographical, chemical, thermal, metallurgical and mechanical. Usually, machining is concerned with topographic characteristic of the product, frequently associated to roughness and other morphological features (15). The mechanical properties covers physical properties of a material when it is under application of loadings or forces, tensile strength and fatigue resistance are among these properties. Thus, the damages inherent made during machining of composite materials may vary, affecting both phases with fibre pull out, matrix crack, uncut fibres, streaks and delamination (16). Generally, an increase of cutting forces is related to more mechanical damage and lower surface quality (4).

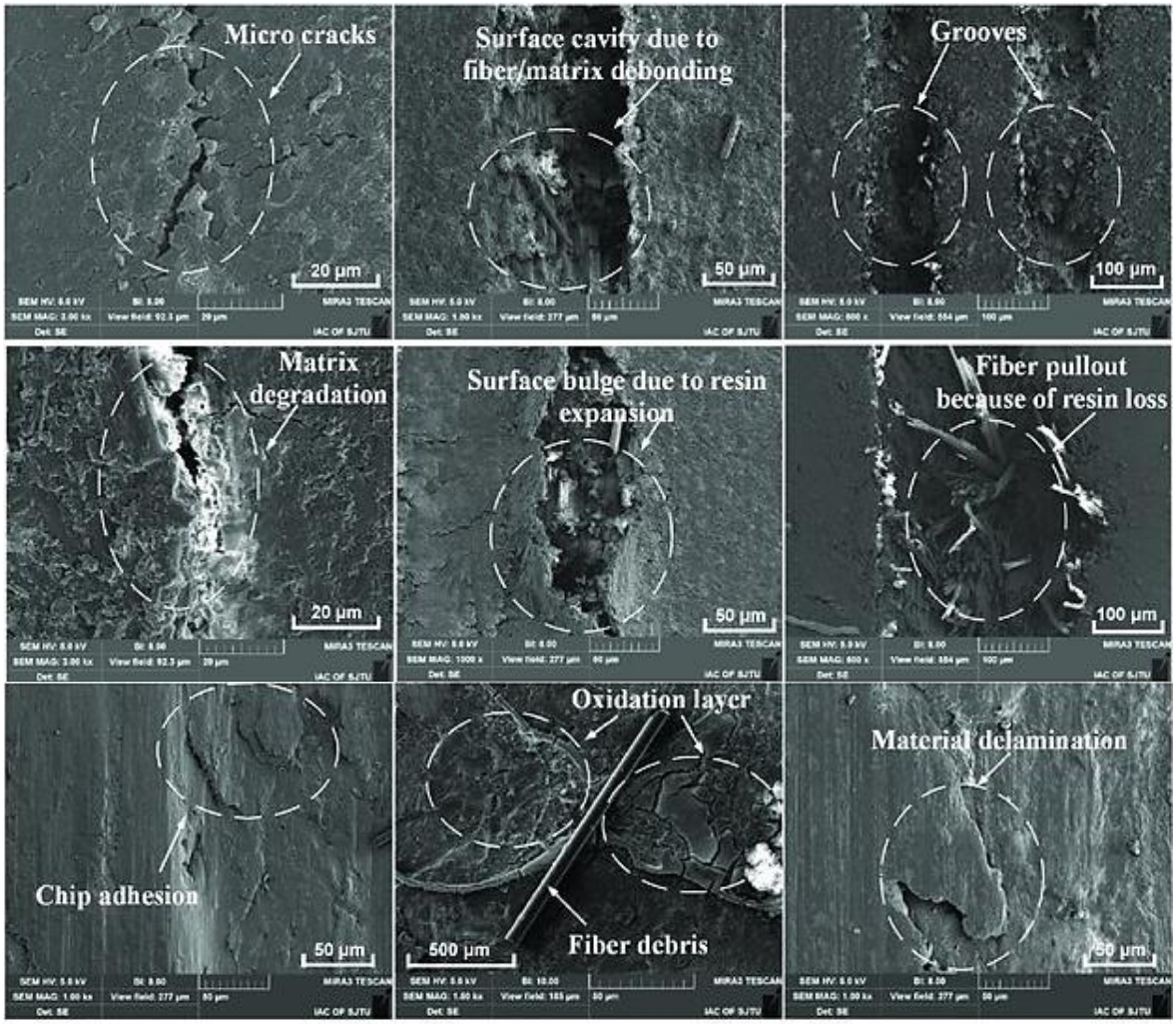

Figure 1 – Common defects caused by different machining processes, adapted (17).

Regarding damage caused by machining processes, drilling cutting often causes delamination of the up or bottom layers, a process well known as peel-up and push-out, respectively (18). Processes of milling and trimming are significantly influenced by feed and cutting speeds, with a high impact on the surface quality and damage generation that may impact mechanical properties (19).The phenomenology of delamination during edge trimming of unidirectional top layers CFRP was described in terms of its development and propagation (20). The findings showed that fibre protrusion is related with delamination, having two main mechanisms of protrusion being distinguished. Modelling and analysis of recorded cutting forces showed that the so-called active force is the cause of initial damage of the laminate, leading to fibres to deflect instead of being cut. Machining temperature is a relevant factor in composite materials,

since a high temperature can generate damage, particularly in matrix phase. A study showed that it is possible to delineate the correct band of temperature for composite machining varying cutting speed, which can facilitate the machining process in terms of cutting forces and reduce tool wear, without causing matrix damage (21).

Regarding trimming or milling, a study monitored a trimming process and showed a relationship between cutting forces and machining parameters. The results indicate that lower levels of tool wear and feed speed, as well as an increase in cutting speeds, reduced cutting forces (22). A non-destructive technique (NDT) for monitoring milling process of a CFRP is using vibration analysis, aiming to relate damage caused by milling and the acquired signals (23). The vibration signals analysis indicated a relationship between vibration and defects and were used to modelling milling parameters for avoiding delamination and resin burnout presence. Acoustic emission is also used with the aim of monitoring machining process, sometimes having the results analysed with cutting forces or vibration analysis. Infrared thermography is a NDT for monitoring machining process, capable of relate temperature variations with defects and damages, especially those damages caused by heat affected zones (24).

The milling process of aeronautic aluminium was also monitored by acoustic emission, which is another NDT, and by the cutting forces, aiming to monitor tool and work piece surface integrity (25). The results presented good evidence of the use of acoustic emission (AE) sensory to monitor anomalies in milling operations, with similarity between AE signals and measured cutting forces. The amplitude of AE signals are similar, more sensible and correlated to cutting forces, the tool wear also affected the energy of AE signals (MARSE). Based on signal measures of AE, cutting forces and cutting length the authors determined which conditions for milling processing generated damage-free or anomalous machined surfaces. A later study

proposed to implement online monitoring for milling process with different tools. The results indicate the existence of a signal pattern for normal finishing surfaces and anomalous, different techniques for evaluating signal processing were tested to identify the differences of cutting tools events with appropriated results (26). A similar study showed the same relationship for a machining process of metal, in terms of relationship tool wear and acoustic emission signals (27).

A turning process was monitored by acoustic emission signals. The results showed that chip formation had impact in the amplitude of AE signals, with a negative relationship between AE mean values and shear angle. For conventional machining and work piece, acoustic emission signals were distinguished during chip formation process and its variation in terms of tool wearing and impacts of machined surface (28). Another study used acoustic emission to analyse the surface finishing of end-milling of extruded aluminium, showing a relationship between surface roughness and acoustic emission signal features. The variation of machining parameters caused different levels of surface roughness, amplitude and RMS of acoustic emission signal (29).

The measurement of cutting forces, surface analysis and acoustic emission signals in trimming CFRP specimens was studied by mathematical modelling (30). Using three different tool geometries, also different cutting and feed speeds, the results showed the influence of tool geometry in cutting forces, surface roughness and delamination. It was possible to develop regression equations and artificial neural network models to predict cutting forces in the different trimming parameters of cutting and feed speed. The surface analysis permitted the identification of the damage mechanisms. The magnitude of AE signals were considered to be related as a measure of cutting tool, in which higher the AE signal indicates worsening of tool performance.

Online monitoring of abrasive water-jet using acoustic emission with different machining parameters presented several results. For example, cumulative counts and energy were useful for detect changes in machining parameters, with cumulative of the featured signals being connected to quality of machined CFRP. The method was unable to establish effects for single burst signals and specific defects, such as delamination (31).

The aim of this work was to demonstrate the possibility of monitoring the cutting process using non-destructive methods. This research used different variables of influence and response, with comparisons of different milling parameters and focusing in their impacts in acoustic emission signals, infrared thermography and surface finishing, with suggestions of evaluation and prediction methods of machined surface, in order to understand the mechanisms behind variables of control.

1.1 Justification

The aim of this study was to establish relationships between the qualities of CFRP machined surface using techniques of acoustic emission signals and infrared thermography. Furthermore, this study aims to evaluated the relationship between surface quality and NDT for CFRP, which is justified by lack of in literature and the possibility of reducing costs industrially. These relationships studied here are aimed to enable the monitoring of the process in real time, allowing estimate surface quality and predict defects based on acoustic emission features and infrared temperature. The study enables the analysis of cutting changes through signal processing, as well as the use of recorded temperatures to identify the effect on surface finishing, having a key differentiation from other studies by establishing relationship between surface finishing of composite materials and opening the possibility of online monitoring surface finishing of CFRP by using NDT. The acoustic emission features and their behaviour with variables of influence are also analysed, regarding cutting path and relation with surface

finishing. The milling process was conducted using a 4-flute end-mill by a CNC in a CFRP plate with 2 different stacking sequences, using 2 different cutting speeds, 3 feed directions and 2 tool wear conditions in a full factorial design of experiments. The process was monitored by an infrared camera and acoustic emission sensor. The machined surface was characterized by microscope images, topography and roughness; the results were compared with monitoring data.

1.2 Study structure

In chapter one an outline of the subject was made, with initial considerations covering the study theme being developed by the PhD thesis. It aims to contextualise the readers to subject of research, as well as, presenting the objectives and relevance of the study.

Chapter two is a literature survey of the non-destructive testing methods (NDT), machining of composite materials and includes their issues and related issues. The themes covered are: composite materials for aeronautical applications; primary manufacturing process of composite materials; machining process of composite materials; use of non-destructive testing in composite materials; acoustic emission and infrared thermography for monitoring and evaluate composite materials during mechanical tests and tool wear in machining process.

Chapter three covers the experimental setup that was used in this study, from the CFRP manufacturing, through acoustic emission and infrared thermography methods, to milling parameters and methods of surface finishing evaluation. The methodology employed during experiments, as well as, the basis for analysis parameters of results are described.

In chapter four the outcomes of the use of non-destructive techniques (NDT) during milling process of CFRP, regarding surface finishing and phenomenology of machining process, are

discussed. The significance of the results, mainly in terms of relationship of NDT results and surface quality are emphasised and are the base of next steps for the thesis development.

Chapter 5 summarises the main conclusions obtained from the result analysis of results, as well as, proposes next steps with the chronogram to develop these steps. Thus, stabilising the overall basis of thesis development, including questions to clarify.

2. State of Art

2.1 Composite Materials for Aeronautical Applications

Composite materials have been being used, with success, as part of aircraft structures for decades. Due to its capacity of combine a wide variety of properties, such as high specific strength, specific modulus, design ability, fatigue and corrosion resistance. These advantages, allied to weight reduction of aircraft structures of up 30%, make composite materials show better performance over steel and aluminium alloy structural materials, turn composite materials useful for a large number of applications (32).

Carbon fibre reinforced resin matrix composites (CFRP) have high strength-to-weight ratio, high temperature resistance, and excellent fatigue resistance, for example, CFRP is largely used on civil aircraft and in aerospace industries. The trend is to develop of more cost-effective process and materials; European aircraft industries objective is a wider application for carbon fibre resin matrix composite materials on aircraft, aiming to reduce aircraft weight by 30% and thus reducing flight costs up to 40% (33).

Resin-based composites is one of the most employed structural material on aviation industry, just after aluminium alloy, steel and titanium alloy. Resin-based composite materials are widely used in modern high-tech fields such as aerospace, as the leading material of the 21st century; the amount of usage of composite materials has become an important sign of the advanced nature of aircraft industry, and even of the advanced nature of aviation as an overall (34).

In the development of science and technology of aviation, modern materials has always played a leading and significant role. The state of development of materials employed in aircraft structure is related to the highest technology of material development for a company of country. In terms of commercial civilian passenger aircrafts, such as Airbus series, composite materials

are used up to 20% of aircraft structure and it is expected to increase this percentage through years. In addition, composite materials give aerospace and civil aircraft industries new useful increments like special damping characteristics, anti-vibration and noise (35).

There are different types of composite materials, with conceptual differences in the classification by authors. Composite materials is usually referred to materials with fibres, fabrics, whiskers, other materials made from particles and reinforcing matrix materials (36). Alternatively, by substrate composite materials can be divided into resin-based composite materials, metal-based composite materials, carbon-based composite materials and ceramic-based composite materials. The function can be divided into conductive composite materials, magnetic conductive composite materials, protective composite materials among others. Usually, in aerospace industries composite materials are mainly made from resin-based, ceramic-based and carbon/carbon for example (37).

Aramid fibre composites polymer (AFRP) also have high strength-to-weight ratio, high elasticity modulus, high thermal stability and resistance. Commonly used as a composite material for armour, it provides strong protection. Recently the interest of using this material in civil aircraft is increasing; this material may be used as a light shielding material, a composite material reinforced by fibres and aramid fibres (38).

Metal matrix composites are made of light metals such as Al and Mg, typically employed where requirements of low density must be meet. Metal matrix composite materials are commercially attractive in many applications, specially in aviation and aerospace to replace beryllium (39). Extensive research and application of metal matrix composite materials allowed rapid development. Metal-based composite materials have been implemented worldly, mainly mechanical parts. For example, to increase wear-resistant, these materials have reinforcement of particles of aluminium-based/zinc-based composite (40).

Ceramic-based composites are used as heat-resistant structural materials. Potential applications for ceramic matrix composites are aerospace, energy, automotive industry, environmental protection, biology and chemical industries. Ceramic matrix composites have high bending strength, fracture toughness, anti-oxidation properties, high temperature resistance, small coefficient of thermal expansion and working temperature up to 1650 °C. Carbon ceramic-based composite materials are also very heat resistant, used at temperatures higher than 1650°C. These materials can be used as engine parts, due to high temperature exposure (41). Specifically, beyond 500°C only composite materials made of ceramic matrices or carbon fibre are useful as structural components due to their thermo-mechanical properties.

Developed countries invest significant amount of their GDP in research, including research of new material, with United States of America (USA), Japan and Western European countries, for example, focus on aviation and military applications (42). USA Department of Energy began implementing research on ceramic matrix composites for NASA, with investments of funds and work force. NASA developed a research project for use of ceramic components in heat engines, developing blades and combustion chambers with success in terms of thermal tests (43). In Europe, Airbus developed a ceramic-based composite to use in rocket engine, it passed ignition tests and due to the use of ceramic matrix composites the structure weight reduction (44).

2.2 Manufacturing of CFRP

The CFRP materials are among the materials with high employability, having a lightweight, high strength and long life span. These characteristics make this material suitable for many different aeronautical applications. Different techniques are used to manufacture CFRP, aiming to combine carbon fibre and resin to deliver a proper material to meet the different requirements for the variety of applications.

Carbon fibre fabric may be divided in two main architectures, unidirectional/tape or bidirectional/woven, in Figure 2 the difference between unidirectional and bidirectional fabrics are showed by two sets of images. On left side, the unidirectional tape of carbon fibre is showed with the concept of unit cell with two fibres at 0° direction or aligned at horizon. In this concept, a unit cell must have repeatability through all the material. Unidirectional is a non-woven sort of carbon fabric, where all fibres are aligned to one direction in parallel. On the right side of the same figure, a bidirectional woven fabric of 0°/90° (perpendicular fibres), with the unit cell having one fibre of each direction. Bidirectional woven may have many different configurations, regarding the woven architecture there are three fundamental types of textile, namely: plain weave (Figure 3, top right), satin weave and twill weave. The fibre alignment is usually consisted by perpendicular layers, but it may vary. The woven fabric usually displays a non-uniform strain distribution on uniaxial loading, due to the existence of crimped fibre bundles (45). Composite materials manufactured of fabrics can have a three-dimensional reinforcement not in-plane, but through thickness. This kind of reinforcement, 3D reinforcement or though thickness, is usually employed to increase strength out-of-plane. It is possible to divide the manufacturing process on fibre and resin state being or not being separated before manufacturing. While pre-preg form is a combination of resin and fibre, fibre and resin can be separated before manufacturing. It is also possible to separate manufacturing process in two main fields, out of autoclave and in autoclave processes.

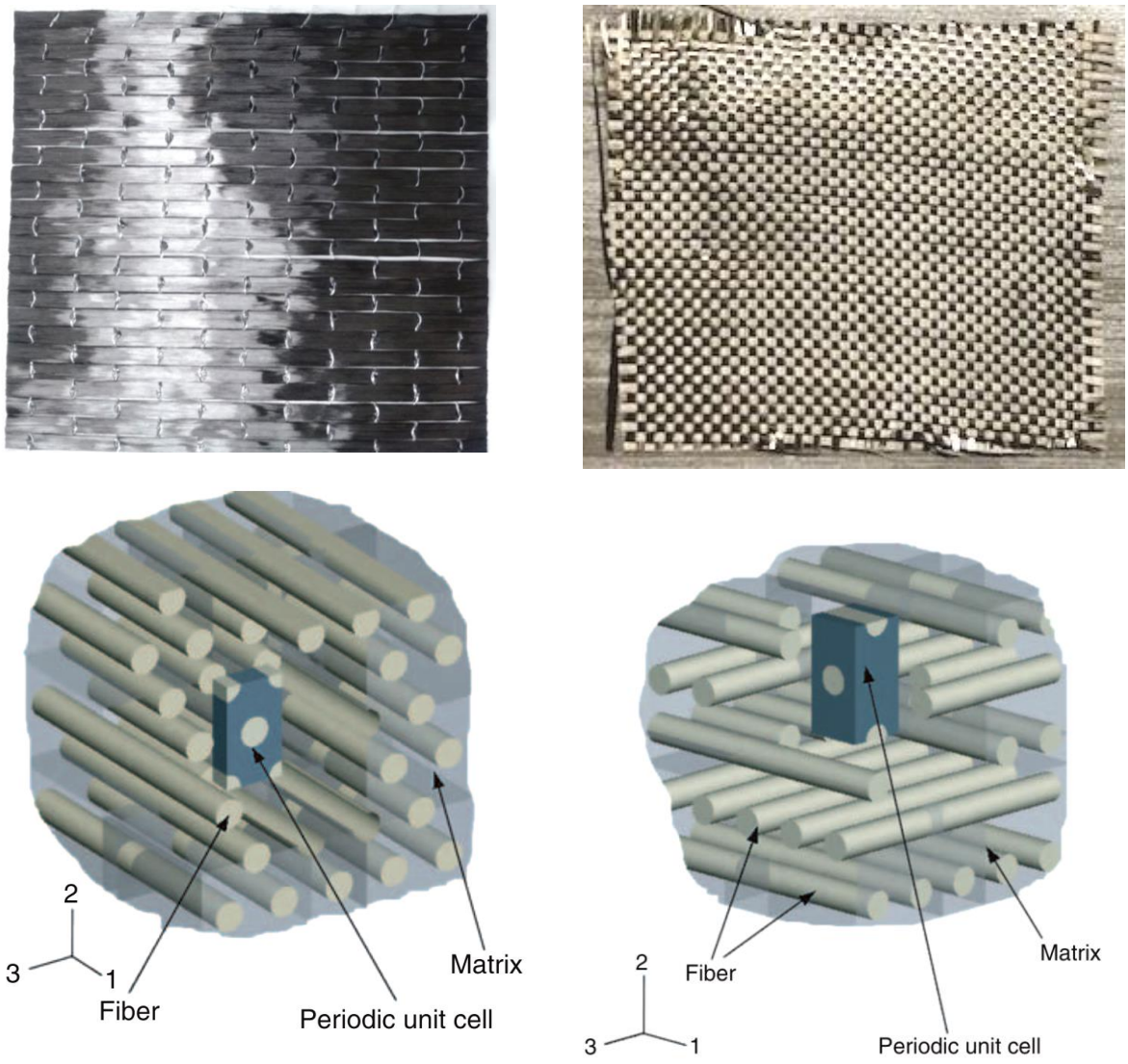

Figure 2 – Unidirectional (left) and bidirectional (right) carbon fibre configurations [Author, (46).

The use of pre-preg or fibre and resin, as well as, in or out autoclave manufacturing is a decision based on the desired final product, regarding factors of quality, budget and size for example. The autoclave manufacturing of composite materials is costly, requires high level of temperature and pressure in the curing stage and usually provides higher final product quality. Alternative methods of manufacturing are also common, some of those out of autoclave techniques are Resin Transfer Moulding (RTM) and Vacuum Resin Transfer Moulding (VaRTM). These two process are have similar principle, with the resin flow injection throw a mould by pressure (47).

In the RTM process there is a closed mould that shapes the fibres to be manufactured, this mould is closed and kept closed in order to receive the resin injection by compression into the mould. Appling pressure in the resin inlet causes resin flow, aiming that resin fulfil the mould, once reached this state, resin injection stops and starts to cure process. After finishing cure, the mould is open and the composite piece is removed from it.

A process derived from the RTM process is the VaRTM, where there is a bottom mould and a vacuum bag on the top, vacuum bag that must be proper sealed to permit vacuum creation. In this process there is an inlet for resin and an outlet of vacuum vent, the resin flow begins when vacuum pressure is achieved. After all the preform is fulfilled of resin, the inlet of resin is closed. Similarly to RTM, resin is cured before removing the manufactured piece. Additionally, some consumable products are employed for facilitate to remove the finished piece from moulding or aiding resin flow.

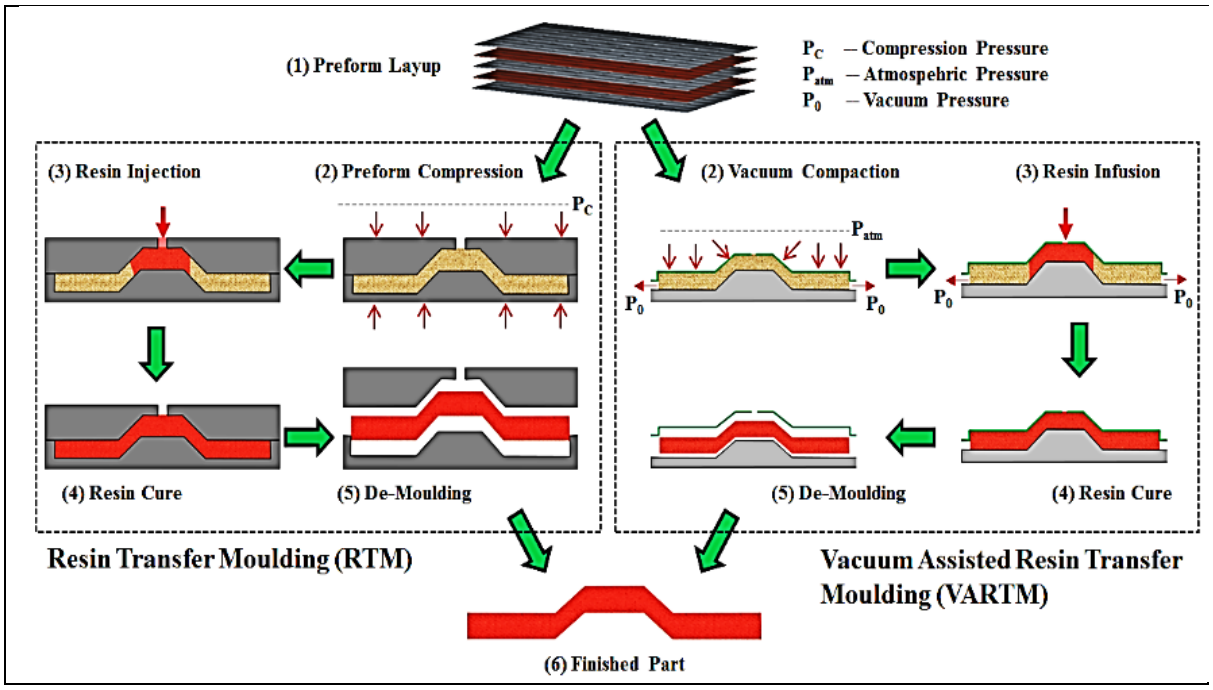

Figure 3 – Schematic comparison of the processes of RTM and VARTM (47).

CFRP manufacturing is subject to a wide variety of defects, with defects of type void being the most common (48). Void defects may decrease mechanical performance and lead to fail in

service, RTM and VaRTM usually have a higher volume of voids. Establishing a level of acceptance of this defect is important, for not risking the CFRP piece to fail in service or discard products that would have acceptable performance (49). Void formation is influenced by mould temperature, a low difference of temperature between resin flow and mould is related to less void formation (50).The pressure is another significant factor, with low levels of pressure increasing void formation and high pressure decreasing void formation (51). Resin viscosity and curing cycle, as well as, fibre lay-up and fibre content also impacts on void formation (52) (53).

Composite materials exhibits an exclusive class of failure mechanisms, also classified as damage or defects. Some defects are generated during the first stages of manufacturing, others during subsequent manufacturing process and also during life in service. Although the classification and nomenclature may vary, defects like fibre-failure, fibre pull-out, fibre-matrix debonding, matrix cracking and delamination are among the most common. The main characteristic of fibre-matrix debonding is the formation of cracks due to excessive interphase stress. Fibre pull-out occurs as an effect of cracks caused by high stress concentration in fibres, which pull-out fibres from the surrounding matrix. Fibre failure or fracture can occur by different reasons, as transversal impact and compression fatigue cycle. Since fibres are the main constituent, fibre failure has severe impact on composite strength. Matrix cracking is a term used to classify long cracks, usually centred and localized in rich resin zones and are linked to low energy impacts or cycling loadings. Delamination damage is a kind of defect that develops inside composite materials and generates failure, sometimes without visible surface damage. Moreover, delamination has serious consequences in the mechanical properties, reducing material stability and may lead to failure at low loadings (54).

2.3 Machining Process of Composite Materials

Composite parts for aeronautical industries usually are manufactured near to the final shape, which frequently means that a secondary manufacturing is necessary. The most common secondary manufacturing process for composite materials is machining. Machining of composite materials has a few different aims, such as of making holes for attaching or fixing parts to or into, trimming edges for fitting or milling complex shapes on inner area to fit other parts. The use of a cutting process depends mainly of the application for the composite material part. However, machining of composite parts is a complex process, involving material properties and the cutting process generates damage. The phenomenology of fibre and matrix with cutting tool has a high level of variability if compared with other class of materials.

Due to CFRP are anisotropic and have inhomogeneous properties, making those materials highly abrasive and leading to high tool wear rates with high cutting forces and possibly having negative impacts on surface finishing of the work piece. The impacts on surface finishing appears as damages or defects like cracks of matrix, matrix thermal degradation, fibre pull out and delamination (55). For example, the investigation of mineral cutting fluids performance in CFRP showed that its use can aid temperature control during the machining process and reduce of tool wear, as well as with insignificant loss of material properties (56).

Quality of metal machined parts is often evaluated by surface roughness, a component of surface texture. The typical way of measuring roughness of a surface is through a set of parameters that uses the measured profile to indicate quality level quantitatively. There are many parameters, with Ra and Rz being the two most common and used. For example, Ra or average roughness uses the measured profile to calculate the area between the roughness profile and the mean line, while Rz is the calculated average of the five highest peak to valley heights (57).However, measuring surface roughness may not be a precise way for evaluating surface

quality of composite materials machining, with some studies indicating alternative methods to measure surface quality, such as volume crater formation (58).

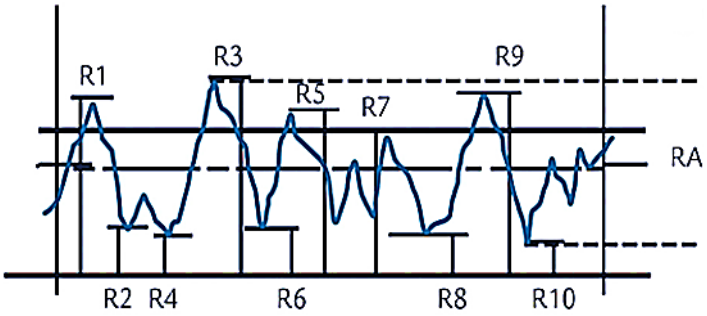

Figure 4 – Example of a theoretical roughness profile showing the parameters of Ra and Rz (59) modified].

A study regarding surface roughness and composite parts quality after trimming was conducted. The analysis of different machining processes to evaluate their impact on mechanical properties of CFRP over quasi-static and tensile fatigue tests. Tool geometries and trimming parameters, such as feed speed and cutting speed were used as influence factors with surface quality and mechanical properties used for the analysis. The results, regarding the same cutting mechanism, showed a strong relationship between the surface quality of the machined part and mechanical resistance. Additionally, different trimming conditions generated similar roughness with different defects, these defects may influence the mechanical behaviour. In this study, the results indicated that surface roughness was not related to fatigue limit, with similar values of Ra having different values of fatigue limits, especially for different trimming processes showing similar fatigue limits, from different Ra values for the same trimming process. The trimmed surfaces by a diamond-cutting tool showed the presence of wrench areas, with the possibility of removing them, by grinding process. However, the wrench area removal does not interfere on the interlaminar shear strength. Thus, the results indicate that using different techniques is possible to obtain the same surface roughness and with different mechanical properties (60).

In order to reinforce composite materials in the Z direction a through thickness reinforcement can be employed to increase material strength in that direction, offering enhancement damage resistance by impact. There are different sorts of 3D reinforcement techniques, like knitting, stitching and z-pinning. The techniques have different ways to perform the reinforcement and provide different mechanical properties, for example stitching uses a needle to carry the yarn throw thickness and z-pinning insert pins of the desired reinforcement throw thickness. A study used Z-pins insertion for reinforcing woven fabric was conducted, the aim was to enhance resistance through thickness to avoid delamination. The test results showed that Z-pin insertion increased material resistance to delamination (61).

The complex set of inputs of machining of composite materials shows how these parameters affect surface finishing and are behind the mechanisms for cutting or fracturing the material in machining, also impacting in chip formation and local mechanical properties. For example, delamination amount is increased with feed rate and cutting speed. While an increase in cutting speed generates smaller chips and reduces delamination frequency, an increase of feed rate is linked to more delamination damages and larger chip thickness (62). Thus, although most of the machining parameters for milling or trimming of composite surfaces are easily calculated, it is essential to understand how these parameters are connected, in order to avoid machine damaging and excessive tool wear. For example, for the same tool, an increase of cutting speed requires a higher spindle speed, which does not influence feed speed but does increases feed per tooth.

Regarding damage caused by machining processes, delamination is one of the most common, it is caused by high loadings during the processing are in direction of thickness, with delamination being one of the most common defects generated by machining (63). The influence of drilling holes distance from the tufting reinforcement on the ultimate strength of

composite materials subjected to quasi-static loading tests was performed (64). The results showed that the tufting located closer to drilling hole have mechanical properties more sensible to the change of drilling tool. The measured roughness indicated that the twist drill had lower roughness values than the core drill. The research showed that the machining process configuration was significant for changing the composite strength.

Machining processes generate damage during the process and measuring surface damage with further characterization of this damage on the composite material have been a challenge. A research investigated the influence of process parameters of trimming in CFRP, specifically cutting and feed speeds, on cutting forces, temperature, tool wear and machining quality. Machining quality was measured by different means and all outputs were analysed. In addition, a new parameter, namely crater volume, is compared to roughness and x-ray tomography images. The tool wear, measured as cutting distance and that means the tool distance covered during a machining process, impacted cutting forces, as well as other variables of influence of cutting and feed speeds. An increase of tool wear or an increase of feed speed also increased cutting forces, while cutting speed increase decreased cutting forces. All temperatures measured are inferior to glass transition and feed speed as the key parameter influencing surface damage. The crater volume parameter seemed to be more representative for the trimming damage characterization. The x-ray tomography also showed that the damage in depth, using the depth of scanning, increases with cutting distance (14).

Regarding properties of a trimmed CFRP plate surface by abrasive water jet, a study investigated the relationship between surface quality and damage induced by the machining process. The CFRP plates made from unidirectional prepreg in autoclave, the abrasive water jet had 4 variables of influence, Jet pressure (4 levels), Jet Transverse Speed (3 levels), Scan Step (3 levels) and Standoff distance (3 levels). After milling process, the specimens were

analysed by profilometre, topography and x-ray topography. Tensile test were performed to study the impact of damage from machining process, with 3 conditions of machining being designated and each condition with different surface quality. The findings shows that jet pressure is the main factor of influence in terms of surface roughness and craters and broken fibres are the most significant form of damage. Tensile tests showed that the finest surface finishing provided the highest tensile strength, however medium and poor surface finishing had insignificant surface quality and significant difference of tensile strength. Crater volume seemed to be significantly related to tensile strength, where specimens with increasing presence of craters having tensile strength reduction (65).

Regarding the interaction between the cutting angle of the machining tool and fibre direction of the composite material, different relative angles may be achieved. The different relative angles between fibre and cutting tool have influence on the cutting mechanism, affecting in surface finishing and thus on damage mechanisms. A numerical and experimental study evaluated the influence of cutting tool and fibre directions, showing that the cutting phenomenon is different for different angles, influencing the sort of damage caused (66). There are many possible different cutting angles, which influences the process of cutting the fibre and matrix and develops different fracture modes. The 4 most common relative angles found in aeronautical structures are shown in Figure 5, each one have a different cutting mechanism for cutting the fibre and it exerts a significant influence on resin fracture. Additionally to relative angle, cutting edges and feed direction senses also influence the cutting mechanism. For example, a large cutting edges causes fibre debonding and small radius cutting process is dominated by crushing fibres (67).

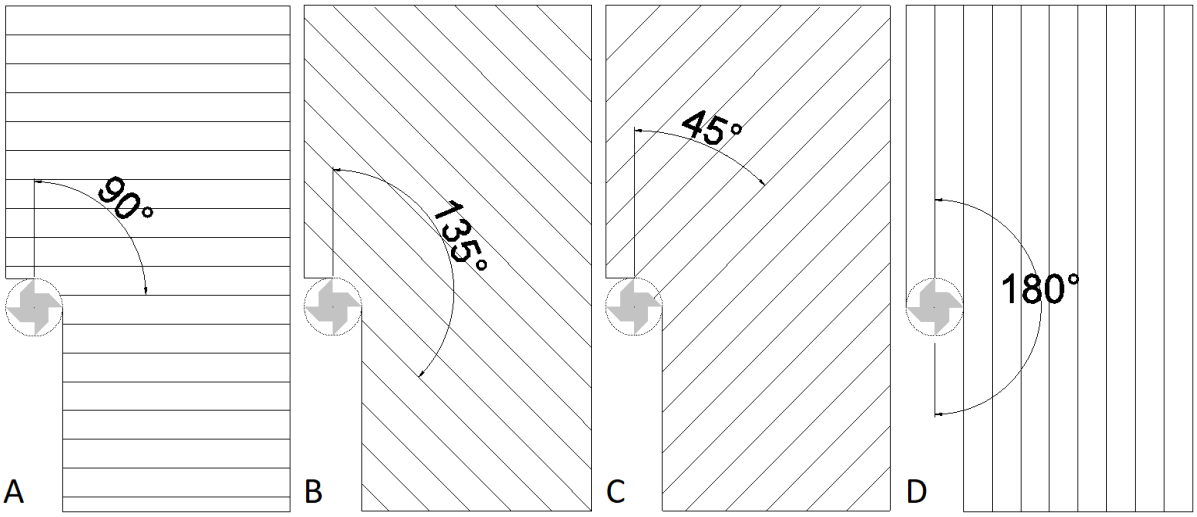

Figure 5 – Different relative angles between the cutting tool feed direction and fibre angle.

2.4 Non-Destructive Testing

Non-destructive testing is a group of techniques of analysis used to detect, locate and assess materials or structures defects or flaws. The defects may be initiated during manufacturing process or caused by corrosion or even by structure loading. The non-destructive testing is by definition a way to detect critical flaws before they have grown to a level that would compromise the component use; this inspection may occur during service life and does not change material properties or cause significant damage (68). There are several NDT techniques, with a range of these techniques used to evaluate damage in composite materials, with passive or active methods and interacting with chemical, electromagnetic or physical spectrum. The most common techniques used in composite materials are visual inspection, ultrasonic inspection, acoustic emission techniques, dielectric techniques, radiography testing, infrared thermography, eddy-current techniques, microwave techniques, shearography, and electron probe imaging (69).

Visual testing is a NDT method that relies on sight, requiring adequate illumination and proper eyesight, recording equipment or lens to enhance visual capabilities. Although common and

sees as simple, this method often involves training and knowledge of product or process. The product material is checked regarding surface, shape, evidence of crack or leaking and internal side defects (70). Examination of internal structure to detect defects and flaws is the main purpose of high frequency waves by radiography testing. The source, x-ray or gamma-ray, emits radiation towards the material and generate images that can be analysed in a screen or film. The radiation that penetrate the material is attenuated by material properties, with denser areas absorbing more radiation and creating the image (71).

Ultrasonic testing is applied to metallic and composite parts and structures in aerospace industry. Usually, the ultrasonic methods check discontinuities inside the material, using a wide range of frequencies, waveforms and techniques. The principle of this technique is based on transmission, reflection, refraction, scattering and other mode changes of mechanical waves inside the material. In aerospace applications the ultrasonic waves, small mechanical disturbance transferring energy through material medium, frequently covers frequencies from 1Mhz to 10 MHz. It is possible to detect delamination, corrosion, porosity and inclusions. The ultrasonic techniques vary, with two being more common. The through-transmission measures sound attenuation caused by a solid, with one transducer emitting and the other receiving the waves. The pulse echo ultrasound uses the pulse reflection, with the same equipment of source receiving the waves (72).

Analysis of infrared thermography is based in areas that shows difference of temperature, cold or hot spots. The temperature of surface material changing is caused by heat flow, this heat flow may have many causes, such as internal defects or flows, voids, disbands, inclusions or heat generation by material failure. Basically, there are passive and active ways of test thermography, with both using an infrared detector to perceive the temperature field distribution of a material surface. Passive thermography uses an infrared camera focused on

the object of study, generating temperature map from thermal image. The active thermography involves heating material surface using an external source of heating and observing the surface with an infrared camera throw time, analysing how the temperature decreases in the material surface (73).

Acoustic Emission may be defined as the transient elastic wave released by a material when there is a sudden change in the material structure, caused by a plastic deformation or crack growth, for example. This rapid redistribution of stress from a localized source on the material also gives the name of the technique of monitoring transient elastic energy signals (74). Acoustic emission technique has been used as a method of NDT for more than 60 years, with the main difference being the capacity of detecting energy release intensity and source without input and in the moment of occurrence, thus being a passive method of monitoring (75).

Since AE technique is a passive method of monitoring, it is necessary to apply a loading for detect the effect, which makes this method particularly useful for mechanical tests for instance. Acoustic emission are ultrasonic signals from 20KHz to 1MHz, with tests being performed, usually, at ranges from 50 KHz to 400KHz. The tests are performed using a piezoelectric transducer (sometimes referred as sensor or probe), the transducer is bolted into surface structure using a coupling substance. A coupling substance is not necessary but desired for many sensors in order to facilitate the signal acquisition and reduce friction (76).

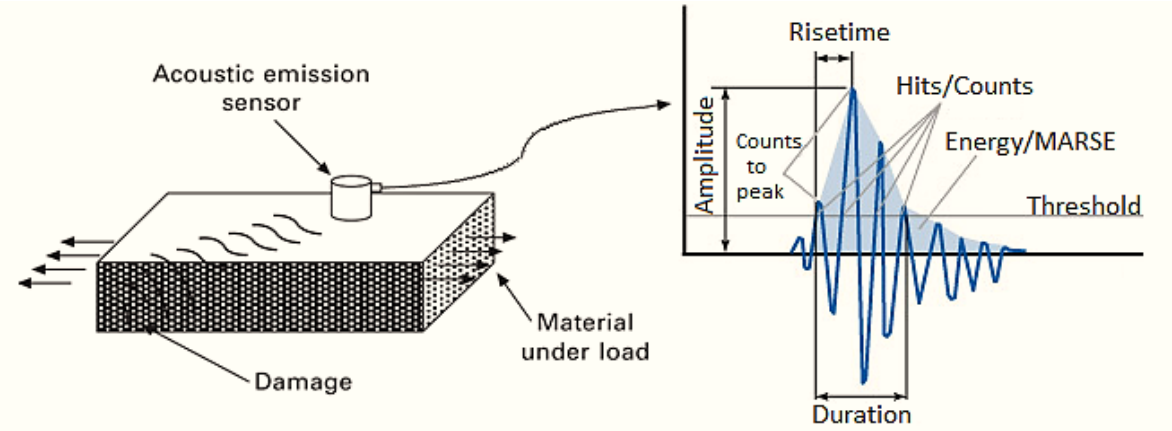

Figure 6 – Acoustic Emission principles (77)adapted].

Regarding AE signal and parameters for analysing waveform (Figure 6), there are a few features or signal characteristics that are extracted from the signal. Beginning with the definition of event, an event starts to be registered any time that occurs a detection of an acoustic emission by a sensor, by way of explanation, an event is detected every time that a signal crosses the threshold. Furthermore, an event may be detected by multiple sensors and times. Thus, every time that an event happens, the wave is recorded with its waveform characteristics, these characteristics are used to distinguish signal from different sources and emission behaviours. The threshold is a setting; it is the minimum level of amplitude that a signal must exceed, in order to be recognized and counted. Thus, each time a signal crosses the threshold, it counts as a hit, and hits is one of the features of an AE signal. Other relevant signal characteristics are amplitude, which is the peak of a signal waveform of an AE event. The feature duration is the time between the first and last threshold crossings. Denominated as risetime, it is the time between the first threshold crossing and the peak of amplitude. Similarly, counts to peak is the number of threshold crossings between the first threshold crossing up to the peak of amplitude. Another signal feature, or signal characteristic, is energy (sometimes referred as MARSE), which is the envelope area under the waveform signal. Energy is particularly sensitive to changes and values of other AE features, specially amplitude and duration (78,79).

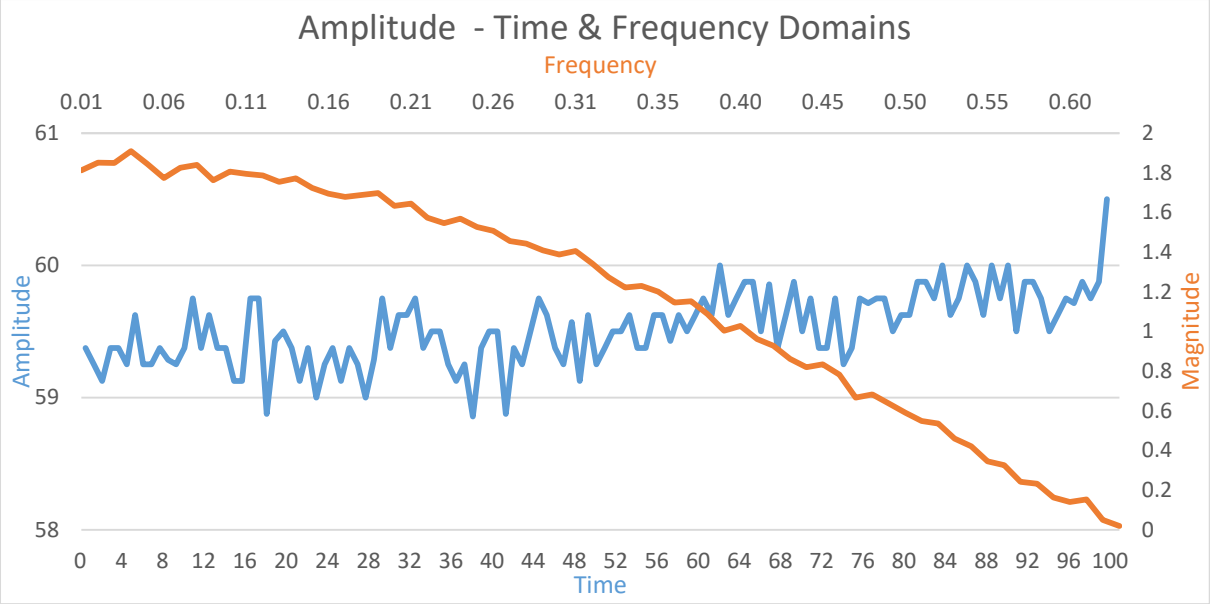

Figure 7 – Example of Time and Frequency domains representation over the same data.

On the subject of data analysis, there are two modes of analysing AE signal data, analysis in time domain or in frequency domain, an example of amplitude data from AE signal is shown at Figure 7. Denominated as time domain, it is a method of analysis of data that relies on time, where the data of an AE signal characteristic is plotted as one axis and time is the other axis, frequently as X and Y axes, respectively. Alternatively, frequency domain is performed using mathematical function over the AE signal feature and is appropriated to analysis that a periodic pattern is expressed. One of the common ways to transform data from time domain to frequency domain is by using Fast Fourier Transform (FFT), converting the AE signal into addition of sinusoidal waves. Thus, the AE signal feature is displayed in one axis and frequency in the other axis, instead of time. Both, time domain and frequency domain, are useful ways to analyse data, in terms of showing patterns, shapes or periodic signals (80).

2.5 Non-Destructive Testing Uses for Damage Analysis

Aeronautic materials and structures must not fail in use, showing resistance in severe conditions. An aeronautic structure failure may lead to aircraft incident fall. Identifying the damage in early stages or avoiding the occurrence of damages during manufacturing processes

is necessary. Methods of monitoring and measuring composite materials damage have been developing, specially by non-destructive testing, significantly about what concerns damages in early stages and damage effects in life cycle of components (81).

Composite materials offer several advantages for industrial applications. However, composite structures are in general costly, which makes non-destructive techniques a useful and often necessary manner to analyse material damage, prevention of premature failure and capable of provide more service life (77). Several techniques have been employed, aiming to detect and monitor damages in early stages.

As the manufacturing process by itself can produce damage in composite materials, several techniques have been employed on the fabrication stages. The ultrasonic inspection is able to evaluate composite cure-state, voids presence, porosity, delamination fibre orientation for example (82). Despite ultrasonic technique reliability, it is not able to monitor process or tests. Acoustic emission is an efficient and consistent method of real-time monitoring material structure. The transient elastic waves are generated by energy release of the material making AE a high sensible, global monitoring and able to be used in any stage of the material life. The evaluation of AE sources and signals are often able to identify damage mechanisms, such as matrix failure, delamination and fibre breakage (83). Similarly to AE, infrared thermography is a NDT able to monitor damage dynamically. Particularly, infrared thermography has been successfully applied for inspection of resin degradation to water presence, disband or delamination or machining induced defects on multi-ply composite materials. The non-need of contact between specimen and NDT equipment allied to the capability of mapping large areas is among infrared thermography advantages (84).

An acoustic emission signal has different features, they help the analysis of identifying the damage with the event. A noise may be considered any sort of residual or undesired signal that

mixes with useful signal, generating interference on processing or interpretation of AE signal. The AE signals are all signals that are directly related to damage mechanisms and aids in damage detection (85).

The damage sources of acoustic emission vary from the kind of material and loading applied, with various forms of damage being subject of study. The plastic deformation of a cutting tool was monitored by acoustic emission, with evaluation of tool wear by the turning process also being monitored. Grinding steel by a carbide tool showed that tool wear and plastic deformation where evaluated indistinctly. The featured AE signal of amplitude increased with tool wear, depth of cut or material rate removal (86).

Investigation of fluid leaks by corrosion in storage tanks are a common industrial application of acoustic emission, for monitoring any initial leak or identifying the leaking location. A study focused on a steel tank above ground leak by corrosion, with monitored by acoustic emission. The results showed that corrosion development has relationship with AE features of counts energy, with increase of these features. Sudden and significant increase of these features indicate macro-crack propagation. Micro-cracking and pitting corrosion are other main causes of AE sources, the signal frequency and duration time are other features that helped on identification of damage type (87).

A theoretical formula was proposed to address energy release, in form of acoustic emission energy for phase transformation of metal. The proposed formula is a refined model of Gibbs thermodynamic potential and used the phase change from martensitic to austenitic to obtain the relationship between stress-induced phase transition and temperature. The formula showed a peak of AE energy release with the initial phase transformation (88). Acoustic emission have been used to identify failure by fatigue for different tests and materials, the high frequency elastic waves are detected from fracture process and then submitted to analysis.

The fatigue crack initiation and growth for metals was investigated by two different studies. The first study proposed a method to investigate crack propagation by theoretical analysis and acoustic emission test. A steel structure was the subject to cyclical loading; the results showed that the theoretical analysis integrated with AE tests can be used in practical engineering cases (89). The second study evaluated the interaction between grain size and acoustic emission energy signal. A NiTi alloy with three different grain sizes was subjected to fatigue tests and monitored by acoustic emission. For all tested conditions, three different stages were found and are related to crack development and the so-called accumulated acoustic energy decreased with grain size. Due to the identification of different stages for different levels of energy by grain size, the results indicate that acoustic emission may be used to monitor cycling damage of practical application of NiTi alloys products (90).

Composite materials have a higher degree of variability of properties if compared with other classes of materials, with AE signals having different behaviour and sources in the occurrence of different damage or defects. Acoustic emission was used for failure criteria of a foot prosthetic made of CFRP during cycling test. The prosthetic foot is designed to substitute a foot, with cycling loading being applied, simulating a walk, it is an appropriate way to test the product service life. The AE failure criteria is compared with displacement criteria and it is based in AE feature signal of hits, with cumulative damage and damage growth instead of only AE hits of damage growth. Common threshold for hit detection proved to be inadequate, both fixed and floating. The findings indicated that when the failure criteria of 10% of displacement is reached, the AE features suddenly rose in 2 up to 4 sub signals. In order to establish similar behavior of AE in comparison with displacement criteria, the study determined that AE featured signal of hits with peak-to-peak threshold showed the best results. Thus, the study concluded that AE and displacement criteria can be interchanged, with AE potentially detecting earlier stages of damage that would lead to failure (91).

Comparative studies of the use of different non-destructive testing show how often these techniques are complementary for each other and that a technique must be careful selected for an appliance. The infrared thermography and ultrasonic techniques were used to evaluate impact damage in composite material. In this study the infrared thermography was unable to detect minor impact damages, while ultrasonic inspection was not just able to identify it, but also able to provide precise level of damage detail (92).

In another study, IF thermography and AE were used to monitor static mechanical testing. The signals of damage mechanisms were collected and used as input for unsupervised pattern recognition, the results indicated a relationship between thermal sources and acoustic emission sources for fibre debonding and fibre pull out. The authors asserted that AE performed better for identify matrix collapse and IF thermography for evaluate debonding and fibre pull-out (93). The NDT detection of defects in composite materials for aeronautics by pulsed thermo analysis has been used in composite materials, being an effective way to characterize the defects.

Damage caused by impact in CFRP panels were used to compare ultrasonic testing and pulsed thermography reliability. Using 35 panels were damage by a low energy impact, the panels thickness varied from 2.6mm to 4.0mm. The ultrasonic testing transmission type immersed the panels under water, while pulsed thermography using a halogen lamp of 1000 W during 3 seconds and observation for 30 seconds. The experimental results were used as input for a probability of detection algorithm. The final analysis shows that infrared pulsed thermography detected smaller defects and was more reliable, indicating that pulsed thermography can be used for aerospace industry as an alternative or complement non-destructive testing (94).

A study explored the possibility of addressing delamination defects on multilayer CFRP using infrared thermography with laser stimulation, since delamination is one of the most common

defects that occurs in CFRP. Experimental tests used a wavelength of 808nm and power of 32W, a FLIR camera was used to record the thermal changes. Additionally, a numerical simulation was conducted using ThermoCalc, the results were used to define experimental tests and an algorithm was used for aiding thermal image processing. To analyse experimental images an algorithm with lock-in function was used, showing that is possible to use this technique of laser heating to analyse thermography of CFRP. The author suggests that laser beam density could be increased and thus enhancing capabilities of detection of deeper defects (95).

2.6 Non-Destructive Testing in Machining Processes

Non-destructive testing has been used in machining process, in general by two points of view. The first is after processing on evaluation of machined parts response to cutting parameters and evaluating the cutting tool wear. The second concerns on monitoring cutting process to evaluate the response of machined surfaces and material properties on machining parameters. A study performed in composite materials during conventional milling used cutting forces and surface quality to evaluate different machining parameters, such as feed and cutting speed, as well as, relative angle. The 3D surface topography and surface roughness indicated an increase of roughness values with cutting speed decrease and feed speed increase. The relative angle has impact in cutting forces; a relative angle of 90 degrees indicated the lowest force values (12).

The milling parameters of a CFRP were analysed using vibration monitoring, aiming to relate damage caused by milling (23). The acquired vibration signals analysis indicated a relationship between vibration and defects and were used to modelling milling parameters for avoiding delamination and resin burnout presence. Thus, the study showed the possibility of using monitoring process in machining to prevent damage formation in CFRP.

The waveform of acoustic emission was used to investigate chip formation of a low cutting speed of metals. In this study, the phenomenology of cutting process is divided in two main mechanisms of cutting, one with continuous chip and the other with discontinuous chip formation. Both process had the same parameters of cutting for testing; the only change was the work-piece material from bronze and copper. Differentiation of discontinuous or continuous chips formation was identified by AE signal analysis and the use of Short-time Fourier transform to analyses AE waveform identified that discontinuities of chip formation coincided with low frequency of AE signals. Thus, the nucleation and propagation of the crack from chip formation generated a low-rise AE burst (96).

Acoustic emission applied to monitor of metal machining use to show a strong relationship with the plastic deformation of the material during the cutting process. Precision and quality are industrial requirements that demand use of reliable way to monitor the process, the outcomes of an ultra-precision turning process of a copper workpiece by diamond tool showed the possibilities of using AE as a way of monitoring quality and precision. Acoustic emission signal was used to analyse crystallographic orientation effect during machining, with AE feature of amplitude showing the effect of material grain structure. The idea is that if cutting parameters are constant, then AE signal is proportional to the energy required to initiate material deformation. Thus, variation of AE signal is caused by slip systems in function of grain orientation. This represented a significant step on using acoustic emission signal analysis towards full automatized manufacturing in terms of quality control (97).

Delamination damage frequently occurs in drilling of CFRP, being a significant concern in aircraft industries since the CFRP panels drilled are common. Delamination may generate fibre peel out and reduce material strength. A study used thermography pulse to evaluate delamination on drilling holes of a CFRP. Using different drilling parameters of spindle speed,

point angle and feed rate. The results were modelled to correlate variables of influence and response, ANOVA statistical method was also used. Among the drilling parameters, point angle is the most significant variable of influence affecting delamination factor. Feed rate increase also increases thrust force, which may leads to delamination. Comparing predicted and measured values showed a significant equivalence between them, indicating that it can be used for evaluate delamination factors of CFRP drilling with confidence level of 97% (98).

The temperature characteristics of a CFRP drilling were recorded by in a high frame frequency camera for a passive infrared thermography method. The study evaluated mainly exit drill temperatures and the interaction of material properties. The findings show that fibre orientation, cutting stage and temperature are related. Temperature analysis of drilling process display that maximum temperature is located at hole center and that tool penetration pushes CFRP without cutting it. The temperature at drill exit relates to phenomenology of cutting process, having unrupted, unremoved and clean-cut regions, with the clean-cut regions having lower temperature by material removal. Fibre orientation and temperature have significant effects on frequency and kind of damage, providing future viewpoints for design and optimization of CFRP drilling process (99).

3. Materials and Methods

The multi-layer composite plate was manufactured using the VARTM processing and the milling process performed by a router-milling machine, both processes were done at NTC laboratory in UNIFEI (Figure 8). The manufacturing process with its variables of influence (input parameters) and the variables of response (output variables) for analysis are described in the subtopics below.

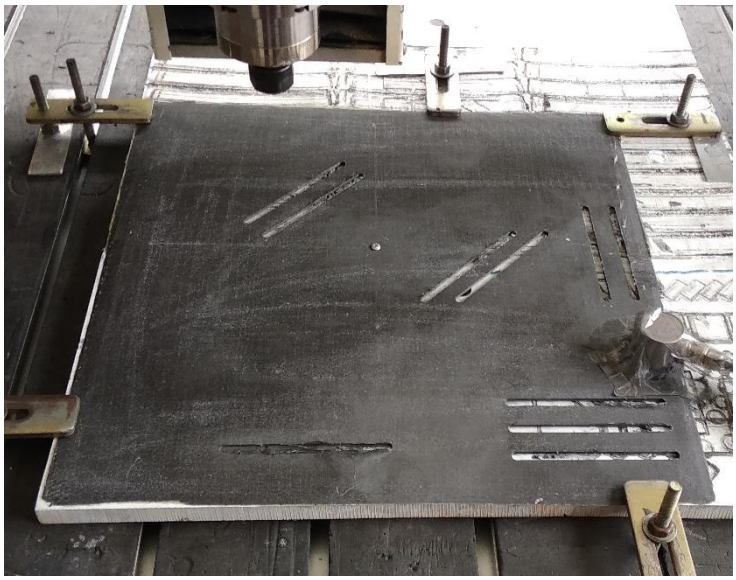

Figure 8 – Machining process of the CFRP plate paused for switching for a new cutting tool.

There are four variables of influence or input parameters: CFRP Layup, Cutting Speed, Tool Condition, and Feed Direction. The CFRP layup has 2 levels, with layup type I as [0/90/45/-45/90/0]s and layup type II as [0/90/0/90/0/90]s. The milling Cutting Speed also has two levels, as 113m/min (A) and 221m/min (B), it is calculated based in the tool diameter and machine RPM. The variable of influence of Tool Condition has two levels, namely New and Worn. The definition of tool New and tool Worn is based on the concept of Cutting Distance, that is explained in subsection of Milling Process. In addition, a tool New is a tool that has a cutting distance of 0 meters and a tool Worn is considered when the tool has reached a cutting distance equal to 1.31 meters. Finally, the input parameter of Feed Direction has three

levels, which are 0°, 45° and 90°. This variable of influence refers at the direction that the milling tool moves towards to and is relative to a fibre direction of 0°.

Regarding variables of response, or output variables, three analyses have been made, in both views of qualitative and quantitative, namely: Analysis of AE Signals, Analysis of Infrared Thermography and Analysis of Surface Quality. First, Acoustic Emission analysis consisted of how the behaviour of the featured signals of Amplitude, Energy, Cumulative Energy, Hits and Cumulative Hits performed through milling process. Secondly, Infrared Thermography allowed the analysis of recorded temperatures during each of the milling processes. Surface Integrity was the object of analysis for quality of the machined surface, roughness profiles and parameters were explored, as well as the surface topography and microscope images of the milled surface.

The variables of influence and response are summarized at Table 1. A full factorial design was done, using randomization of the process, in which three replicas were done for each condition. The aim of the use of statistical design of experiments was to avoid influence of other unknown or undesired variables and to ensure the minimal impact of those unknown factors.

Table 1 – Experimental factors of influence and response analysis

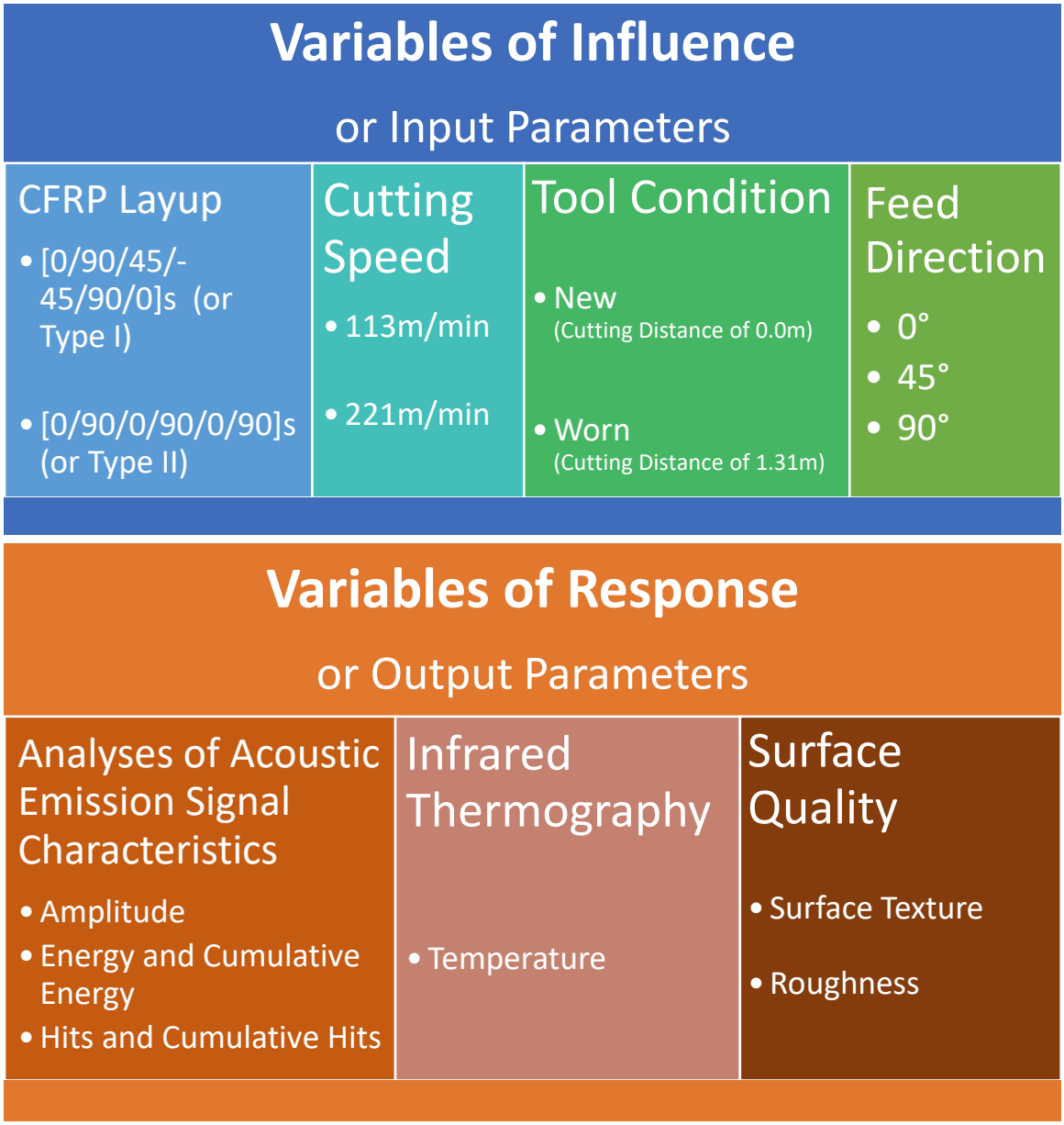

CFRP Plate Processing of Manufacturing

In this research dry unidirectional sheets (142g/m²) of carbon fabrics from Hexcel® (GA045) with epoxy resin Araldite® LY 5052 Resin / Aradur® 5052 Hardener were manufactured using a VaRTM process. The lay-ups are closely related to common sequences used for aeronautic applications and have a total thickness of approximately 2.5±0.3mm, having 12 layers and each layer with approximately 0.21 mm of thickness.

The carbon fibre unidirectional weave tape was cut, in order to deliver a total of 24 square sheets, each sheet having the necessary adjustment for shaping in order to provide the orientations of 0°, 45°, -45° or 90°. The dimensions of each the square sheets, that were manually cut, had approximately 400mmx400mm. The stacking sequences or layups used were: $[0/90/0/90/0/90]_s$ and $[0/90/45/-45/90/0]_s$. The carbon weave sheets were manually placed in metallic mold, with a vacuum bag covering the assembled unidirectional weave layup, there were no air leaks. In sequence, a total of 400 grams of resin mix were pumped through the weave at vacuum pressure. After complete resin infusion, the metallic mold was moved for stating the effective resin cure. The curing process retained vacuum pressure, at room temperature for 20 hours and then moved to an industrial curing oven at temperature of 100℃ for additional 4 hours.

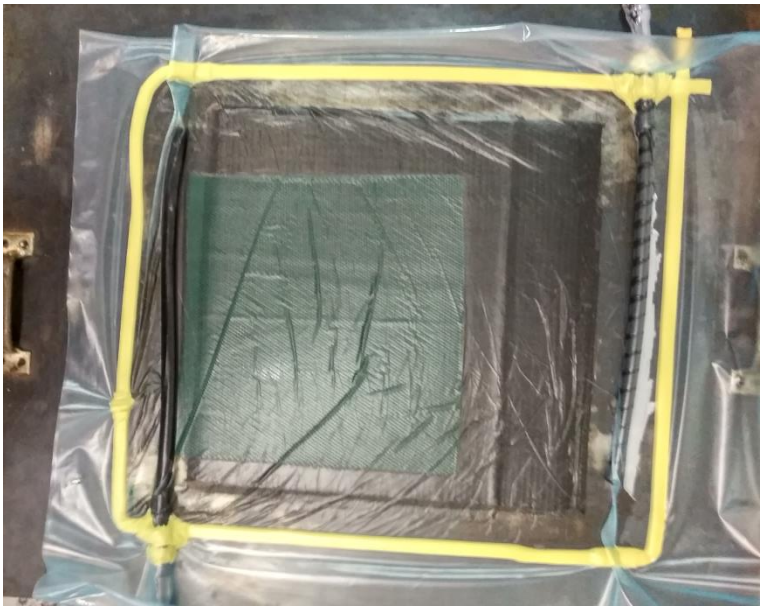

Figure 9 – CFRP manufacturing through VaRTM, before resin infusion.

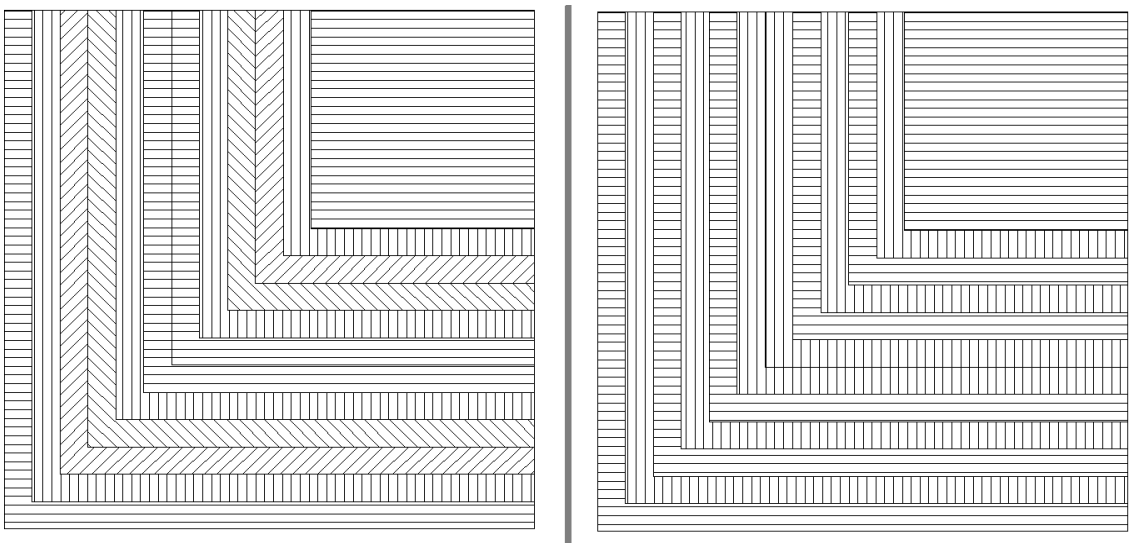

Figure 10 – Schematic illustration of lay-up orientation, $[0/90/45/-45/90/0]_s$ *at left,* $[0/90/0/90/0/90]_s$ *at right.*

Machining Process

The experimental investigation of milling parameters regarding cutting speed, tool wear and relative angle were conducted using end-mill tool. Table 2 summarizes the machining input parameters used. The machining process were carried out in a CNC SHG 1212 Router, the feed speed (or table feed) was set constant and equal to 1000mm/min and the cutting speed varied in two speeds. The spindle speed range is from 60 up to 24000 rpm, leaving a wide range of possible cutting speeds. The choice of spindle speed was based on common below high cutting speeds for aeronautical composite materials cutting and the chosen cutting speeds were 113 m/min and 221m/min. Thus, the spindle speed used were equal to 12000 RPM for a cutting speed of 113m/min and 23450 RPM for the cutting speed of 221m/min. The milling process was performed following a linear shape (Figure 11 at left), in which each of the 6 steps had a total linear cutting distance of approximately 218 mm and axial depth of 0.5mm. Three feed directions, or performed trajectory, were tested, namely 0°, 45° and 90° (Figure 11 at left). These feed directions are in reference to the 0° fibre layer orientation and produced different relative angles, since the fibre orientation varied through thickness. The cutting tool is an end-

mill tool made of carbide with a diameter of 3mm, having 4 helical flutes 9mm long, helix angle equal to 38° and follows the standard DIN 6527 (Figure 11 at right).

As stated before, tools were divided in two conditions: New and Worn. The tool condition as New or Worn follows the principle of cutting distance, which is the total distance that the tool has performed the cutting process. For example, in this work a tool is considered as Worn when the cutting distance reaches 1.31m, which is equivalent to a complete milling cut at Feed Direction of 0°, at Cutting Speed of 113m/min at plate layup [0/90/45/-45/90/0]s. A total of 36 tools were used, for each input parameter and then each tool was later used as worn, again for each input parameter. This value of cutting distance considers the entire perimeter of the machined area and is equal to sum of each axial step depth. Additionally, the end-mill overall design and material are appropriated for machining process of aeronautical composite materials.

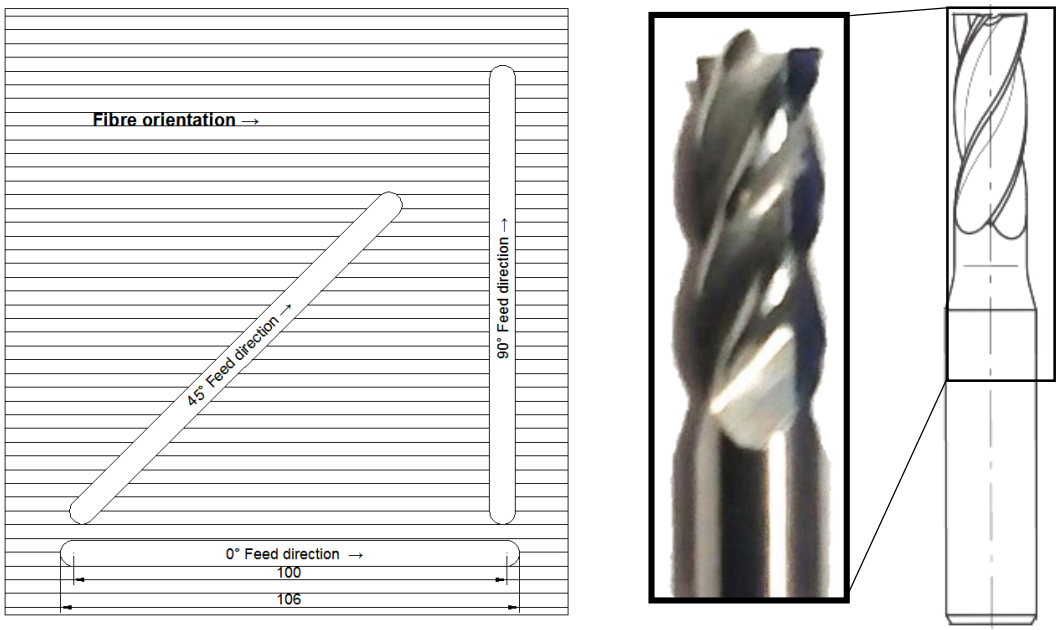

Figure 11 – Schematic view showing the milling positions with feed direction (left) and Carbide cutting tool DIN 6527 (right).

Table 2 – Input parameters used for milling the CFRP plate.

Input Parameters	**Values**

Cutting Speed (vc)	$113m/min$ – $221m/min$
Spindle Speed (n)	12000 min^{-1}– 23450min^{-1}
Feed per Tooth (f)	$0.02mm/t$ – $0.01mm/t$
Feed Speed (vf)	$1000mm/min$
Tool Condition	New – Worn
Cutting Distance	$0m$ – $1.31m$
Tool Diameter $\emptyset$	$3mm$
Number of Teeth (z)	4
Axial Step Depth	$0.5mm$

Monitoring

An acoustic emission sensor bolted directed in the CFRP plate using a gel-based, namely Ultragel ULTRA® from Multigel, coupling phase monitored milling operations (Figure 12). Previous tests showed that the sensor location was not significant for change signal acquisition. It was an expected result, since the plate dimensions are small compared to other applications of acoustic emission, such as leak detection in pressure pipe.

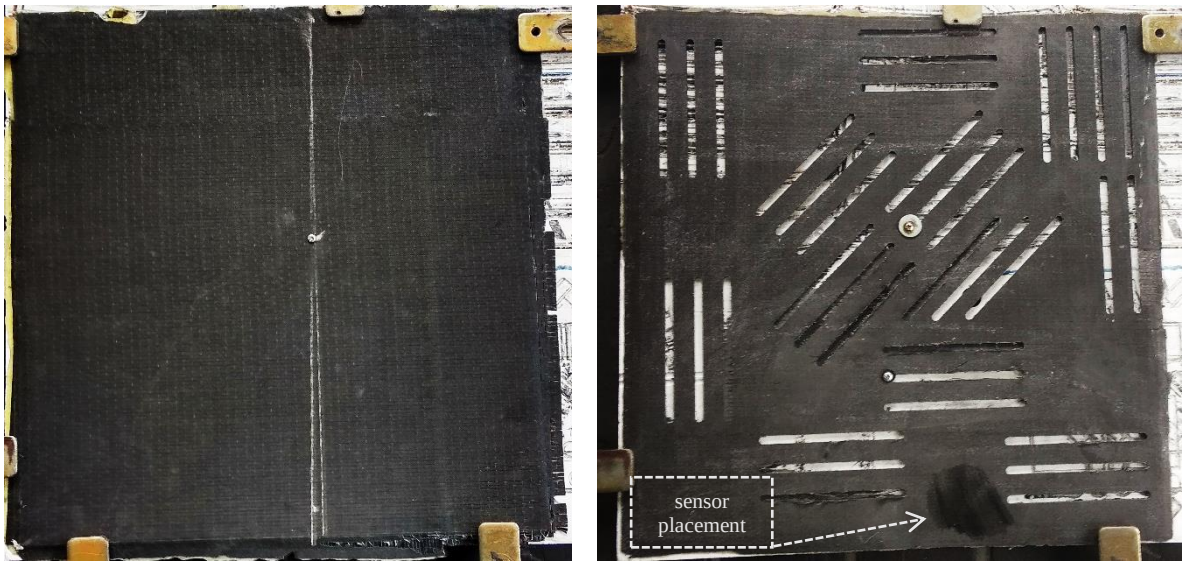

Figure 12 –Plate before and after milling process, $[0/90/0/90/0/90]_s$ *lay-up.*

A Physical Acoustics Sensor ModelR151I-AST was used; it has an integrated preamplifier with gain of 40dB and frequency range from 50 kHz to 400 kHz. The acquisition device is a PCI multichannel board of 18 bit 40MS/sec, the whole equipment is manufactured by Mistras Group and it is setup in a dedicated desktop computer. Mistras Group qualifies the system with a high speed and resolution, a low noise, which is recommended for research purposes. For data processing and post analysis the AEWin Post software was used, it allows reviewing the data, applying additional filters, generation of charts and statistical analysis of data. The filter used in this research intended to avoid signal from machine vibration and dust/chip formation, with a setup of 40 dB (Figure 13). After signal acquiring, an AEWin Post signal treatment was used, it had an aim to clarify the featured signal, pondering the burst of signals by location and filtering weak waves (Figure 14). The AE signal was analysed regarding signal characteristics, with analyses in time and frequency domain being performed as complementary to each other. Additionally, statistical analysis of AE signal features data were done, using basic summary of statistics, which includes the largest observation and the smallest observation of replica samples.

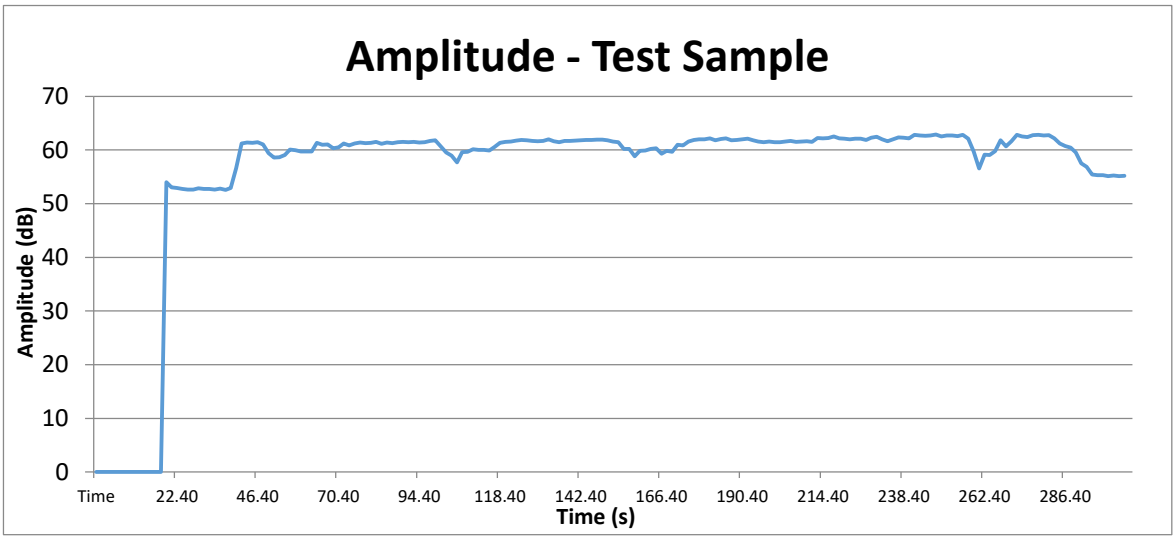

Figure 13 – Test sample without threshold.

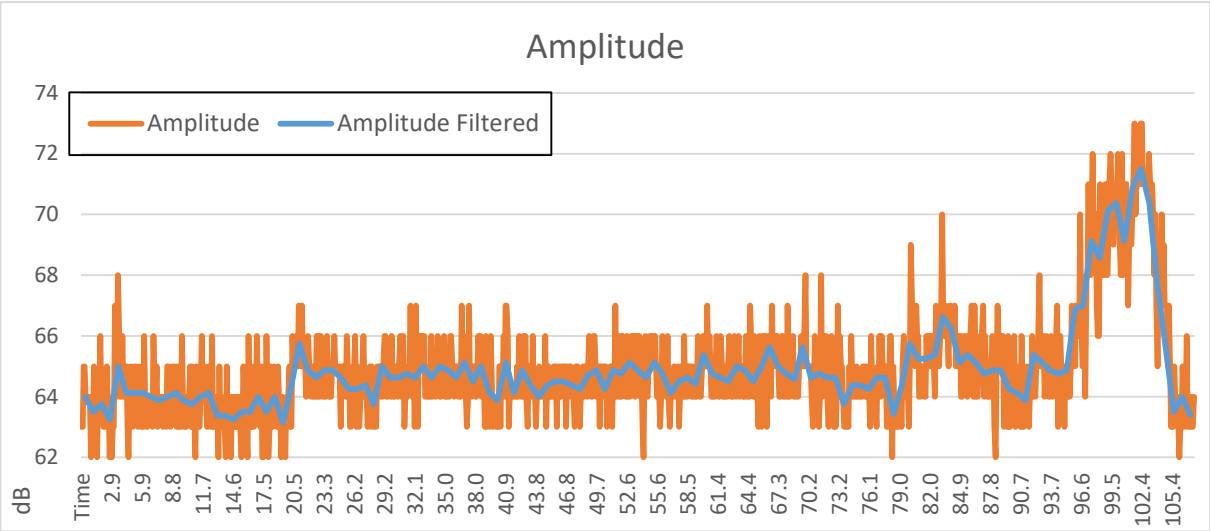

Figure 14 – Amplitude feature filtered before and after treatment for test samples.

The temperature was monitored using an infrared camera FLIR E30, which was placed at a distance of approximately 1 meter from the cutting tool and plate contact, with manual movement to follow the cutting path. All the process was recorded in video to allow further analyses. The camera has a thermal sensitivity of 0.1℃ degrees and a temperature range of -20℃ to 250℃, capable of register more than 25000 points of temperature. The camera is able to adapt the colour range according to the temperatures and to focus in a point, which is the centre of the target (Figure 15). In this case, the camera was pointed at surface regarded as the boundary region of the tool and workpiece as shown in Figure 15.

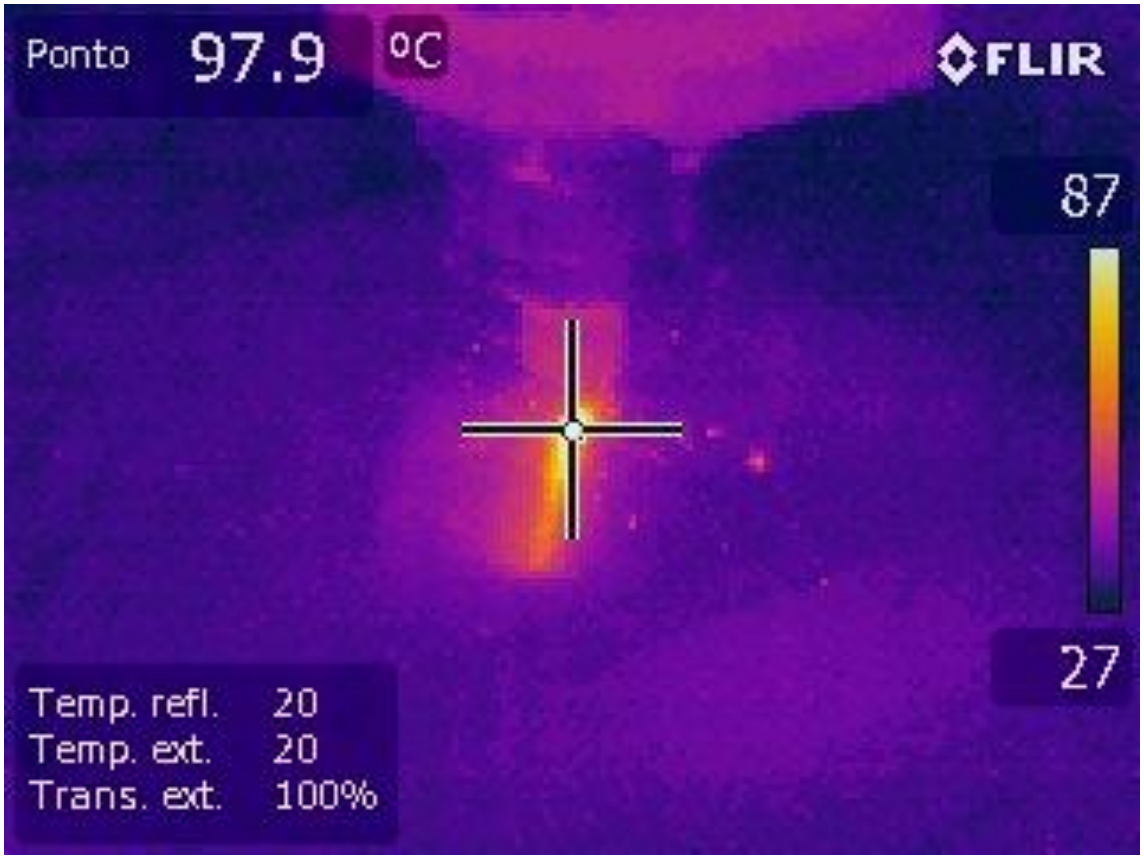

Figure 15 – Infrared FLIR E30 camera screen during milling cutting.

Machined Surface quality

The quality of the machined surface was evaluated using digital microscope and rugosimeter. The digital microscope camera, Dino-Lite Microscope, has a magnification of more than 200X and allows measurements over the HD pictures. A 3D optical measurement equipment, Alicona Infinite Focus, captured images and created 3D surface profiles roughness, providing the combination of images and roughness measurements of scanned areas. It also provided topography, roughness of areas or lines (Figure 16A). The surface roughness was measured by system Mitutoyo tester model SURFTEST SJ-500, which is able to plot the surface profile as data for later processing, with profile and values of Ra and Rz being recorded for each replica in different positions, namely A, B and C (Figure 16B). The position A is located the cutting process has started, with B being the intermediate area and C the last milled section.

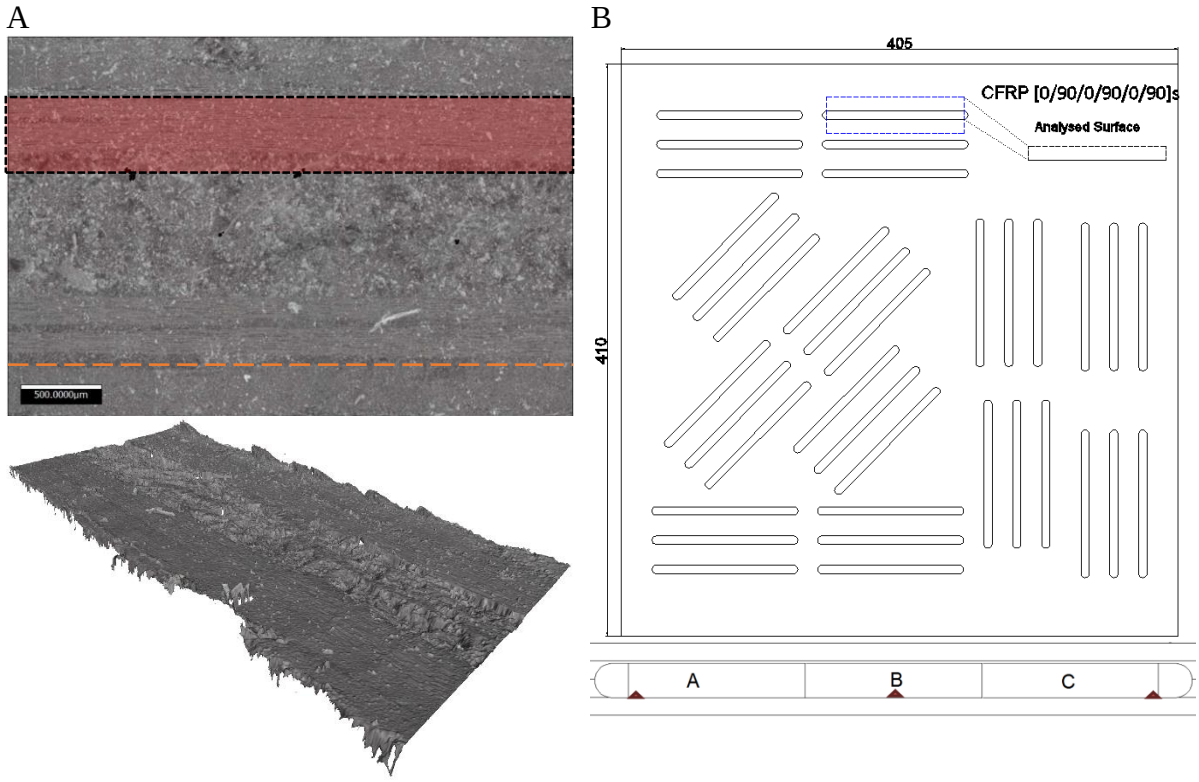

Figure 16 – A) Scanned surface areas, with roughness profiles by areas (red) and lines (orange), topography (down); B) Schematic view of roughness measurements areas (up) and positions (down).

4. Results and Discussion

Temperature

The statistical analysis was based on ANOVA, in which the maximum temperatures were evaluated by variables of influence. The Analysis of Variance showed that cutting speed and tool wear have significant impact on temperature, as shown in Figure 17.

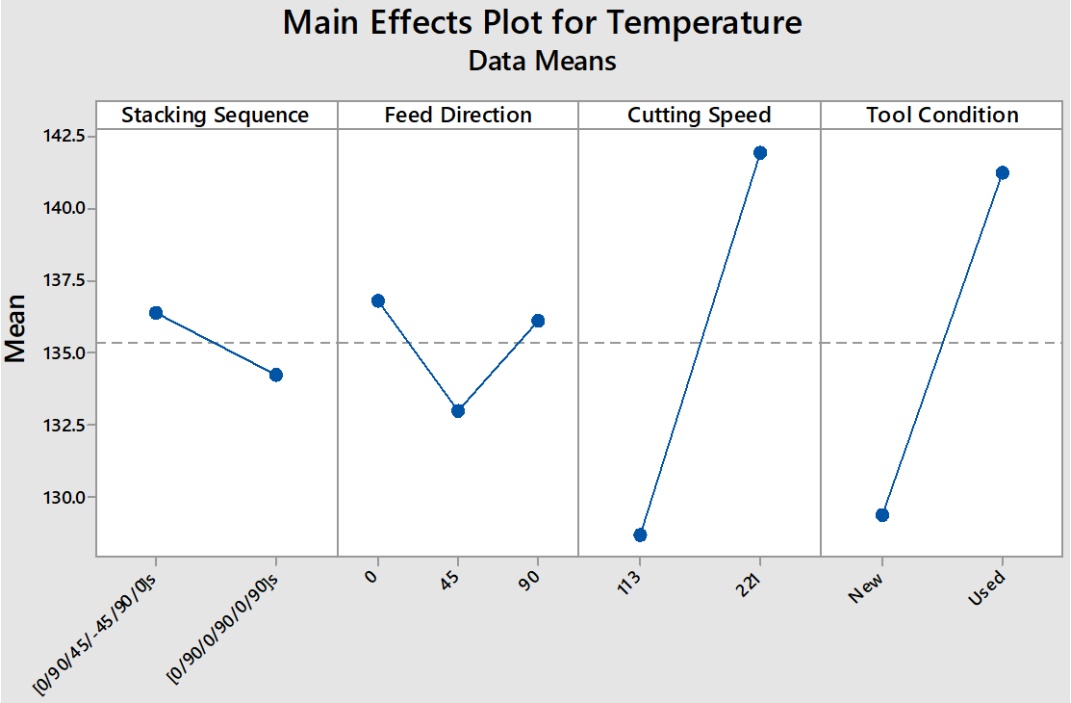

Figure 17 – Main effects for maximum temperature during the milling process.

Regarding feed direction, the 45 degrees feed direction showed a lower temperature than feed directions of 0 and 90 degrees, with the comparison between 0 and 90 degrees showing insignificant (p-value<0.05) difference of temperature. The cutting speed and condition showed higher influence in temperature, with the increase in cutting speed or tool wear leading to higher maximum temperatures of machining. A variation of cutting speed added to a constant feed speed means a variation of feed per tooth, which doubled from 0.02mm/t to 0.01mm/t for the cutting speed of 113m/min and 221m/min, respectively. The findings, similar to other studies, indicating that tool wear and cutting speed have a significant influence in temperature

during machining process (21) (100). On the stacking sequence, the layup plate of $[0/90/45/-45/90/0]_s$, showed a slight higher temperature, a difference of less than 3 degrees Celsius during machining. The plate layup and feed direction are close related, since they determine the relative angles of the cutting process and it is the main factor of influence for the machining phenomenon. Considering that feed direction of 45 degrees offers a different relative cutting angle if compared with 0 and 90 degrees, especially if considering the stacking sequence variation, this change may be responsible for the lower temperature. For the stacking sequence of $[0/90/0/90/0/90]_s$ the relative angle is equal to ± 45 degrees, while for $[0/90/45/-45/90/0]_s$ the relative angle varied from 0, ± 45 and 90 degrees. The maximum recorded temperatures, regardless of replica or condition, are below matrix degradation, since overall maximum temperature was 171℃.

The development of temperature during milling process is showed in Figure 18, as the highest temperature during each axial step depth and regarding each variable of influence. The values are the mean of the three replicas and consider the highest temperature reached during one axial step depth. Regarding Figure 18, firstly, it is possible to observe that although machining processes start with tool and workpiece at room temperature of around 25~30 Celsius degrees, before reaching end of the first axial step depth, the temperature for any analysed condition is already higher than 90℃. Secondly, as the process goes through it has a further increase in temperature to up to an approximately stable stage in this higher temperature. The stable stage temperature varies according to machining conditions, but were kept higher than 105℃. Additionally, this approximately stable stage of temperature is maintained during most of the process, at the end of milling, which coincides with the last axial step of depth the samples presented a decrease in temperature, to values near 100℃.

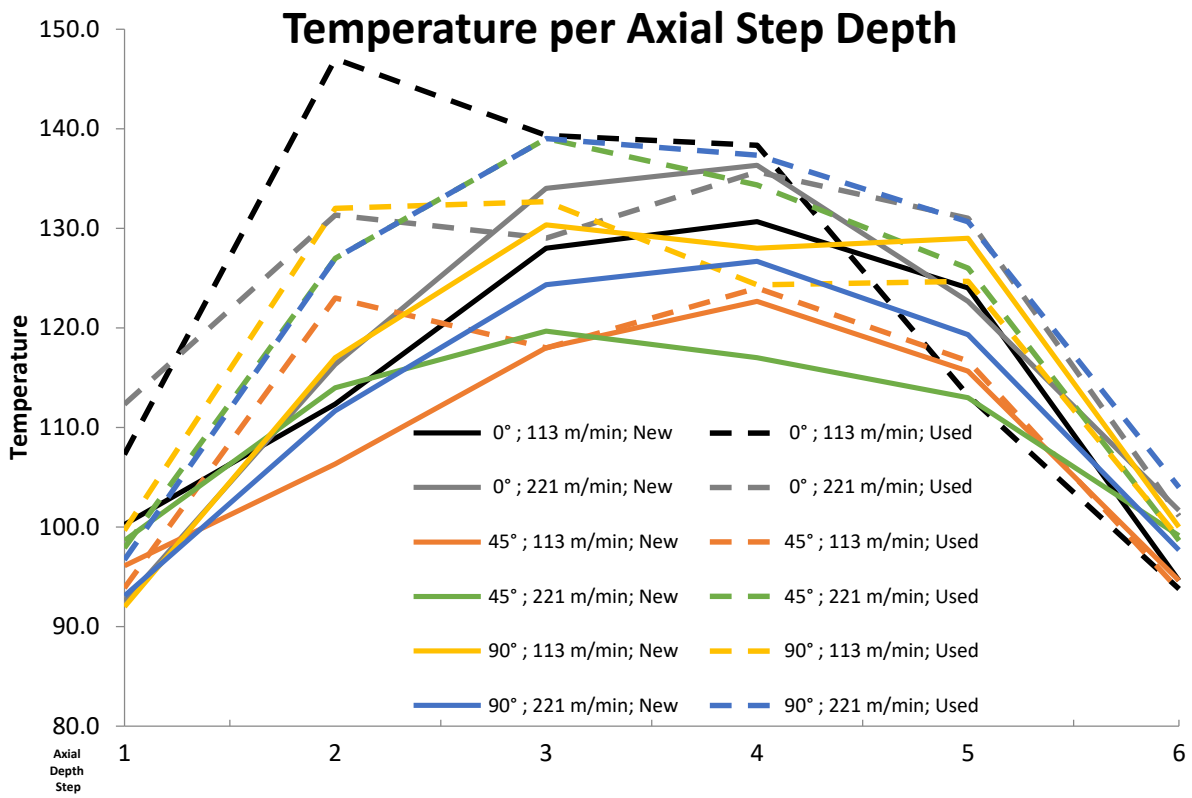

Figure 18 – Average highest temperature for the three replicas, developed during each axial depth step for $[0/90/0/90/0/90]_s$ *lay-up, regarding Feed Direction, Cutting Speed and Tool Condition.*

The effect of temperature variation between begin-middle-final stages, is especially explored for the final step of milling. The decrease in temperature at the final stage may be related to thickness variation and plate misalignment. Considering that, the axial depth step is $0.5mm$ and the attachment of 400x400mm size VaRTM plate on a router table, VaRTM is a process that commonly causes minor thickness variation, then it is plausible establish this relationship. Moreover, the infrared video recordings of the machining process show that the final step has less chip formation and material removal, with some samples showing no cutting in the last axial step at all. Also, the infrared thermography recordings shows that chip formation is composed mainly by dust of low temperature, a result of its low heat dissipation capacity. The findings in this study agree with previous other findings, in which higher cutting speeds impacted in tool life, increasing tool wear (101). The results showed higher temperatures, mainly on the combination of tool wear and higher cutting speed samples.

Surface Finishing

The surface of CFRP plates, post milling, were evaluated in terms of visible damage, topography and roughness, regarding the impacts of each of the variables of influence. Using two different digital microscope cameras in this analysis, it aimed the evaluation of milling surface defects on the specimens, employing a minimum magnification of 34.1 times. It was found that samples with feed direction of 0°, tool New and cutting speed of 133m/min have a small number of defects, mainly due to mechanical degradation (Figure 19A). The tool wear effect is showed in Figure 19B, since the same cutting speed and feed direction of Figure 19A were used. Thus, the tool wear seems being the main cause of interlaminar delamination and fibre pullout. Similarly, at Figure 19C with cutting speed increased to 221 m/min (other variables of influence were maintained) caused interlaminar delamination and matrix smearing.

The changes in feed direction to 45° and 90°, with cutting speed of 133m/min and tool New have also impacted the surface quality. The 45° feed direction (Figure 19D) showed a larger amount of mechanic degradation areas and fibre pullout. The feed direction of 90° (Figure 19E) showed the presence of fibre pullout, matrix smearing and interlaminar delamination, with less damage caused by mechanic degradation. These results show how variables of influence had impact in surface finishing, with variation of the type of damage according to feed direction, cutting speed and tool wear for the same stacking sequence of $[0/90/0/90/0/90]_s$.

A – Feed Direction 0°, Cutting speed of 113 m/min, Tool Condition New.

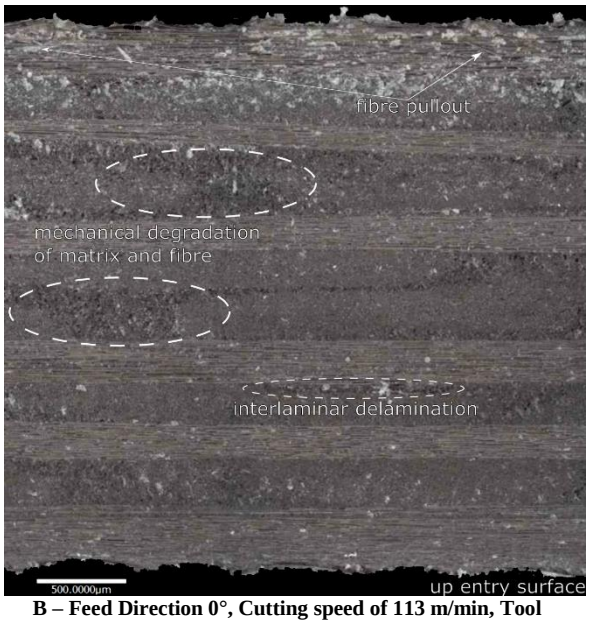

B – Feed Direction 0°, Cutting speed of 113 m/min, Tool Condition Used.

C – Feed Direction 0°, Cutting speed of 221 m/min, Tool Condition New.

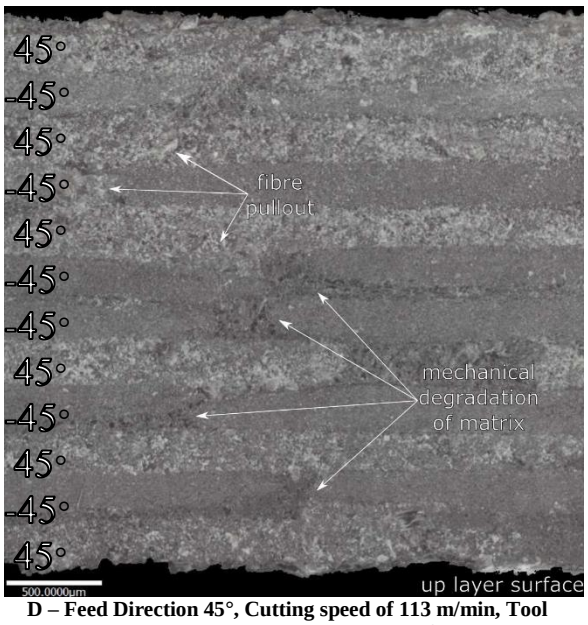

D – Feed Direction 45°, Cutting speed of 113 m/min, Tool Condition New. The relative angles between feed direction and fibre orientation are at the left.

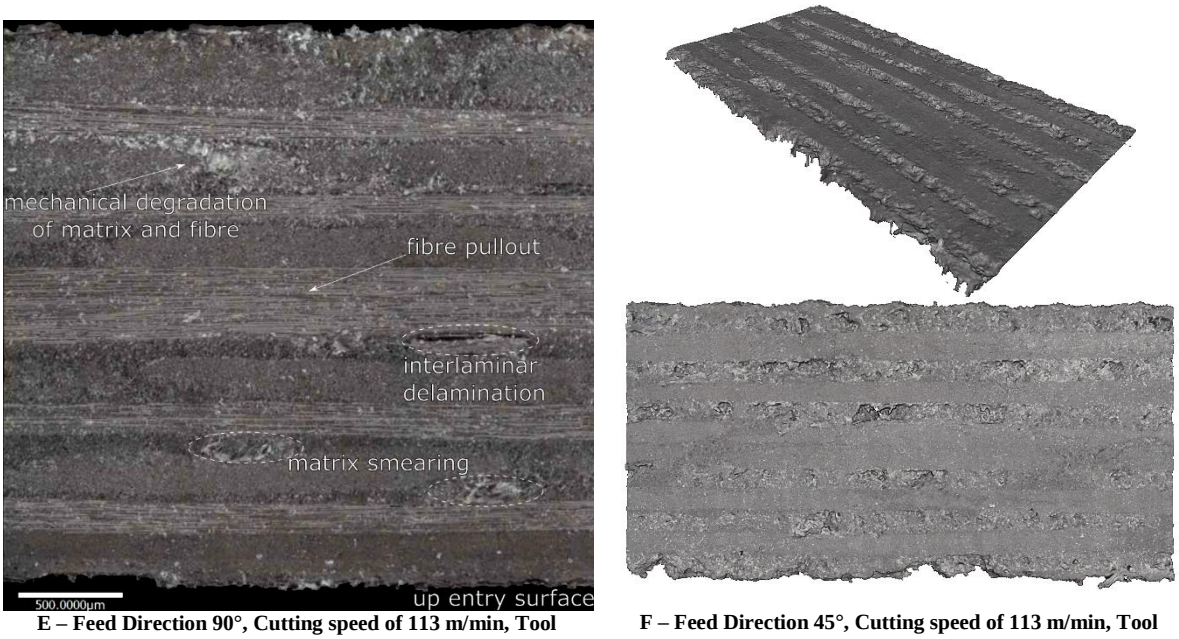

E – Feed Direction 90°, Cutting speed of 113 m/min, Tool Condition New.

F – Feed Direction 45°, Cutting speed of 113 m/min, Tool Condition New.

Figure 19 –Digital microscope observations of the milled surface using different parameters and stacking sequence of $[0/90/0/90/0/90]_s$.

The feed direction variation offered different relative angles regarding the fibre orientation, especially the 45° feed direction (Figure 19D and F). Visually, there is difference between the relative angles caused by feed direction and fibre alignment, with -45° relative angle having brighter and flatter surfaces, 45°relative angles having darker surface finishing with presence of significant areas of deep craters, as indicated by relative angles in Figure 14D. As expected, the feed direction as variable of influence combined with fibre alignment affects surface finishing (102).

A topographical analysis also shows the impact of the relative angle between feed directions in surface finishing. The topography of the machined surfaces, regarding feed direction of 45° and layup of $[0/90/0/90/0/90]_s$, for both tool conditions allows the analysis of tool wear and is shown at Figure 20. In order to distinguish clearer the topographical differences, two height sub-ranges were employed, at Figure 20 left the height sub-range is between $40\mu m$ and $-40\mu m$, at the right is from $100\mu m$ to $-300\mu m$. Following the analysis, in Figure 20A, the presence of black areas indicate deep damage, confirmed by Figure 20B showing that depth is

approximately 100μm. These areas are present for relative angle of 45° and for entry/exit surfaces. Tool wear impacts surface finishing, increasing presence of damaged areas, as seem in Figure 20C and D, which were cut with tool worn having a cutting distance of 1.31m. In addition, the last axial steps, at image top area, show more damaged areas, it is also being related to tool wear.

Regarding surface topography and microscope images, it seems that the main mechanism related to poor surface finishing is due relative angle, followed by tool wear. Surface finishing containing damaged areas in the depth are related to worse mechanical properties (103).

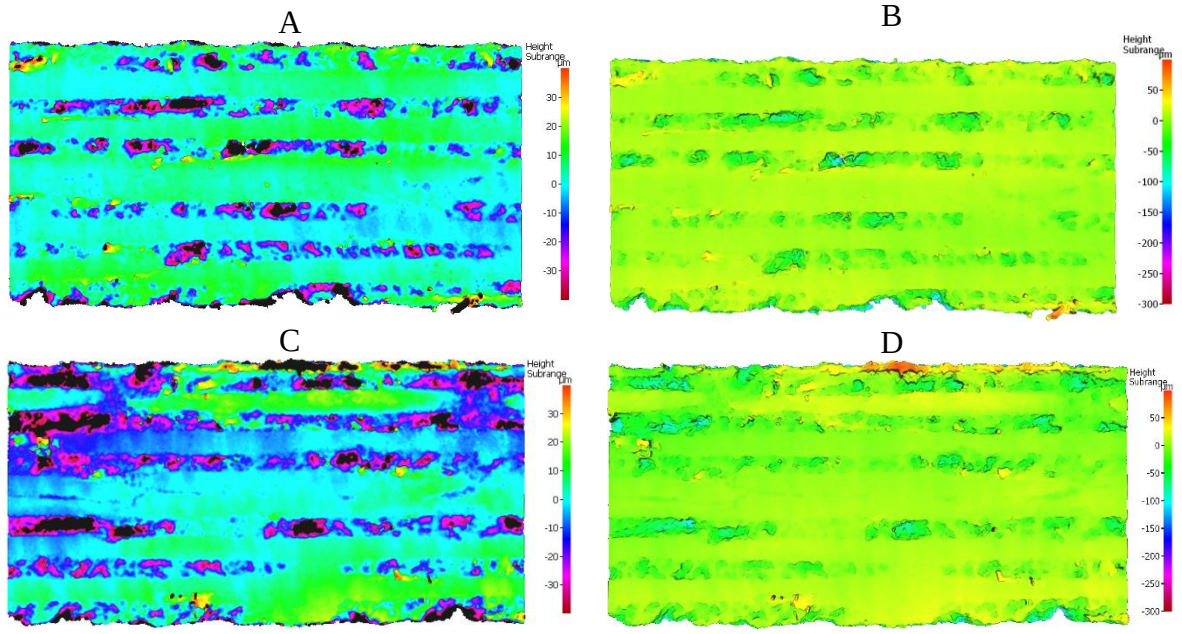

Figure 20 – Topography of machined surfaces with feed direction of 45°, cutting speed 113 m/min and stacking sequence of $[0/90/0/90/0/90]_s$*. A and B new cutting length of 0m and C and D cutting length of 1.31m.*

The plate configuration of $[0/90/45/-45/90/0]_s$ showed the occurrence of non-cut fibres on up layer, or fluffing, specifically for samples with feed direction of 45° as shown in Figure 21, these defects are not similar to defects of plate $[0/90/0/90/0/90]_s$. Figure 22 exhibits in details the delamination of the non-cut fibres in two different positions of the sample, the length of the fluffing defect is close to the specimen width. Similar fluffing defects with less intensity are observed on other replicas with varied cutting speed and tool condition, but same feed

direction and around the same plate area. Thus, these defects may be a result of the synergy of all these factors, since higher cutting speeds and tool wear produced more defects with longer lengths (104). Moreover, specifically this replica had its bottom layer not machined, regardless the axial step depths for all replicas being the same. It may be result of VaRTM process, as pointed before, this process causes thickness variation and resin concentration on certain locations of the plates, especially significant for high precision post process like machining.

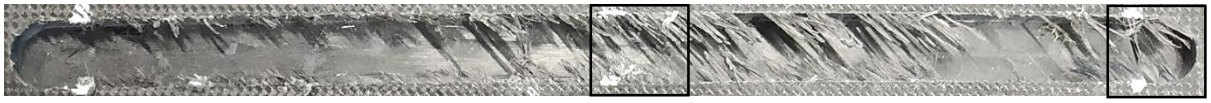

Figure 21 – Defects caused by the milling process for $[0/90/45/-45/90/0]_s$ *plate, 45° of feed direction, with cutting speed of 221m/min and worn tool, black squares indicating right end and central zones.*

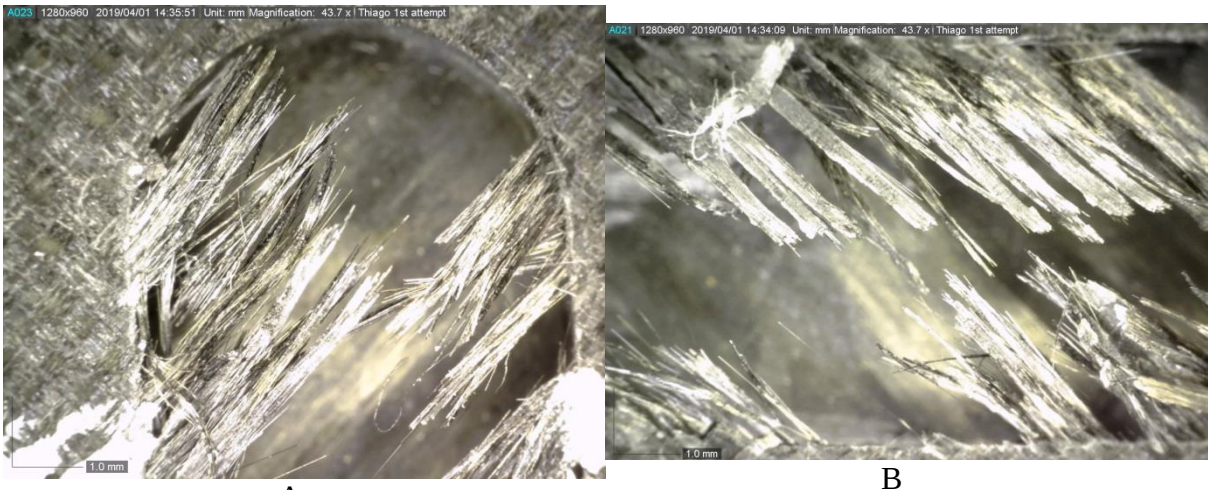

A B

Figure 22 – Surface defects after milling process with Magnification of 43.7X, for $[0/90/45/-45/90/0]_s$ *stacking sequence, 45° of feed direction, with cutting speed of 221m/min and used tool; A) Right end zone; B) Central zone.*

Regarding only stacking sequence variation, in this case from $[0/90/0/90/0/90]_s$ to $[0/90/45/-45/90/0]_s$, Figure 23, generated a different surface finishing for all tested conditions. Comparing Figure 19 and Figure 23, there are more visible damage caused by machining process, this damage presents deeper craters and volume of voids.

Comparing conditions for the same stacking sequence, the feed direction also impacted surface quality, Figure 23E and F show the topography of 0° and 45° feed directions. The feed direction

of 0° has a smoother topography and all height sub range inside the range of -40µm to 40µm, with worse quality located in the fibres of 45° and -45°. The feed direction of 45° shows a centred are with deeper craters beyond the height sub range, concentrated on fibre directions of 0° and 90°. Compared to stacking sequence of $[0/90/0/90/0/90]_s$, the feed direction of 45° presented more and deeper craters. All these analyses show the major impact of relative angle on mechanisms of the cutting and types of defects during milling processes. Furthermore, regarding tool condition, the comparison between Figure 23 A and B shows the effect of a tool worn, causing significant more damage and impacting negatively the surface finishing of the composite plate.

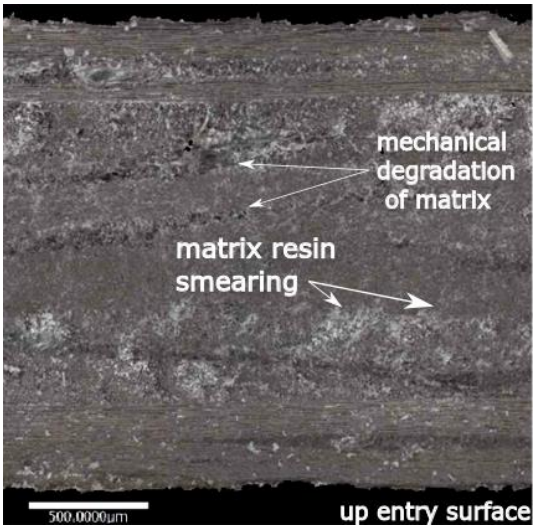

A – Feed Direction 0°, Cutting speed of 113 m/min, Tool Condition New.

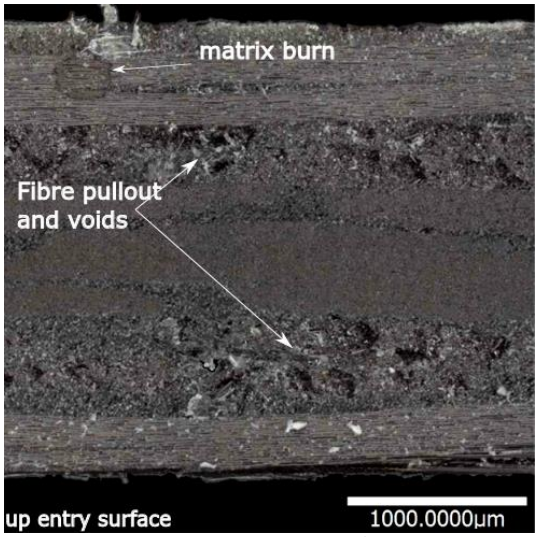

B – Feed Direction 0°, Cutting speed of 113 m/min, Tool Condition Used.

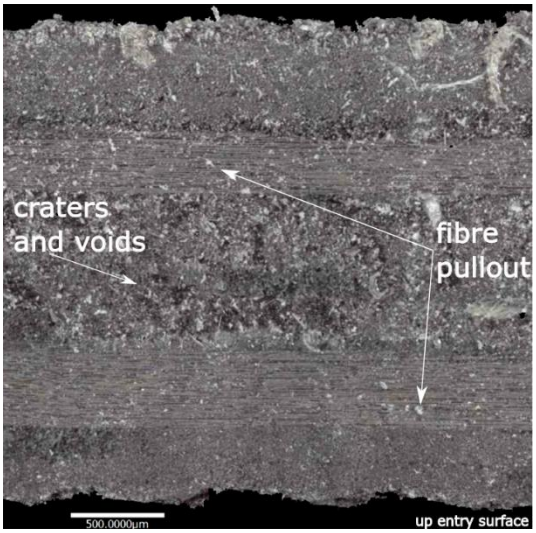

C – Feed Direction 45°, Cutting speed of 113 m/min, Tool Condition New.

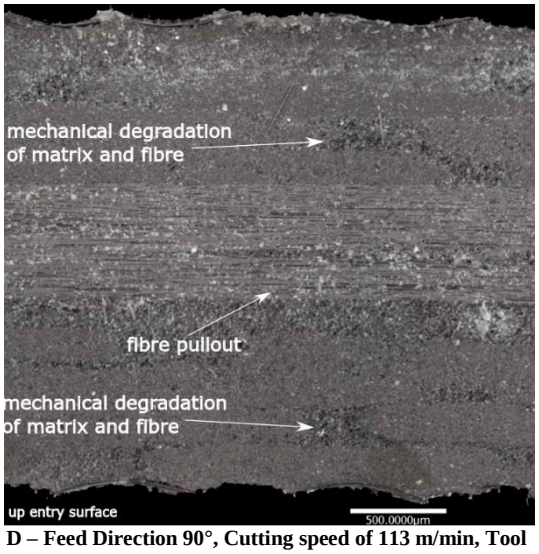

D – Feed Direction 90°, Cutting speed of 113 m/min, Tool Condition New.

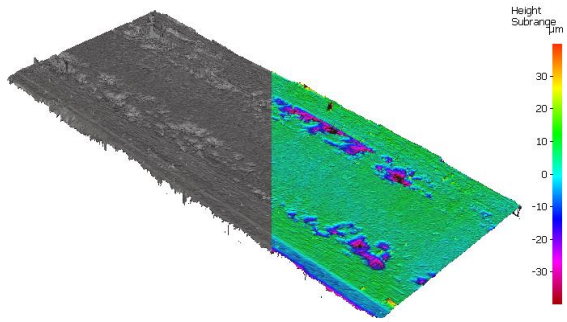

E – Feed Direction 0°, Cutting speed of 113 m/min, Tool Condition New

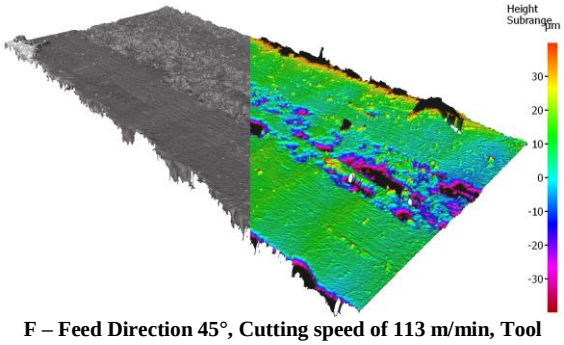

F – Feed Direction 45°, Cutting speed of 113 m/min, Tool Condition New

Figure 23 – Digital microscope observations of the milled surface using different parameters and stacking sequence of $[0/90/45/-45/90/0]_s$.

These results shows the high level of influence due to relative angle between feed direction and fibre direction. Figure 24 shows the different relative angles between fibre directions and the feed direction of 45°, the relative angles are similar for different feed and fibre directions. The mechanisms of cutting are different, causing different effects on surface finishing, as is possible to conclude by microscope images.

The relative angle of 45° and -45° (or 135°) is shown at Figure 19F. The fibre direction of 45° and feed direction of 0°, as in Figure 24A, tends to generate fibre pull-out and thus having deeper craters due to material pull while the fibre direction of -45° for the same 0° feed direction (Figure 24B) has a smoother topography and surface finishing less defective. Relative angle of 90°, Figure 24D, has a smooth topography and dark surface, thanks to perpendicular cut, generating a good surface finishing and small amount of defects. Finally, relative angle of 0°, Figure 24C, are perpendicular to fibre direction, having a bright surface and smooth topography. However, due to micro misalignment, not all the fibres are completely 0° oriented through all the length, originating pull-out defects in significant scale.

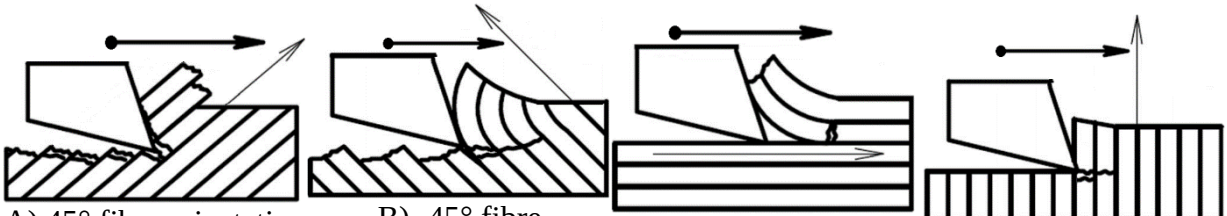

A) 45° fibre orientation
45° of relative angle

B) -45° fibre orientation
-45° of relative angle

C) 0° fibre orientation
0° of relative angle

D)90° fibre orientation
90° of relative angle

Figure 24 – Relative angle variation for feed direction of 45 degrees for different fibre orientations.

Regarding surface roughness though thickness, the machined surface was analysed in different positions, as shown by highlighted areas in Figure 16B. With an aim of evaluating the effect of tool wear, the results of surface finishing for surface roughness shows that feed direction, cutting speed, feed per tooth and tool wear have impact on roughness. In this method of evaluation, the feed direction of 45° as the highest Ra and Rz, with 0° and 90° having no significant difference. In terms of cutting speed and tool wear, an increasing cutting speed and cutting length increases roughness.

The comparative of roughness profile heights for Figure 25 and Figure 26 had a measurement length equal to 2.5mm (two measurements of 1.25mm), with a total of 12500 points, a Gaussian filter and a cut-off (Lc) of 0.8mm. The comparative of the normalized roughness profiles shows that from the position A to position C, there is a significant change in roughness height due to tool wear. The axis distance is measured from the top of the machined specimen, showing also that top profile having lower values of roughness due to shorter cutting distance (tool wear).

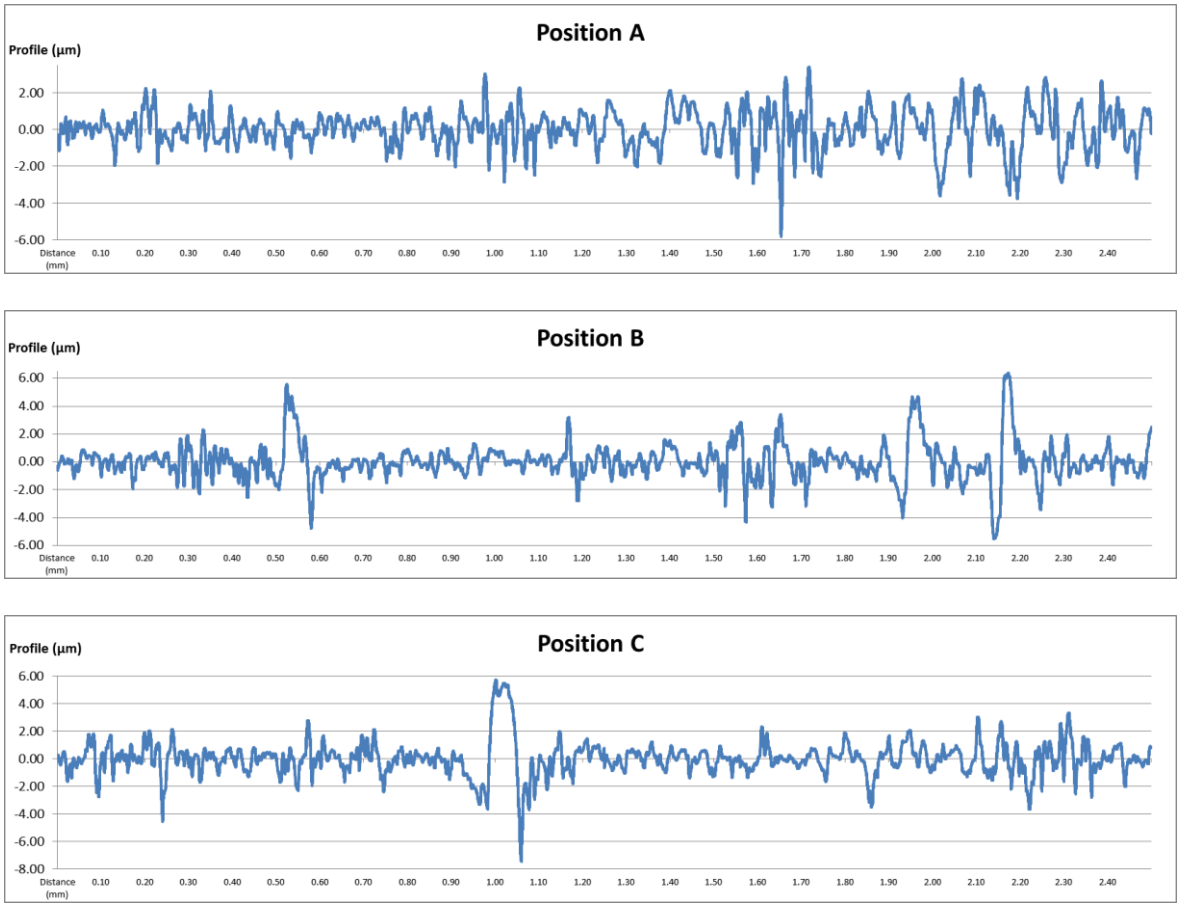

Figure 25 –Roughness profile height for different positions, cutting speed of 113 m/min, feed direction of 90°, tool new and stacking sequence of $[0/90/0/90/0/90]_s$.

Linear roughness profile heights also showed that surface finishing has significant changes with feed direction, as the comparative of Figure 25 and Figure 26 shows. The feed direction of 45° has deeper valleys and upper peaks, with cutting speed having more impact than tool wear. Additionally, comparing the feed per tooth variation of 0.02mm (cutting speed of 113m/min) to 0.01mm (221m/min), position C in Figure 25 and Figure 26 respectively, it seems that a higher feed per tooth speed provides a general smoother surface, if the valleys and peaks are not to take in account. The variables of influence have impacts in surface finishing, with digital microscope images and roughness describing this influence. Although it is possible to obtain the surface roughness by different processes and thus having different impacts on mechanical behaviour, as emphasised before, for the same process a higher roughness may indicate damage presence (Figure 20) and poorer mechanical properties (22).

Figure 26 – Comparison of different conditions for roughness profiles with feed direction of 45° ($[0/90/0/90/0/90]_s$ lay-up).

Regarding the results of surface roughness and microscope images, there is a relationship between the variables of influence and the surface finishing. The variables of influence have impacted the surface roughness and are related to results from microscope images. For example, the tool wear have increased the surface roughness and surface defects of feed direction of 45°, which has higher Ra, worse surface quality and deep craters. The results of

surface quality coinciding with steps and feed direction agrees, showing increasing of roughness with tool wear (Figure 27). The sections simulating five steps are drawn in Figure 27, with white lines indicating areas with approximately 0.5mm of height, as an axial depth step (called by step). These areas contains 125 profile lines, where the roughness was measured and the Ra values used in the analysis are the average of three replicas for each condition. The areas inside green outlines were excluded from this roughness analysis. These areas contain surfaces that are entry and exit of the tool, irregular though thickness areas and have different mechanisms acting, thus it would interfere in the results with imprecision. The entry and exit areas, at the up and bottom layers are more subject to defects and discontinuities, for example, this affects the average results of profile straight lines.

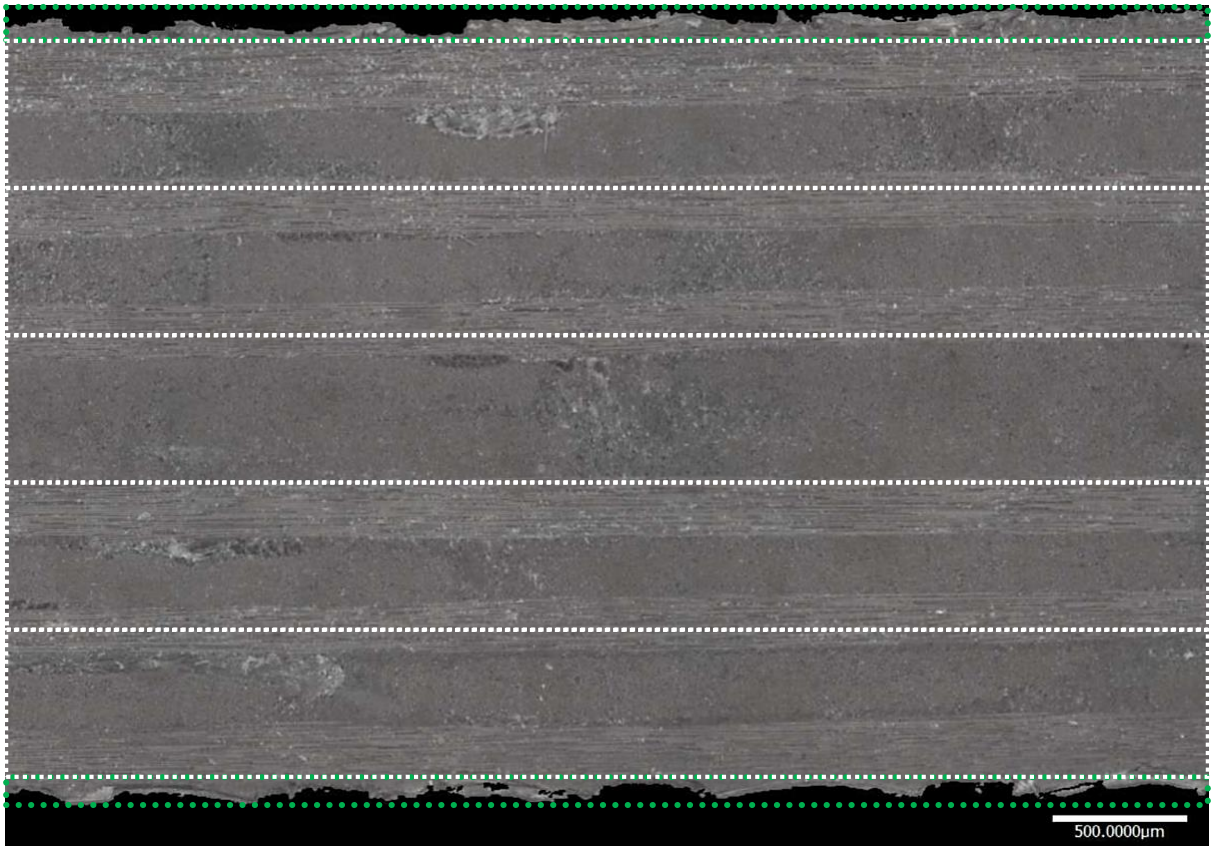

Figure 27 – Surface analysis of roughness profiles divided in areas equal to 0.5mm of depth.

Analysing the profile areas with relation to variables of influence shows the significant influence of tool wear, with increasing of average Ra roughness related to axial depth steps,

represented by Areas at Figure 28 and Figure 29. The results show that an increase in cutting speed leaded to higher surface finishing quality, with reduced roughness (Ra) values (Figure 28). This relationship between higher cutting speed and lower Ra is valid when comparing results for the same feed direction, since feed direction is also a significant factor of influence for the cutting process phenomenology. Regarding Figure 23 and Figure 29 is possible to observe the impacts of feed direction in surface quality, supporting that different feed directions have different mechanisms of cutting. The results also indicate that Ra values increases from Area 1 to Area 5, due to tool wear and that areas near the edge (which corresponds to axial step depths 5 and 6) have the highest Ra values. Regarding the results for feed direction of 45° (the feed direction that has the worst surface quality) at Figure 29, Ra values starts with 1.48μm, increasing quickly to stable value of Ra 3.5μm and finishing the cutting process with Ra equal to 5.6 μm at step 5. Thus, tool wear seems to reach a certain stage, which increases roughness rapidly, up to 3 times higher values than at the step 1, this affects negatively surface quality.

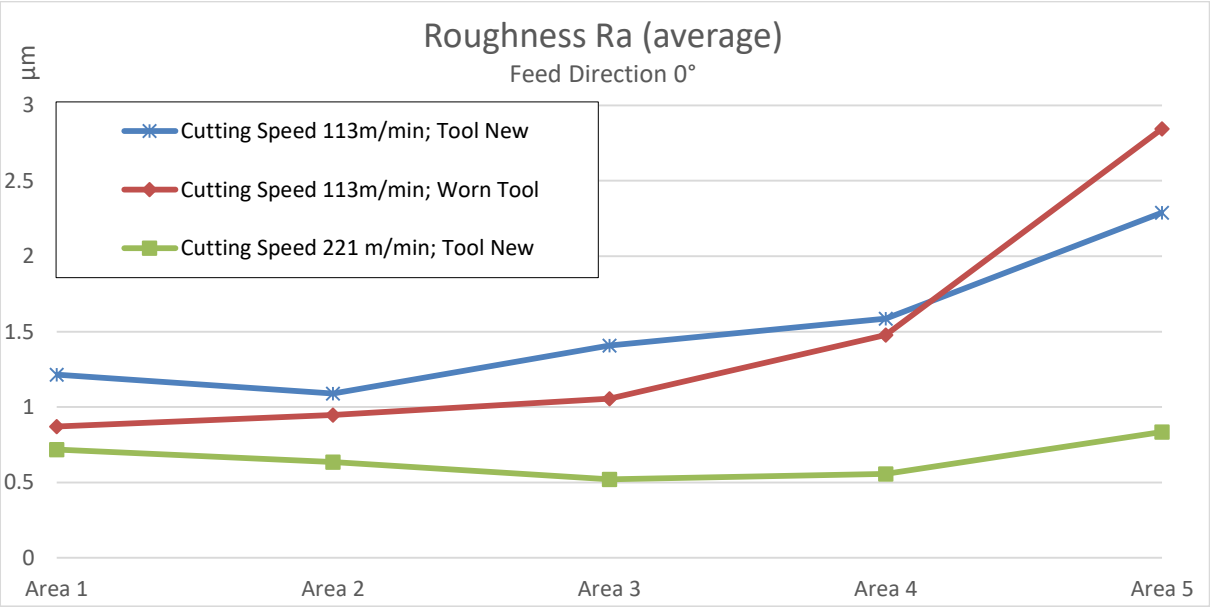

Figure 28 – Average Roughness Ra for same feed direction with variation of cutting speed and tool wear (stacking sequence of $[0/90/0/90/0/90]_s$*).*

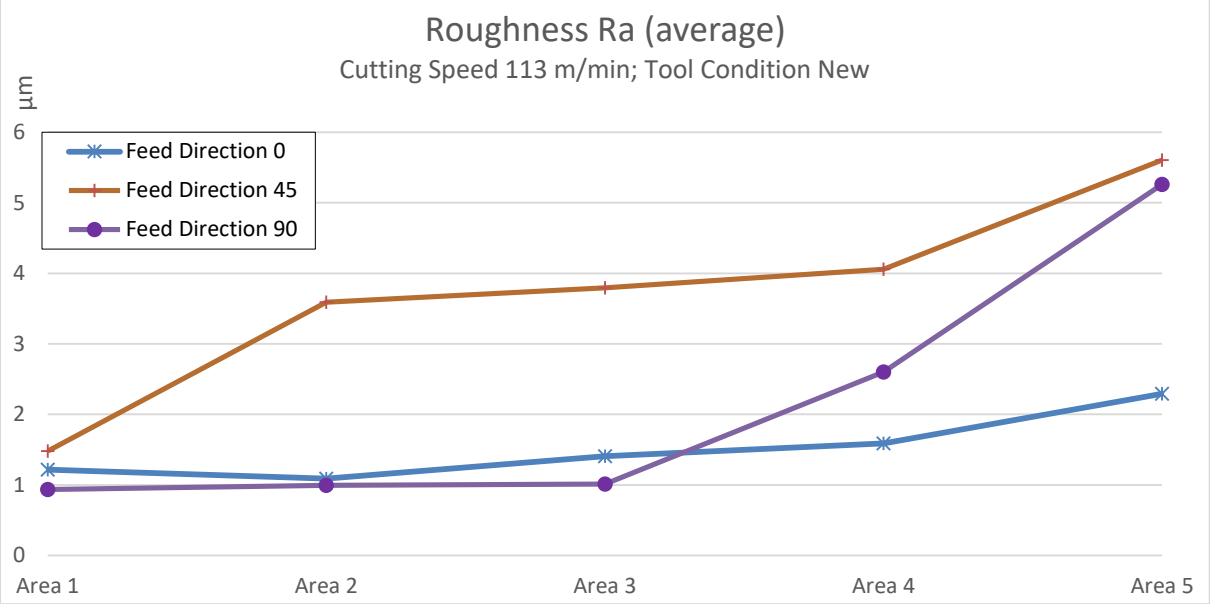

Figure 29 – Average Roughness Ra for different feed direction, same cutting speed and tool wear (stacking sequence of $[0/90/0/90/0/90]_s$).

Acoustic Emission

The acoustic emission signals were analysed as a function of time and frequency, in terms of its commonly studied features, namely: Amplitude, Hits, and Energy. The milling operations took around 100 seconds, with 11 changes of feed direction and some of these feed direction inversions occurs with axial depth step. The characteristic signal of Hits (Figure 30) showed a significant relationship with the cutting path, regardless of the variables of influence. The red light lines, connecting the valleys to time axis, indicate the feed direction turns. The time between feed direction changes vary from 9.6s to 10.4s for each cycle of axial depth step, this 0.8 seconds delay is related to axial depth step that happens during feed inversion.

The feature of Hits in acoustic emission can be applied to show AE activity, since Hits counting are recorded for each time a signal crosses the threshold. In this case, the Hits feature shows a clearer relationship with the cutting path, since the signal feature only changes when the feed direction varies or the process stops/beings.

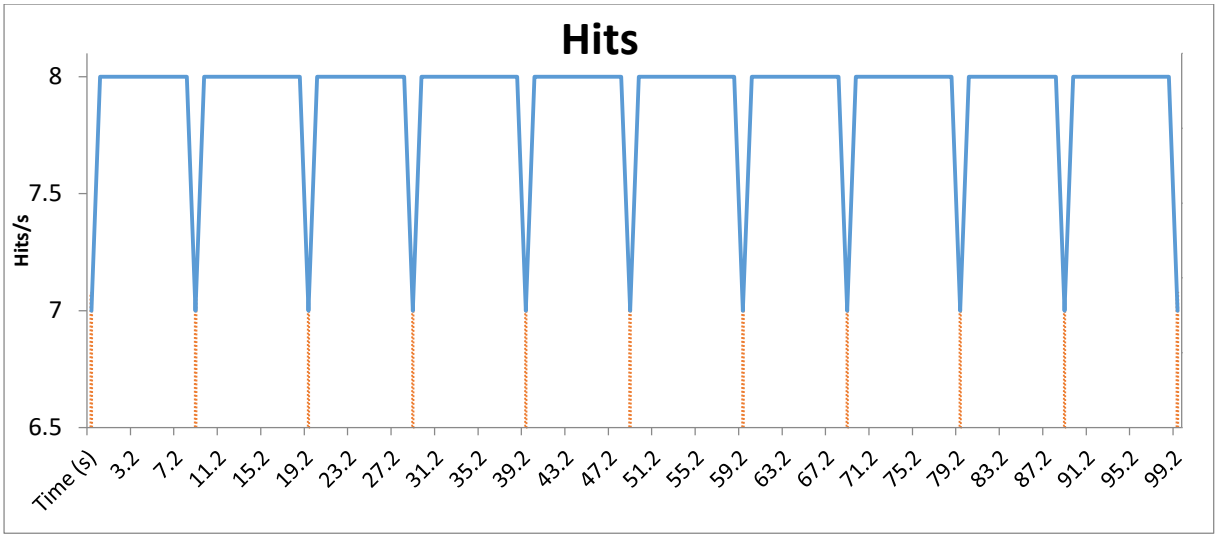

Figure 30 – AE signal of Hits by time with pattern related to cutting path, the valleys indicate feed direction inversion. Sample with: Feed Direction of 45°, Cutting Speed of 113 m/min and New Tool.

In order to analyse AE hits in frequency domain, instead of time domain, a Fast Fourier Transform was performed as using Excel and it is shown in Figure 31. The FFT of hits shows the magnitude of different cycles during the same machining process of Figure 30, in which the most significant cycle is at 10s (0.1Hz), with magnitude of 0.35. The frequency with highest magnitude is between the two cycles observed in time domain that repeats at 9.6s and 10.4s, which in frequency domain are represented by frequencies of 0.095Hz and 0.105Hz, or cycles of 10.5s and 9.5s, having high magnitude. Additionally, there are two frequencies that seems relevant, with cycles of nearly 3.2s (0.305Hz) and 1.03s (0.97Hz), both having similar magnitudes of 0.15. The first one correspond to the changings occurring during feed inversions during machining process, which takes 3 seconds to conclude, and the second is about the steps during the feed inversion. For example, while a feed inversion takes approximately 3s to conclude, it has a sudden decrease (1s), a bottom reach (1s) and is followed by a re-increase (1s) of hits per second and with 3s in total. Thus, the analyses of hits concerning time and frequency domains show similarity, with both being related to cutting path events, in which the most significant is response to the feed direction inversions occurring during the process.

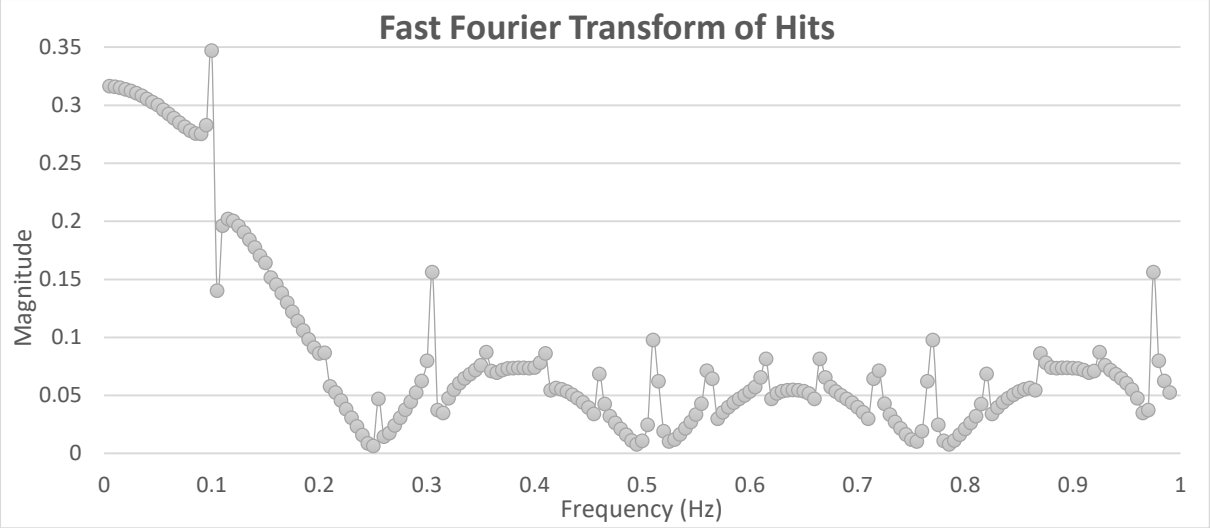

Figure 31 – Acoustic Emission Hits per second in frequency domain.

Figure 32 shows the Amplitude of an AE signal, it seems more sensible to cutting path than hits feature signals, as there is no pattern variation of the dB signals through the cutting path. The amplitude of the AE signal represents the highest voltage acquired for a waveform, thus the experiments show that the behaviour of the amplitude feature is not clearly related to feed turn direction nor axial step depth for time domain. However, it is possible to perceive an increase in the amplitude through time, which may be caused by tool wear. Regarding characteristic amplitude of AE signal in frequency domain (Figure 33), the magnitude of the signal decreases with frequency, has only one peak near 0.04Hz (25s cycle). This peak has similar magnitude to adjacent points and does not allow further conclusions about the behaviour of amplitude AE feature, showing that for time and frequency domain there is no clear relationship between cutting path and the signal characteristic. Since the magnitude of frequencies also decay with higher frequency, it reinforces the idea that a periodic pattern is not present for AE signal characteristic of amplitude. Similarly, the AE signal feature of energy showed no relevant frequency peak, with the highest magnitude of 79 being near to 0.06Hz (16.7s cycle) and then with frequency magnitude decaying as frequency time increases. Thus, it is possible to assert that with the current result analyses there is no evidence of periodic pattern for energy AE signal characteristic.

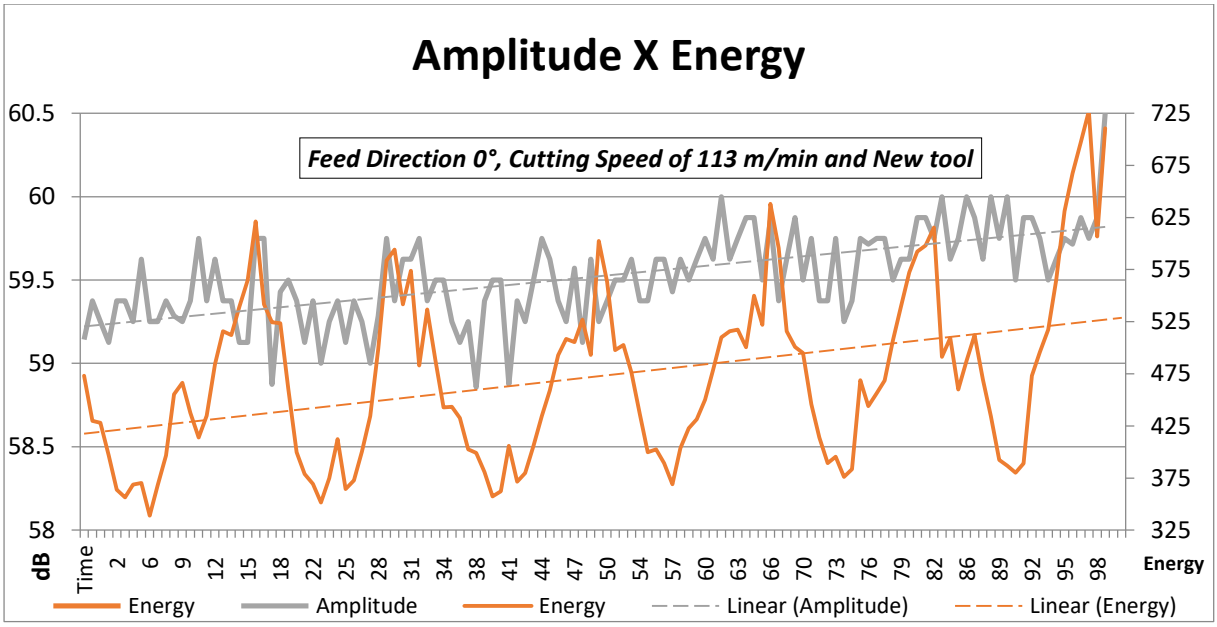

Figure 32 – Evolution of the AE signals (Amplitude and Energy) vs. machining time during milling process. With: Feed Direction 0°, Cutting Speed of 113 m/min and New tool.

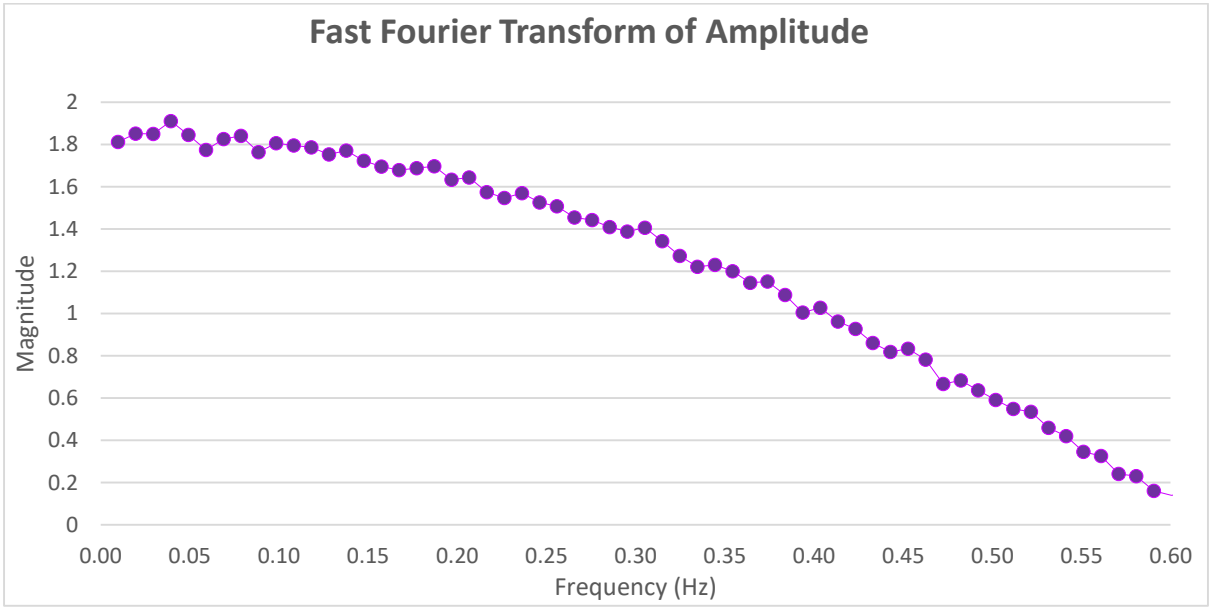

Figure 33 – Acoustic Emission Amplitde in frequency domain.

Figure 32 also compares the AE signal of the same process in terms of Amplitude and Energy. Similar to amplitude, energy shows a slight increase in magnitude during the cutting process (Figure 32 *trendlines*). Regarding energy behaviour, it seems that there is a periodical pattern, in which valleys and peaks occurs periodically during cutting process, this idea is reinforced Figure 34.

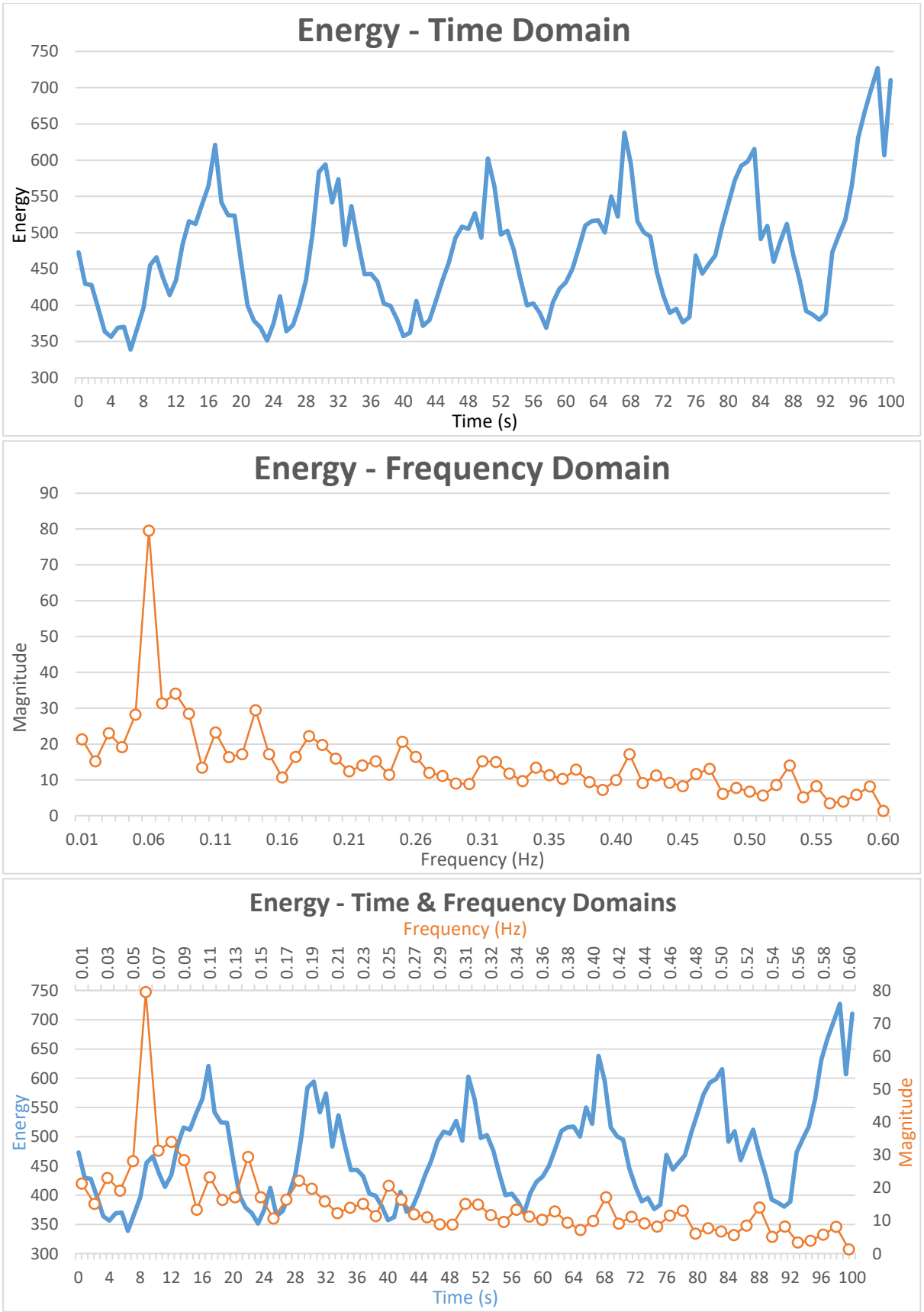

Figure 34 – Comparison of Acoustic Emission energy in frequency (FFT) and time domains.

The comparison between Energy and Amplitude features with Hits, agrees with the concept of AE signals and the cutting path relationship. Figure 35 shows that for the same signal, while hits has a valley each inversion of feed direction over cutting path, energy oscillates between valleys and peaks. In the same way, energy has a similar behaviour of hits, energy shows valleys at the time that feed direction inversion happens. However, compared to hits, energy feature shows peaks of when a step in axial depth occurs (axial step depth is always combined with feed direction inversion). The peaks have larger amounts of energy, meaning that more waveforms are counted, in way of speaking there are more hits per second. Since not only hits are connect to energy, as seem that valleys are connect to energy behaviour, these peaks are also related to waves have higher amplitude and duration. Thus, by observing the behaviour of hits and energy signal characteristics, it is possible to assert that during feed direction inversion there is a higher amount of hits with low energy (mainly because of waves with low amplitude and duration). Additionally, the peaks occurring during feed direction inversion combined with axial step depth have more waves to count and these waves have high energy (mainly due to higher amplitude and longer duration of the wave).

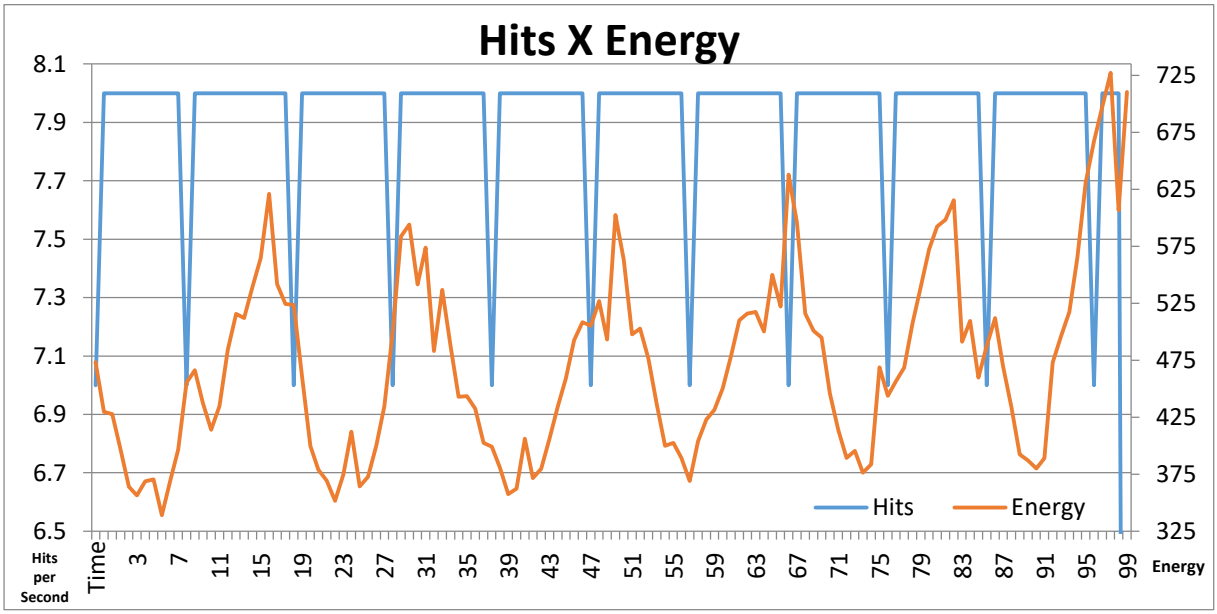

Figure 35 – Comparison between Hits and Energy through time, milling with New Tool. With: Feed Direction 0° and Cutting Speed of 113 m/min.

Based on the ANOVA statistical analysis, the results of AE signals were analysed aiming to relate the variables of influence and the responses in terms of signal characteristic, temperature and surface finishing. Regarding the statistical analysis of the AE signal features, the Main Effects for Cumulative Energy (Figure 36), Maximum Energy and Average Energy were analysed, showing that all factors of influence had impact in different levels. While feed direction and stacking sequence had particular interaction, cutting speed and tool condition had impact on cumulative energy of AE signal, as shown in Figure 36. The particularity between the interaction of feed direction and fibre direction is that relative angle varies and that an angle equal to ± 45 degrees is related to more surface damage and thus is expected to have high cumulative energy values. This supposition is reinforced by analysing Figure 36, regarding the stacking sequence of $[0/90/0/90/0/90]_s$, the feed direction of 45 degrees influenced the mean of cumulative energy to higher values, since the fibres were cut with a relative angle of ± 45 degrees.

Comparing the main effects plot for cumulative energy (Figure 36) and temperature (Figure 17) it seems that for stacking sequence and feed direction, higher values of cumulative energy are related with low temperatures, this comparison reinforces the idea that the cutting mechanism is different in regards of the relative angle. Furthermore, cutting speed and tool condition have similar behaviour for cumulative energy and temperature, with higher cutting speeds and levels of tool wear leading to higher amounts of cumulative energy and higher temperatures.

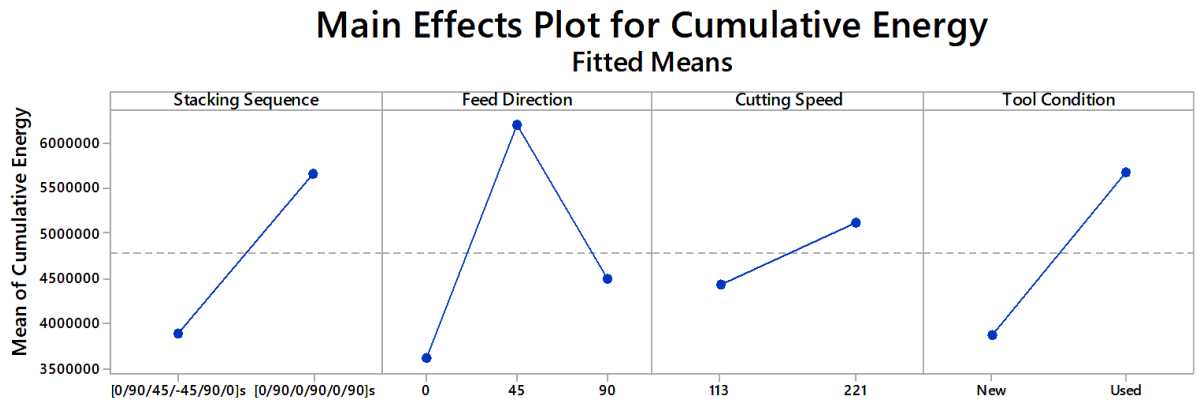

All displayed terms are in the model.

Figure 36 – Main effects in AE cumulative energy, regarding factors of influence and their levels.

Regarding cutting speed levels, the variation of 113m/min to 221m/min was tested for equal variances. It is showed in Figure 37 that the variation of cutting speed is significant, reinforcing the effect on the main effects. It indicates that although the difference of means for cumulative energy by cutting speed levels is lower, if compared to other influence factors, the test of equal variances shows that the difference is significant and that a higher cutting speed leaded to higher levels of cumulative energy.

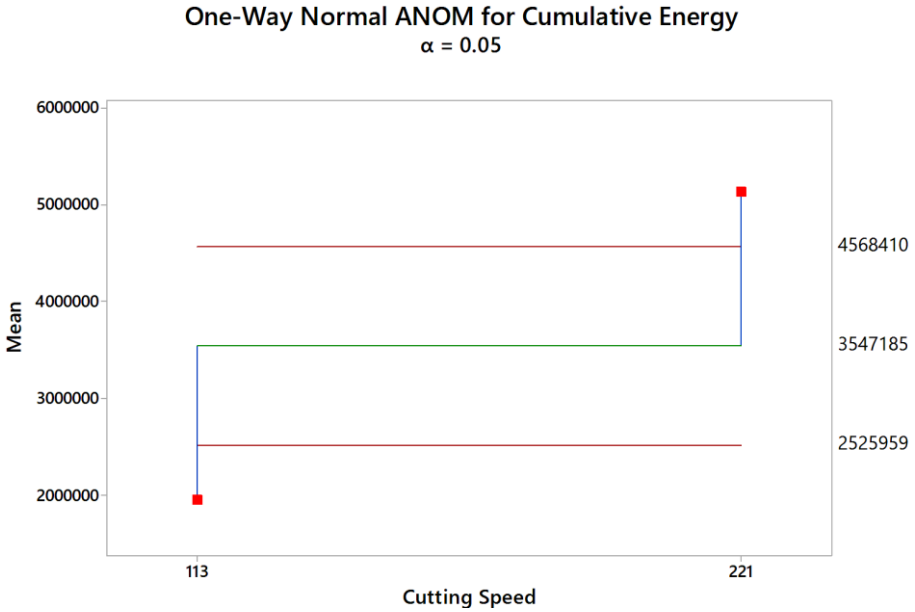

Figure 37 – Test of equal variances for cutting speeds of 113m/min and 221m/min.

Furthermore, a scatterplot of AE signal characteristic of cumulative energy and maximum energy shows that the highest values from both variables of response are related to the higher

cutting speed and higher levels of tool wear (Figure 38). Samples in lower speed, of 113m/min and with the starting cut using a new tool had values lower as 10^7 energy units for cumulative energy and $3x10^4$ energy units for maximum energy, far from the maximum of nearly 2.5 $x10^7$ energy units and $7x10^4$ energy units respectively for cumulative energy and maximum energy.

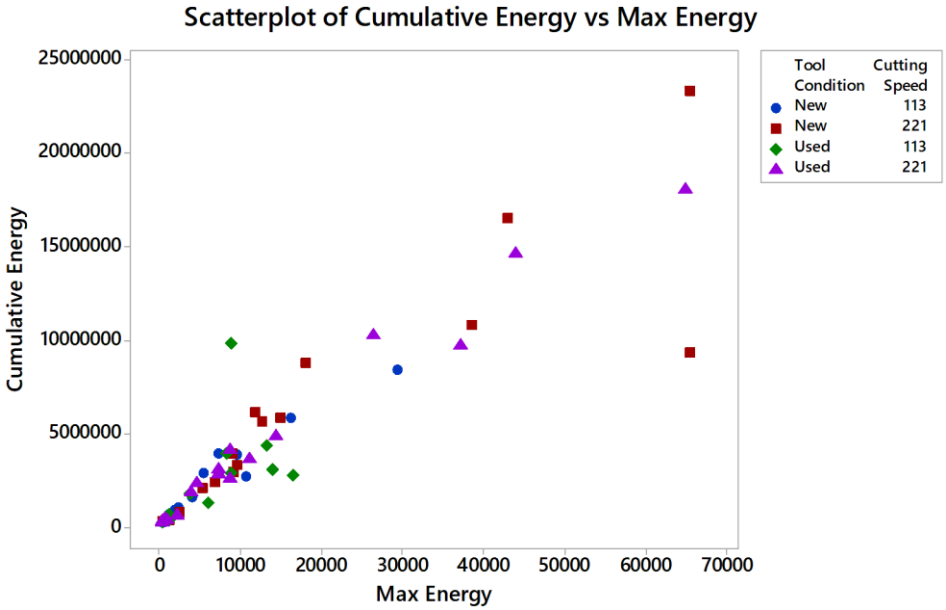

Figure 38 – Cumulative energy and maximum energy values plot regarding tool condition and cutting speed.

Comparing the relationship between cumulative energy with maximum amplitude shows that feed directions varies with this features (Figure 39). The feed direction along with fibre orientation provided different cutting mechanisms, as shown in Figure 24. The results regarding fibre direction of 0° shows that it has most amplitude values around 60 dB and 80 dB with cumulative energy below $5x10^4$units, while the feed direction of 45° shows amplitude and cumulative energy with values of 60-80 dB and highest cumulative energies varying between $10 - 15$ $(x10^4)$ units and the feed direction of 90° having a wider distribution of both characteristics signals. Moreover, the relationship between maximum amplitude and cumulative energy shows that signals with amplitudes above 80 dB are related to higher cumulative energies $15 - 20(x10^4)$units.

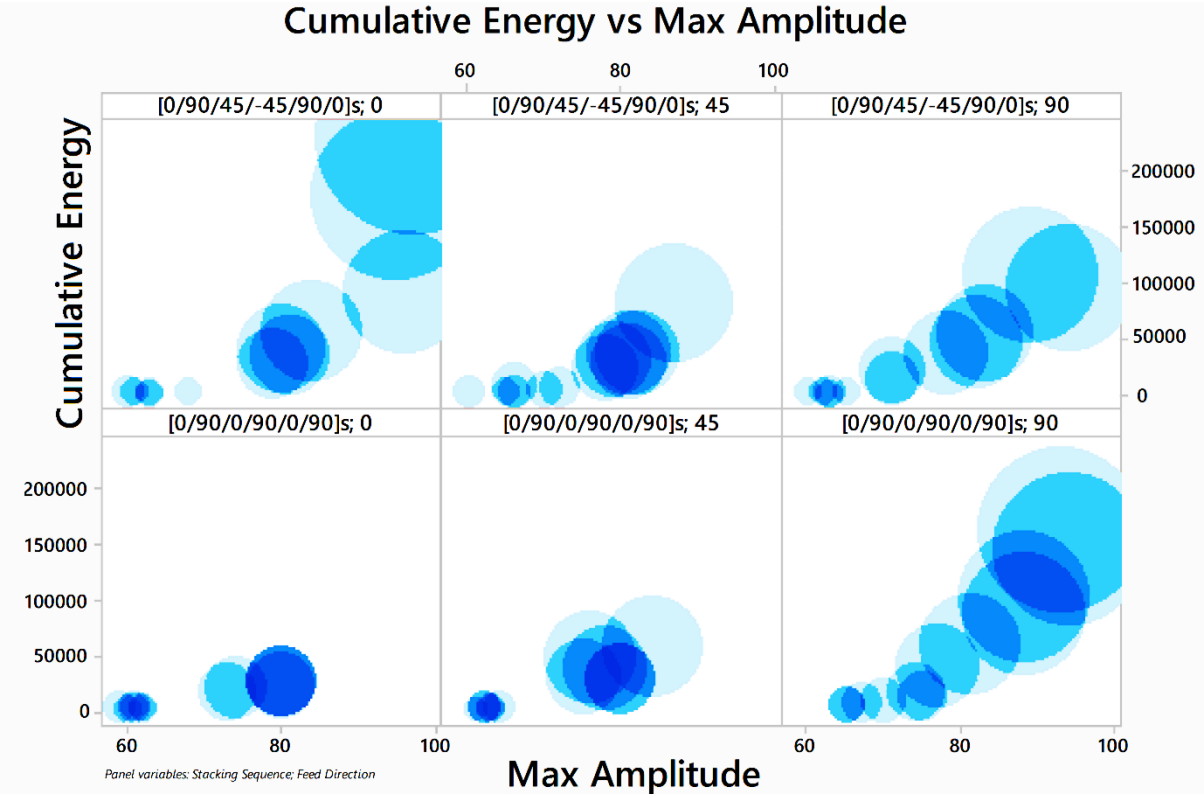

Figure 39 – Comparative of max amplitude and cumulative energy

Different studies proposed the use of several different parameters of Acoustic Emission for damage identification in composite materials, mostly for mechanical testing applications. The characterization of damage for composite material via Acoustic Emission leads to diverse results of a similar conclusion, it is possible to correlate damage to a characteristic of an Acoustic Emission signal (93) (105) (106) (107) (108).

According to some studies, the analysis of amplitude behaviour during testing shows that the damage is related to the signal. These authors were able to relate the damage mode with amplitude range. However, amplitude range varies from one study to another, but this difference can be a result of material composition, processing, equipment and ultimately testing procedures (108). Amplitude values are related to different mechanisms of defects, for example, low values of Amplitude, 40-60 dB, are related to matrix micro-cracking and friction, intermediate amplitudes, 60-80 dB, with decohesion and debonding and the high,80-100 dB, with fibre breakage (93) (106) (107). Similarly, the signal characteristics Hits Energy are

related to material damage, the signal characteristic accuracy can vary with the found damage and testing (105) (109). Thus, it is necessary further verification of the possible relationship between acoustic emission signal characteristics and surface finishing, focusing in evaluating the relation between them. While tool wear impacts in surface roughness and is related to acoustic emission features, cutting speed and feed direction deals with the cutting phenomenon changing how the composite material and its fibres are cut. Particularly, these influence factors impact on the interaction between material and cutting tool, resulting in different ways of cutting. The variation of relative angle from one feed direction to another varies, changing the cutting mechanism influencing the acoustic emission signal features and showing different defects. The feed direction of 45° has a general lower temperature and an intermediate range level of amplitude signal; nonetheless this configuration has more fibres cut at +45° and -45°, showing high surface roughness and significant damage and more deep craters.

The analysis of Acoustic Emission signal for the replica in Figure 21, with stacking sequence of $[0/90/45/-45/90/0]_s$, 45° of feed direction, cutting speed of 221m/min and used tool, revels that the characteristic signals of Hits, Energy and Amplitude had a unlike behaviour in time domain. Figure 40 and Figure 41 show that for initial milling process (green zone Figure 40) there were burst of hits, with low amplitude and energy levels. The presence of non-cut fibres may be related to amplitude signals of below 53 dB. The wave burst (up to 127 hits per second) may being caused by the defective milling process also emitting waves with low energy. After the first axial step, the signals became similar to standard replicas as explored and discussed before. There are a second hits burst (Figure 40 purple area) it is combined with low energy and amplitude signals, which can be a result of milling tool in contact with defect area.

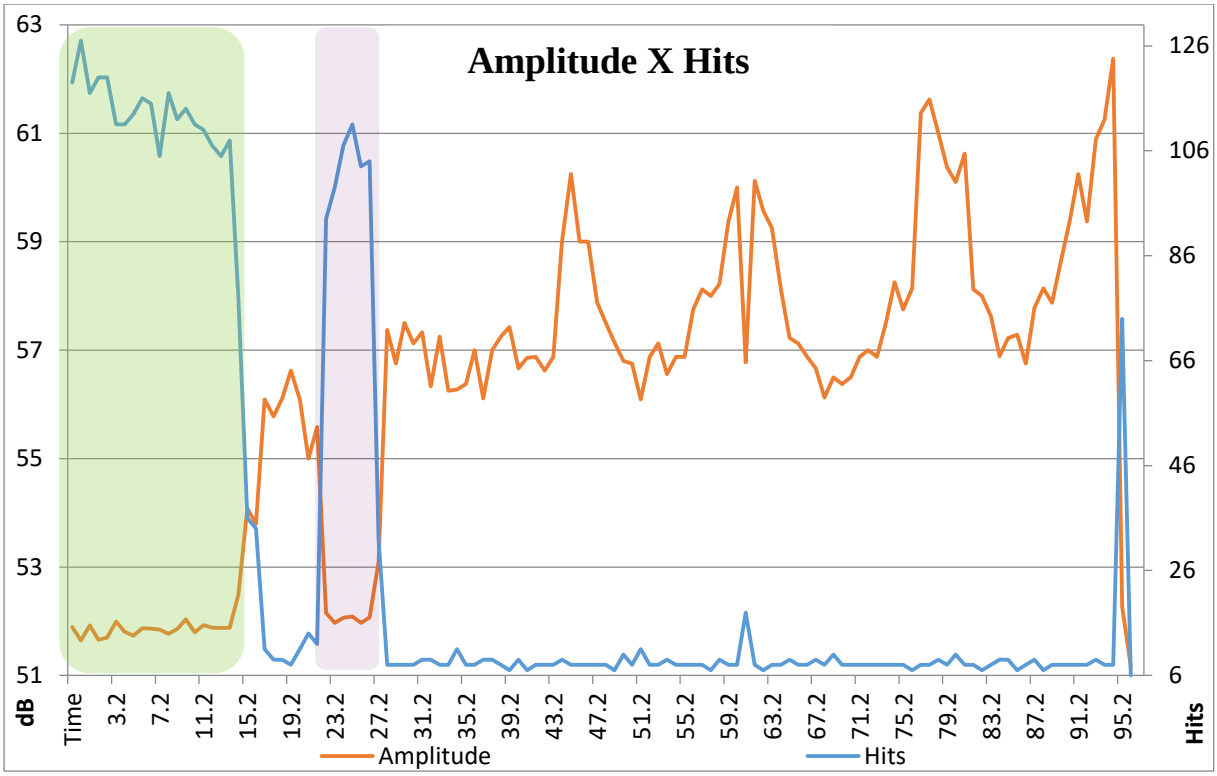

Figure 40 – Amplitude versus Hits of Acoustic Emission signal for $[0/90/45/-45/90/0]_s$ *plate, 45° of feed direction, with cutting speed of 221m/min and used tool.*

Figure 41 confirms that low Amplitude with burst of Hits contains low energy signals, caused by milling process with poor surface finishing. The Cumulative Energy shows that the initial cutting path has a low amount of energy, a region with several uncut fibres. The remaining path shows the common behaviour for the AE signals. Data analysis of AE hits and amplitude regarding frequency domain showed no relevant information, with no frequency peak and general behaviour not being related to an event. Thus, these results shows that amplitude signal feature in milling of composite materials is subjected to mechanism of cutting, being influenced by relative angle between fibre and feed direction.

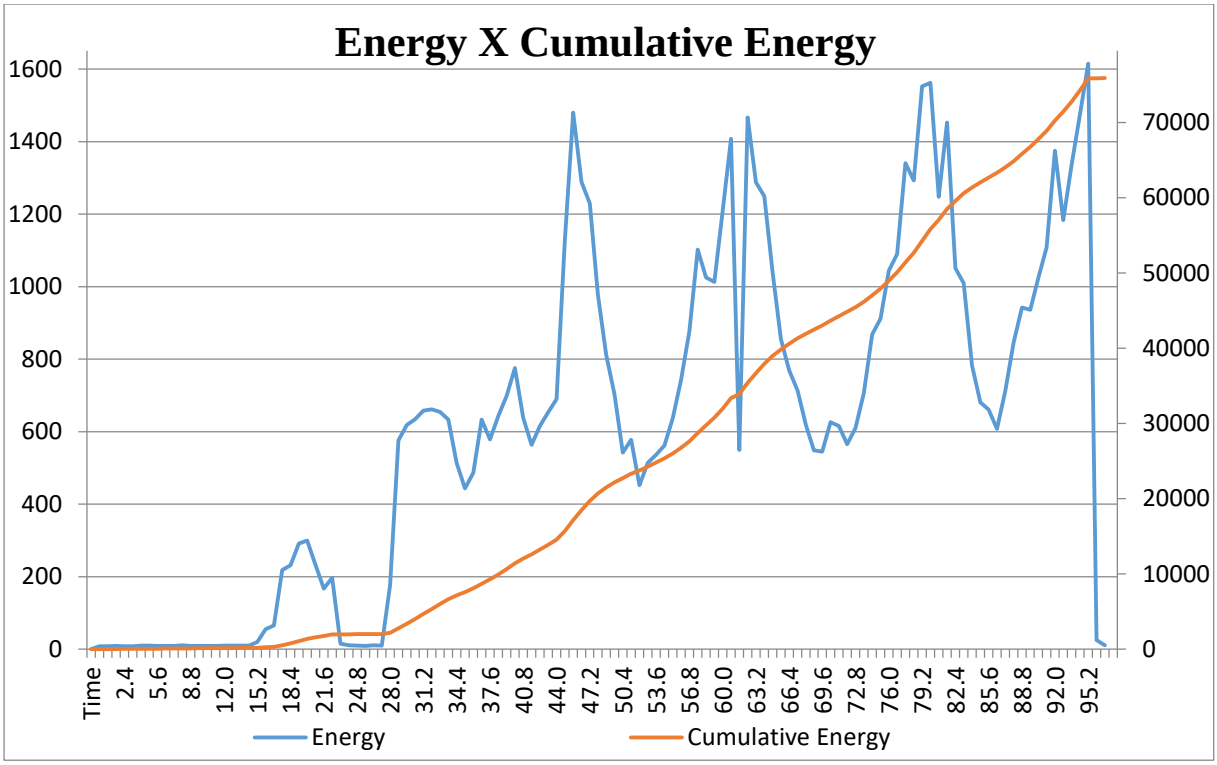

Figure 41 – Energy versus Cumulative Energy of Acoustic Emission signal for $[0/90/45/-45/90/0]_s$ *plate, 45° of feed direction, with cutting speed of 221m/min and used tool.*

Energy and Cumulative energy may be related to surface finishing, the data of cumulative energy trough cutting length by step was compared to roughness profile for the same replica and is shown in Figure 42 and Figure 43. In terms of surface finishing, it was possible to establish a relationship between all variables of influence with cumulative energy and rugosity. The figures show that surface roughness increases with tool wear and that cumulative energy curve has the potential of estimate the Ra value. Also, the values of cumulative energy and Ra varies with cutting speed and feed direction. The comparison for cutting speed shows that an increase of it generates lower levels of energy and lower average Ra by step.

Cumulative Energy X Ra

Feed Direction 0° - Tool New

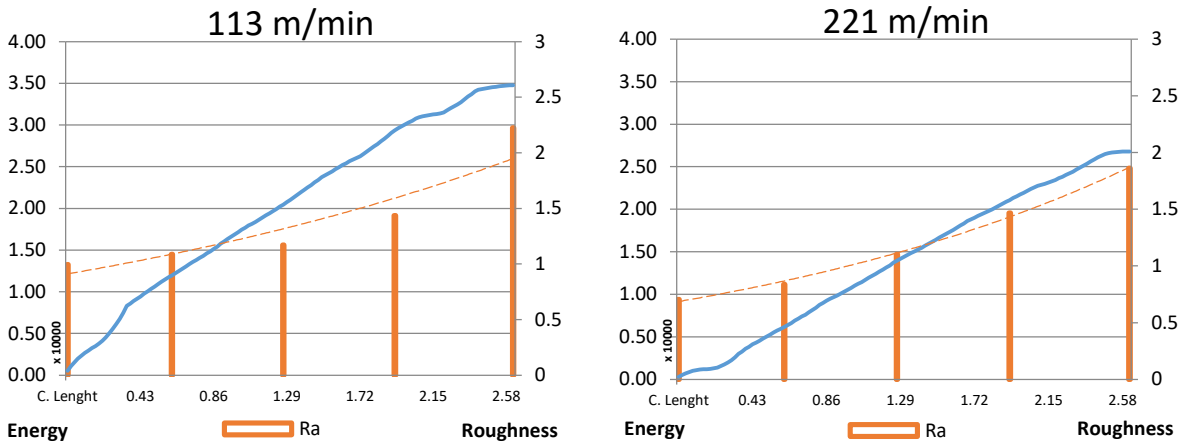

Figure 42– Cumulative energy by average Ra cutting length.

Regarding exclusively feed direction, it has impact in both, Ra and cumulative energy, with the feed direction of 0° having lower values of Ra and cumulative energy than feed direction of 90° (Figure 42 and Figure 43). The feed direction of 45° showed the highest values of average roughness by step and the same relationship with cumulative energy, although presenting lowest values compared with other feed directions. It may be a result of the mechanism of cutting being different, since it has different relative angles of cutting (45° and -45°). The cutting angle is not parallel nor perpendicular as the other feed directions. While presenting higher values of average Ra and more damage in machined surface, the different relative angle generated less energy release, affecting in cumulative energy values. In fact, comparing the values of amplitude median for each direction shows that 45° (68dB) of feed direction have higher values than other feed directions (58-60 dB). Regarding surface finishing, as well as, AE features there is evidence that the cutting mechanism is different, similar to different mechanisms of damages (93,105,107). These results agrees with previous studies, showing that higher amplitude levels are related with fibre pull-out (Figure 19D and Figure 20) and higher roughness levels.

Cumulative Energy X Ra

Cutting Speed 113m/min – Tool New

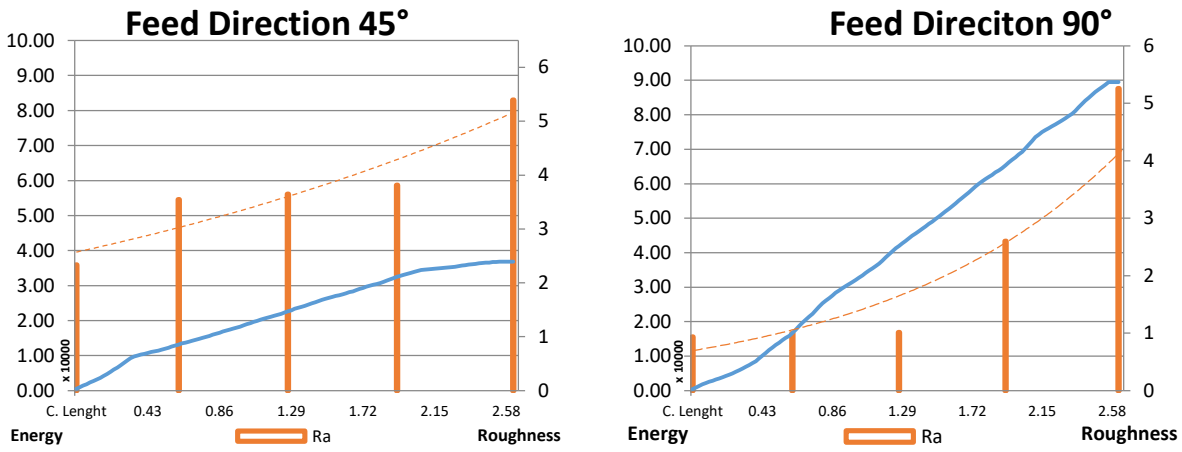

Figure 43– Cumulative energy by average Ra cutting length.

The use of cumulative energy for evaluating tool wear impact in roughness seems plausible. It is possible to estimate the maximum level acceptable roughness based on the amount of cumulative energy for a determined process based in the same cutting mechanism, since for all analysed conditions, the roughness increased with cumulative energy. Furthermore, other signal features are related to cutting path or damage mechanisms, showing the usefulness of using acoustic emission for monitoring machining process concerning workpiece surface finishing.

5. Conclusion

The experimental study of milling of multidirectional laminate plate of CFRP is presented in this research. The effects of variables of influence, regarding machining parameters (cutting speed, feed direction and cutting distance) and stacking sequence on variables of response measured by machining temperature, acoustic emission signal and surface finishing were investigated and analysed. Regarding non-destructive testing, the thermal camera recorded the machining temperatures developed during the process, the acquired acoustic emission signals was used to monitor workpiece response do cutting process. The use of different parameters during conventional milling process allows the following conclusions:

The development of the temperature during the milling process tends to increase from the beginning up to reaching a stable range. The temperature is influenced by tool wear and cutting speeds, with higher cutting speeds leading to higher wear. The recorded temperatures though cutting process are below glass transition temperature, suggesting that matrix degradation seem by microscope images are not caused by temperature. The variation of feed direction, thus implying in variation of relative angle between fibre and tool, varied temperature, with samples of feed direction oriented at 45 degrees having slight lower temperatures.

Microscope images showed the different effects of each variable of influence in terms of surface finishing. Each feed direction caused a different level or type of damage, with tool wear and higher cutting speeds related to higher damage levels. The surface roughness profile showed that for the same cutting sample, the tool wear impacted the surface with higher levels of roughness. The feed direction of 45 degrees showed the highest levels of visual damage and roughness, as result of the mechanism of cutting due to its relative angle.

Acoustic emission signals provided an alternative way to monitor milling process, with strong relationship to cutting path. Moreover, acoustic emission features can be related to the cutting mechanisms and damage phenomenology. Thus, acoustic emission features may be related to damage process, since surface quality varies with variables of influence and showed influence on monitored data. Energy and Amplitude features increases through cutting length and are related to tool wear, having impact in surface roughness that also increases through cutting length.

The study provided significant findings from analysis, offering new perspectives for improvements of real time monitoring CFRP process. The acquired data allows the estimation of tool life and surface quality, signal response through cutting path and relationship between cutting parameters and AE signals response.

6. Future Works

Based on the obtained results, it is possible to further analyse the following future works: Study of the efficiency of other non-destructive techniques during machining of CFRP, aiming to compare with acoustic emission and infrared thermography. The study of other machining processes for CFRP plates with similar configuration using the same non-destructive methods. Evaluation of machining of different matrix resin and/or reinforcements using acoustic emission and infrared thermography. The study of evaluation of acoustic emission signals during machining process, aiming the identification and classification of the featured signal with the damage caused in the composite part. The development of a monitoring system capable of using acoustic emission signals in order to predict surface quality of the machined parts for aeronautical composite parts.

References

1 BOYER, R. . P. N. Aircraft Materials, 2016.

2 FEDERAL AVIATION ADMINISTRATION, U. S. D. O. T. A. T. S. B. **Aviation Maintenance Technician Handbook - Airframe- Volume 1**. [S.l.]: Books Express Publishing, 2012.

3 KIM, D. J. et al. Recent Trends in Composite Materials for Aircrafts. **Applied Chemistry for Engineering**, v. 9, n. 4, p. 252-258, 2016.

4 ZITOUNE, R. . B. H. Machining and drilling processes in composite manufacture: Damage and material integrity. In: BOISSE, P. **Advances in Composites Manufacturing and Process Design**. [S.l.]: Woodhead Publishing, 2015. p. 177-180.

5 CHE, D. . S. I. . H. P. . G. P. . E. K. Machining of Carbon Fiber Reinforced Plastics/Polymers: A Literature Review. **Journal of Manufacturing Science and Engineering**, v. 136, June 2014.

6 MARTINS, F. R. **CARACTERIZAÇÃO DO FRESAMENTO DE CHAPAS DE COMPÓSITO POLÍMERO REFORÇADO COM FIBRAS DE CARBONO**. UNICAMP. Campinas, SP, Brazil. 2014.

7 TURNER, J. E. A. Effect of machining coolant on integrity of CFRP. **Advanced Manufacturing: Polymer & Composites Science**, v. 1, n. 1, p. 54-60, 2015.

8 KARATAS, M. A.; GÖKKAYA, H. A review on machinability of carbon fiber reinforced polymer (CFRP) and glass fiber reinforced polymer (GFRP) composite materials. **Defence Technology**, v. 14, n. 4, p. 318-326, August 2018.

9 FARAZ, A. . B. D. . W. K. . Cutting edge rounding: An innovative tool wear criterion in drilling CFRP composite laminates. **International Journal of Machine Tools and Manufacture**, v. 49, n. 15, p. 1185-1196, December 2009.

10 KPLEV, A. . L. A. . V. T. The cutting process, chips, and cutting forces in machining CFRP. **Composites**, v. 14, n. 4, p. 371-376, October 1983.

11 QIU, X. . L. . P. . N. Q. . C. A. . O. P. . L. C. . K. T. J. Influence of machining parameters and tool structure on cutting force and hole wall damage in drilling CFRP with stepped drills. **The International Journal of Advanced Manufacturing Technology**, v. 97, n. 1-4, p. 857-865, July 2018.

12 ÇOLAK Q., S. T. Cutting Forces and 3D Surface Analysis of CFRP Milling with PCD Cutting Tools. **Procedia CIRP**, v. 45, p. 75-78, 2016.

13 ZITOUNE, R. . K. V. . C. F. Study of drilling of composite material and aluminium stack. **Composite Structures**, v. 92, n. 5, p. 1246-1255, April 2010.

14 NGUYEN-DINH, N. . Z. R. . B. C. . L. S. Surface integrity while trimming of composite structures: X-ray tomography analysis. **Composite Structures**, v. 210, p. 735-746, February 2019.

15 THAKUR, A.; GANGOPADHYAY, S. State-of-the-art in surface integrity in machining of nickel-based super alloys. **International Journal of Machine Tools and Manufacture**, v. 100, p. 25-54, January 2016.

16 KARATAS, M. A. . G. H. A review on machinability of carbon fiber reinforced polymer (CFRP) and glass fiber reinforced polymer (GFRP) composite materials. **Defence Technology**, p. 1-9, 2018.

17 ZOU, F. et al. Hole quality and tool wear when dry drilling of a new developed metal/composite co-cured material. **Proceedings of the Institution of Mechanical Engineers, Part B: Journal of Engineering Manufacture**, v. 234, n. 6-7, p. 980-992, February 2020.

18 KHASHABA, U. A. Drilling of polymer matrix composites: A review. **Journal of Composite Materials**, v. 47, n. 15, 2012.

19 HADDAD, M. . Z. R. . E. F. . C. B. Study of the surface defects and dust generated during trimming of CFRP: Influence of tool geometry, machining parameters and cutting speed range. **Composites: Part B**, v. 66, p. 142-154, 2014.

20 HINTZ, W. . H. D. **Modeling of delamination during milling of unidirectional CFRP**. 14th CIRP Conference on Modeling of Machining Operations (CIRP CMMO). Turin, Italy: Elsevier Procedia CIRP. 2013. p. 444-449.

21 LIU, J. E. A. An investigation of workpiece temperature variation of helical milling for carbon fiber reinforced plastics (CFRP). **International Journal of Machine Tools & Manufacture**, v. 86, p. 89-103, 2014.

22 NGUYEN-DINH, N. . Z. R. . B. V. . L. S. Surface integrity while trimming of composite structures: X-ray tomography analysis. **Composite Structures**, v. 210, p. 735-746, 2019.

23 CHIBANE, H. . E. A. Optimal milling conditions for carbon/epoxy composite material using damage and vibration analysis. **International Journal Advanced Manufacturing Technology**, Londres, v. 68, p. 1111-1121, Abril 2013.

24 FU, R. et al. Drill-exit temperature characteristics in drilling of UD and MD CFRP composites based on infrared thermography. **International Journal of Machine Tools and Manufacture**, v. 135, p. 24-37, December 2018.

25 MARINESCU, I. . A. A. A critical analysis of effectiveness of acoustic emission signals to detect tool and workpiece malfunctions in milling operations. **International Journal of Machine Tools & Manufacture**, v. 48, p. 1148-1160, 2008.

26 MARINESCU, I. . A. D. A time–frequency acoustic emission-based monitoring technique to identify workpiece surface malfunctions in milling with multiple teeth cutting simultaneously. **International Journal of Machine Tools & Manufacture**, v. 49, p. 53-65, 2009.

27 ARUN, A. . R. K. . U. D. . S. A. Tool Condition Monitoring Of Cylindrical Grinding Process Using Acoustic Emission Sensor. **Materials Today: Proceedings** , v. 5, p. 11888-11899, 2018.

28 HASE, A. . W. M. . K. T. The relationship between acoustic emission signals and cutting phenomena in turning process. **International Journal of Advances in Manufacturing Technology**, v. 70, p. 947-955, 2014.

29 MOKHTAR, N. . I. I. Y. . A. M. . Z. H. . A. A. Analysis Of Acoustic Emission On Surface Roughness During End Milling. **ARPN Journal of Engineering and Applied Sciences**, v. 12, n. 4, February 2017.

30 PRAKASH, R. . K. V. . Z. R. . S.-A. J. High-Speed Edge Trimming of CFRP and Online Monitoring of Performance of Router Tools Using Acoustic Emission. **Materials**, v. 9, n. 798, September 2016.

31 LISSEK, F. . K. M. . T. J. . H. S. Online-monitoring for abrasive waterjet cutting of CFRP via acoustic emission: Evaluation of machining parameters and work piece quality due to burst analysis. **Procedia Engineering** , v. 149, p. 67-76, 2016.

32 BOTELHO, E. C. . S. R. A. . P. L. C. . R. M. C. A review on the development and properties of continuous fiber/epoxy/aluminum hybrid composites for aircraft structures. **Materials Research**, São Carlos, SP - Brazil, v. 9, n. 3, July/Sept 2006.

33 ILCEWICZ, L. B. . H. D. J. . F. A. J. Composite Applications in Commercial Airframe Structures. **Comprehensive Composite Materials**, v. 6, p. 87-119, 2000.

34 CHOWDHURY, N. . W. J. . C. K. W. . C. P. Static and fatigue testing bolted, bonded and hybrid step lap joints of thick carbon fibre/epoxy laminates used on aircraft structures. **Composite Structures**, v. 142, p. 96-106, May 2016.

35 HIKEN, A. The Evolution of the Composite Fuselage: A Manufacturing Perspective. In: DEKOULIS, G. **Aerospace Engineering**. 1st. ed. [S.l.]: Intechopen, 2019. Cap. 5.

36 RAJAK, D. . P. D. . K. R. . P. C. I. Recent progress of reinforcement materials: a comprehensive overview of composite materials. **Journal of Materials Research and Technology**, v. 8, n. 6, p. 6354-6374, November 2019.

37 ALEMOUR, B., BADRAN, O., HASSAN, M. R. **Journal of Aerospace Technology and Management**, São José dos Campos - SP, Brazil, v. 11, Mar 2019.

38 MULLER, R. **Aircraft Fuselage**. US 2008/0308676 A1, 18 December 2008.

39 GARG, P. . E. A. Advance research progresses in aluminium matrix composites: manufacturing & applications. **Journal of Materials Research and Technology**, v. 8, n. 5, p. 4924-4939, September-October 2019.

40 OWOEYE, S. S. . F. D. O. . O. B. . B. S. G. Zinc-aluminum (ZA-27)-based metal matrix composites: a review article of synthesis, reinforcement, microstructural, mechanical, and

corrosion characteristics. **The International Journal of Advanced Manufacturing Technology**, p. 373-380, September 2018.

41 BEWLAY, B. P. . J. M. R. . S. P. R. . Z. J. C. A review of very-high-temperature Nb-silicide-based composites. **Metallurgical and Materials Transactions A**, v. 34, p. 2043-2052, October 2003.

42 ZHANG, Q. M. Research on Ceramic Matrix Composites (CMC) for Aerospace Aplications.. **Advanced Materials Research**, p. 321329, July 2011.

43 MILLER, R. A. Thermal barrier coatings for aircraft engines: history and directions. **Journal of Thermal and Spray Technology**, p. 35-42, March 1997.

44 STEFFEN BEYER, F. M. R. D. M. S. D. S. C. W. **Method for producing a component made of a fiber-reinforced ceramic, component produced thereafter and its use as an engine component**. DE102007010675B4, March 2007.

45 MURMAN, S. . S. S. **Modeling Effective Stiffness Properties of IAD**. 21st AIAA Aerodynamic Decelerator Systems Technology Conference and. [S.l.]: [s.n.]. 2011.

46 NAIK, A. . A. N. . K. G. . Z. M. Micromechanical Viscoelastic Characterization of Fibrous Composites. **Journal of COMPOSITE MATERIALS**, v. 42, n. 12, 2008.

47 ALI, M. A. . U. R. . K. K. A. . S. A. Y. **Graphene Coated Smart Fabrics for VaRTM Process Monitoring**. 21st International Conference on Composite Materials. Xi'an, China: [s.n.]. 2017.

48 MESOGITIS, T. S. . S. A. A. . L. A. C. . Uncertainty in the manufacturing of fibrous thermosetting composites: A review. **Composites: Part A**, v. 57, p. 67-75, February 2014.

49 STAMOPOULOSA, A. G. . T. K. I. . D. A. J. Quality assessment of porous CFRP specimens using X-ray Computed Tomography data and Artificial Neural Networks. **Composite Structures**, v. 192, p. 327-335, May 2018.

50 MEHDIKHANI, M. . G. L. . V. I. . L. S. Voids in fiber-reinforced polymercomposites: A review on theirformation, characteristics, andeffects on mechanical performance. **Journal of Composite Materials**, v. 53, n. 12, 2019.

51 CHEN, D. . A. K. . X. C. Reduction of void content of vacuum-assisted resin transfer molded composites by infusion pressure control. **Polymer Composites**, v. 36, n. 9, p. 1629-1637, 2015.

52 YANG B., E. A. Influence of Fabric Shear and Flow Direction on Void Formation During Resin Transfer molding. **Composites: Part A**, v. 68, p. 10-18, January 2015.

53 HAMIDI, Y. K. . D. S. . A. L. . A. M. C. Effect of fiber content on void morphology in resin transfer molded e-glass/epoxy composites. **Journal of Engineering Material Technology**, v. 131, n. 2, April 2009.

54 CANTWEL, W. J.; MORTON, J. The Significance of Damage and Defects and Their Detection in Composite Materials: A Review. **Journal of Strain Analysis**, v. 27, p. 29-42, January 1992.

55 FLEISCHER, J. . T. R. . L. G. . M. P. . M. H.-C. . C. A. Composite materials parts manufacturing. **CIRP Annals**, v. 67, n. 2, p. 603-6026, 2018.

56 ELGNEMI, T. . A. K. . S. V. . N. J. Effects of atomization-based cutting fluid sprays in milling of carbon fiber reinforced polymer composite. **Journal of Manufacturing Processes**, v. 30, n. C, p. 133-140, 2017.

57 NGUYEN, T. T. Prediction and optimization of machining energy, surface roughness, and production rate in SKD61 milling. **Measurement**, v. 136, p. 525-544, March 2019.

58 HEJJAJI, A. et al. Surface and machining induced damage characterization of abrasive water jet milled carbon/epoxy composite specimens and their impact on tensile behavior. **Wear**, v. 376-377, p. 1356-1364, April 2017.

59 ATTAR, E. A.; KATAMISH, A. H.; SALLAM, H. I. Effect of Cutting Tools and Luting Cement on Marginal Adaptation of All Ceramic Restoration. **Egyptian Dental Journal**, v. 59, p. 947-960, January 2013.

60 HADDAD, M. . Z. R. . E. F. . C. B. Study of trimming damages of CFRP structures in function of the machining processes and their impact on the mechanical behavior. **Composites: Part B**, v. 57, p. 136-143, 2013.

61 BORTOLUZZI, B. D. **Desenvolvimento de reforços tridimensional por meio de costura em compósitos de fibra de carbono/epóxi**. Dissertação de mestrado, Universidade Federal de Itajubá. Itajubá, Brasil. 2017.

62 SHEIKH-AHMAD, J.; URBAN, N.; CHERAGHI, H. Machining Damage in Edge Trimming of CFRP. **Materials and Manufacturing Processes**, v. 27, p. 802-808, May 2012.

63 COLLIGAN, K. . R. M. Delamination in surface plies of graphite/epoxy caused by the edge trimming process. **Process Manufacturing of Composite Materials**, Nova Iorque, v. 49, n. 27, p. 113–25, 1992.

64 MARTINS, A. **Analysis of damage mechanisms in composite structures reinforced by tufting**. Université de Technologie de Compiègne. Compiègne. 2018.

65 HEJJAJI, A. . Z. R. . C. L. . L. R. S. . C. F. Surface and machining induced damage characterization of abrasive water jet milled carbon/epoxy composite specimens and their impact on tensile behavior. **Wear**, v. 376-377, n. Part B, p. 1356-1364, April 2017.

66 SU, Y. Effect of the cutting speed on the cutting mechanism in machining CFRP. **Composite Structures**, v. 220, p. 662-676, April 2019.

67 EFFECTS of cutting edge radius and fiber cutting angle on the cutting-induced surface damage in machining of unidirectional CFRP composite laminates. **International Journal of Advanced Manufacturing Technology**, v. 91, p. 3107–3120, January 2017.

68 RAMASAMY, N. . J. M. Innovative Nondestructive Testing Systems and Applications. In: OMAR, M. **Nondestructive Testing Methods and New Applications**. 1st. ed. Rijeka, Croatia: InTech, 2012. Cap. 2, p. 23-53.

69 JOLLY, M. R. . P. A. . S. B. . H. K. . S. R. . T. S. . F. P. . S. A. Review of Non-destructive Testing (NDT) Techniques and their applicability to thick walled composites. **Procedia CIRP**, v. 38, p. 129-136, 2015.

70 BOSSI, R. H. . S. G. C. . S. R. E. Visual Testing. In: THE AMERICAN SOCIETY FOR NONDESTRUCTIVE TESTING, I. **ASNT Industry Handbook:** Aerospace Nondestructive Testing. [S.l.]: [s.n.], 2014. Cap. 5.

71 THE AMERICAN SOCIETY FOR NONDESTRUCTIVE TESTING, I. Other Methods. In: H., B. R. **ASNT Industry Handbook:** Aerospace Nondestructive Testing. [S.l.]: [s.n.], 2014. Cap. 17.

72 LINDGREN, E. A. . L. J. A. . K. D. . F. B. A. . V. A. . K. V. A. . M. W. P. . B. B. B. . B. L. . T. J. G. . W. G. L. Ultrasonic Testing. In: THE AMERICAN SOCIETY FOR

NONDESTRUCTIVE TESTING, I. **ASNT Industry Handbook:** Aerospace Nondestructive Testing. [S.l.]: [s.n.], 2014. Cap. 9.

73 MALDAGUE, X. P. V. . S. S. M. . S. J. A. Thermographic Testing. In: THE AMERICAN SOCIETY FOR NONDESTRUCTIVE TESTING, I. **ASNT Industry Handbook:** Aerospace Nondestructive Testing. [S.l.]: [s.n.], 2014. Cap. 11.

74 YAZDANI, N. . G. E. C. . R. M. Field assessment of concrete structures rehabilitated with FRP. In: PACHECO-TORGAL, F. . M. R. . S. X. . B. N. D. . T. K. V. . S. A. **Eco-Efficient Repair and Rehabilitation of Concrete Infrastructures**. [S.l.]: Woodhea publishing Series in Civil and Structural Engineering, 2018. Cap. 8, p. 171-194.

75 JAYAKUMAR, T. . M. C. K. NDT Techniques: Acoustic Emission. In: JAYAKUMAR, T. **Encyclopedia of Materials:** Science and Technology (Second Edition). 2nd. ed. Kalpakkam, India: Elsevier Inc. , 2016.

76 MOURITZ, A. Nondestructive inspection and structural health monitoring of aerospace materials. In: MOURITZ, A. **Introduction to Aerospace Materials**. [S.l.]: Woodhead Publishing Limited, 2012. Cap. 23, p. 534-557.

77 KARBHARI, V. M. Introduction: the future of non-destructive evaluation (NDE) and structural health monitoring (SHM). In: KARBHARI, V. M. **Non-Destructive Evaluation (NDE) of Polymer Matrix Composites**. Arlington, TX - USA: Woodhead Publishing Limited, 2013. Cap. 1, p. 3-11.

78 ASTM INTERNATIONAL. **Standard Practice for Acoustic Emission Examination of Fiberglass Reinforced Plastic Resin (FRP) Tanks/Vessels**. E1067/E1067M, 2011.

79 ASTM INTERNATIONAL. **Standard Terminology for Nondestructive Examinations**. ASTM E1316, 2020.

80 PORFIRI, M.; SHAMS, A. Pressure reconstruction during water impact through particle image velocimetry: Methodology overview and applications to lightweight structures. In: LANGELLA, A.; LOPRESTO, V.; ABRATE, S. **Dynamic Response and Failure of Composite Materials and Structures**. 1st. ed. [S.l.]: Woodhead Publishing, v. I, 2017. Cap. 13, p. 395-416.

81 KARBHARI, V. M. . E. A. **Methods for detecting defects in composite rehabilitated concrete structures**. Salem, EUA. 2005.

82 HSU, D. K. Non-destructive evaluation (NDE) of aerospace composites ultrasonic techniques. In: KARBHARI, V. M. **Non-Destructive Evaluation (NDE) of Polymer Matrix Composites**. 1a. ed. [S.l.]: Woodhead Publishing, v. 1, 2013. Cap. 15, p. 397-421.

83 HUANG, J. Q. Non-destructive evaluation (NDE) of composites: acoustic emission (AE). In: KARBHARI, V. M. **Non-Destructive Evaluation (NDE) of Polymer Matrix Composites**. 1a. ed. [S.l.]: Woodhead Publisher, 2013. Cap. 2, p. 12-32.

84 LEY, O. . G. V. Non-destructive evaluation (NDE) of aerospace composites: application of infrared (IR) thermography. In: KARBHARI, V. M. **Non-destructive evaluation (NDE) of polymer matrix composites**. 1a. ed. [S.l.]: Woodhead Publisher, v. 1, 2013. Cap. 12, p. 309-336.

85 MATERIALS, A. S. F. T. A. **Standard Definition of Terms Relating to Acoustic Emission.** [S.l.]: [s.n.]. 1982.

86 BHUIYAN, M. S. H. . C. I. A. . D. M. . N. Y. . D. S. Z. Application of acoustic emission sensor to investigate the frequency of tool wear and plastic deformation in tool condition monitoring. **Measurement**, v. 92, p. 208-217, October 2016.

87 BI, H. . L. H. . Z. W. . W. L. . Z. Q. . C. S. . T.-G. I. Evaluation of the acoustic emission monitoring method for stress corrosion cracking on aboveground storage tank floor steel. **International Journal of Pressure Vessels and Piping**, v. 179, January 2020.

88 GENG, R. S. . B. W. G. B. . S. R. W. B. **A Theoretical Model For Evaluating Acoustic Emission Energy Release During Phase Transitions Of A Shape-Memory Alloy**. Ultrasonics International 83. [S.l.]: Butterworth & Co (Publishers) Ltd. 1983. p. 48-53.

89 XU, B. . W. Q. Stress fatigue crack propagation analysis of crane structure based on acoustic emission. **Engineering Failure Analysis**, November 2019.

90 CHEN, J. . K. Q. . L. Q. . Y. H. Effects of grain size on acoustic emission of nanocrystalline superelasticNiTi shape memory alloys during fatigue crack growth. **Materials Letters**, v. 252, p. 300-303, October 2019.

91 UNNTHORSSON, R. . R. T. P. . J. M. T. Acoustic emission based fatigue failure criterion for CFRP. **International Journal of Fatigue**, v. 30, n. 1, p. 11-20, January 2008.

92 KATUNIN, A. . D. K. . D. M. Damage identification in aircraft composite structures: A case study usign various non-destructive testing techniques. **Composite Structures**, v. 127, p. 1-9, 2015.

93 MUNOZ, V. . V. B. . P. M. . P. M. L. . W. H. . C. A. Damage detection in CFRP by coupling acoustic emission and infrared thermography. **Composites Part B**, v. 85, p. 68-75, 2016.

94 DUAN, Y. . Z. H. . M. X. P. V. . I.-C. C. I. . S. P. . G. M. . S. S. . M. J. Reliability assessment of pulsed thermography and ultrasonic testing for impact damage of CFRP panels. **NDT & E International**, v. 102, p. 77-83, March 2019.

95 SWIDERSKI, W. Non-destructive testing of CFRP by laser excited thermography. **Composite Structures**, v. 209, p. 710-714, February 2019.

96 FILIPPOV, A. V. . R. V. E. . T. S. Y. Acoustic emission study of surface deterioration in tribocontacting. **Applied Acoustics**, v. 117, n. Part A, p. 106-112, February 2017.

97 LEE, D. E. . H. I. . V. C. M. O. . O. J. F. G. . D. D. A. Precision manufacturing process monitoring with acoustic emission. **International Journal of Machine Tools and Manufacture**, v. 46, n. 2, p. 176-188, February 2006.

98 KRISHNAMOORTHY, A. . M. J.. K. V. K. S. M. . S. M. K. Delamination Analysis of Carbon Fiber Reinforced Plastic (CFRP) Composite plates by Thermo graphic technique. **Materials Today: Proceedings**, v. 2, n. 4-5, p. 3132-3139, 2015.

99 FU, R. . J. Z. . W. F. . J. Y. . S. D. . Y. L. . C. D. Drill-exit temperature characteristics in drilling of UD and MD CFRP composites based on infrared thermography. **Elsevier**, v. 135, p. 24-37, December 2018.

100 ZITOUNE, R. . C. N. . C. F. . Š. M. Temperature and wear analysis in function of the cutting tool coating when drilling of composite structure: In situ measurement by optical fiber. **WEAR**, v. 376, p. 1849-1858, December 2016.

101 NOR KHAIRUSSHIMAA, M. K. . S. I. S. S. Study on Tool Wear during Milling CFRP under Dry and Chilled Air Machining. **Advances in Material & Processing Technologies Conference**, n. 184, p. 506-517, 2017.

102 ZITOUNE, R. . C. F. . L. F. . P. R. P. P. Experiment–calculation comparison of the cutting conditions representative of the long fiber composite drilling phase. **Composites Science and Technology**, v. 65, n. 3-4, p. 455-466, March 2005.

103 HADDAD, M. . Z. R. . B. B. . E. F. . C. B. Study of trimming damages of CFRP structures in function of the machining processes and their impact on the mechanical behavior. **Composites Part B: Engineering**, 57, February 2014. 136-143.

104 HOSOKAWA, A. et al. High-quality machining of CFRP with high helix end mill. **CIRP Annals - Manufacturing Technology**, v. 63, n. 1, p. 89-92, 2014.

105 BRAVO, A. . T. L. . K. D. . E. F. Characterization of Tensile Damage for a Short Birch Fiber-reinforced Polyethylene Composite with Acoustic Emission. **International Journal of Material Science**, v. 3, n. 3, September 2013.

106 EL MAHI, A. E. A. **Analyse par émission acoustique de l'endommagement des matériaux éco-composites**. 10ème Congrès Français d'Acoustique. Lyon: [s.n.]. 2010.

107 KOTSIKOS, G. . E. J. T. . G. A. G. . H. J. Use of Acoustic Emission to Characterize Corrosion Fatigue Damage Accumulation in Glass Fiber Reinforced Polyester Laminates. **Polymer Composites**, v. 8, n. 20, p. 689-696, April 2004.

108 NIMDUM, P. . R. J. **Use of acoustic emission to discriminate damage modes in carbon fibre reinforced epoxy laminate during tensile and buckling loading**. CCM 15 - 15th European Conference on Composite Material. Venese, Italy: [s.n.]. 2012. p. 8-17.

109 MALOLAN, V. . W. G. . S. A. S. G. . T. T. Comparison of acoustic emission parameters for fiber breakage and de-lamination failure mechanisms in carbon epoxy composites. **Journal of Engineering and Technology Research**, v. 8, n. 3, p. 21-30, May 2016.

110 MOUSMOULIS, G. . K.-D. N. . A. G. . A. I. . P. D. Experimental analysis of cavitation in a centrifugal pump using acoustic emission, vibration measurements and flow visualization. **European Journal of Mechanics - B/Fluids**, v. 75, p. 300-311, May-June 2019.